# Comprehensive Assessment of Low Salinity Water Injection EOR Using Integrated Modeling Framework

Samuel David Fontalvo Guzman

A Thesis

Submitted in partial fulfillment of the requirements for the degree of

Bachelor of Science in Petroleum Engineering

Advisor

Maika Karen Gambús Ordaz, PhD.

Universidad Industrial de Santander

Co-Advisor

Zulfiquar Reza, PhD.

University of Oklahoma

Universidad Industrial De Santander

Facultad De Fisicoquímicas

Escuela De Ingeniería De Petróleos

Bucaramanga

2020

*Dedicated to*

*God, who gave me life and salvation*

*My dear Parents, who are the best gift ever in the World. They are my success*

*My brother, for sharing the most memorable moments*

*My grandparents (included Rosalba), who are always attentive and praying for me*

*Uncle Willy, for giving me such a huge support*

*Uncle David, who inspired me to dream*

*All my family, for believing in me*

*Dr Reza, who gave me this great opportunity to go to OU*

**Acknowledgements**

I want to give thanks to **God**, whom I owe everything, for guiding me throughout my career in every single step I have taken, for giving me strength in hard moments and for being so good to me.

I want to thank my **parents**, my **brother** and all **my family** to be supportive all the time. Thanks for praying for me, for calling me, for giving me so much, for everything. I love you!

My sincere gratitude to my **uncle Willy** and my dear **aunt Nora**, for all the economic support during all the steps of my career. I pray God recompensate you thousand times more. I also value all the advices you gave me from the beginning of my career

I want to say thanks to the "**Universidad Industrial de Santander**" for giving me the opportunity to embrace it as my alma matter. Thanks to every professor who contributed increasing my knowledge and teaching me lessons for my life.

I would like to thank the "**Grupo de Investigación de Recobro Mejorado**" for giving me the opportunity to grow in the academic area. Thanks to **Luis Carlos Prada** for having me patience and give me lots of opportunities. Thanks to all the team members for giving me good feedback in the presentations. It has strongly improved my skills. Also, for laughing of my typical occurrences.

I would like to thank to **Dr. Reza**, who gave me the opportunity to do my research internship at the University of Oklahoma. I appreciate all the time and effort to teach me and to encourage me to do my best. Thanks for having me patience with the long phrases I used to write. I promise I will do better. Thanks for the commitment with my learning process. I also want to thank **Yoana Walschap** for all her support before, during and after the internship. You are such a lovely and kind person. It was an amazing time at OU. I wish you all the best.

I would like to thank to **Dr. Maika Gambus** for her support even in stressful moments, for her collaboration being my thesis advisor and for teaching me those important courses. I admire her methodology to teach and solve problems.

I want to thank **Dr. Olga Ortiz** for her great and unconditional help with every issue during my internship abroad. Her kindness inspires me to help others wholehearted.

I want to thank my colleagues who have been there since the 1st semester (primiparos), **Victor, Erick, Juanchito, Nico, Diegu, Laura, rolo,** etc jaja, also to all the colleagues that I met throughout the undergraduate studies, **Camilo, Pipo, Chía, Jonathan, Fiallo, Angie, Fernanda, Pedro, Sergio, Rachel, Gutierritos** and all that help me grow personal and intellectually.

## Table of Contents

**Pag.**

## List of Figures

**Pag.**

# List of Tables

**Pag.**

# List of Appendices

Pag.

## Abstract

**Title:** Comprehensive Assessment of Low Salinity Water Injection EOR Using Integrated Modeling Framework*

**Author:** Samuel David Fontalvo Guzman**

**Key Words:** Low salinity water injection, enhanced oil recovery, integrated reservoir modeling, lithofacies saturation functions dependence, brine speciation.

**Description:**

Recently, variants of Low Salinity Water Injection (LSWI) emerged as promising enhanced oil recovery methods where the injected water salinity is considerably low compared to that of the formation water. Wettability change toward a more water-wet state and presence of clay minerals are postulated as major contributing factors. In this study, it is investigated the performance of LSWI under realistic reservoir conditions using integrated reservoir models in a comprehensive manner through Design of Experiments (DoE). The effects of various saturation functions, lithofacies mimicking wettability change, brine speciation and fluid model are the main emphases of the investigation.

Integrated reservoir models are constructed using all available geological, geophysical, and other relevant subsurface data. Low and high API crude oil fluid models were used with the aim to evaluate efficacy of the low-salinity effect in these oils. Lithofacies-dependent saturation functions were assigned to capture the effect of wettability change. Brine speciation of water injection must be done in order to accurately model the effects of each brine on LSWI. Brine speciation introduces the presence of other salt ions in the aqueous phase than simply sodium chloride. A two-tier DoE were performed, first focusing on endpoint scaling. Then, it is performed an overall uncertainty with parameterizations for porosity, permeability, anisotropy, fluid properties, production and injection rates and pressures and salinity of the injected water.

Overall recovery factors with lithofacies-dependent saturation functions narrow the range of plausible results and provide a better estimate of the recovery factor. Results provide critical insights on expected incremental recovery of LSWI and how to diagnose and optimize such processes, as well as the ideal static properties of a reservoir candidate to implement LSWI, alongside the main characteristics of the injection water and the formation water.


---

* Bachelor Thesis

** Facultad de Ingenierías Fisicoquímicas. Escuela de Ingeniería de Petróleos.
Director Maika Karen Gambús Ordaz, PhD. Codirector Zulfiquar Reza PhD.

## Resumen

**Título:** Evaluación Exhaustiva de una Técnica EOR de Inyección de Agua de Baja Salinidad Usando un Modelo Integrado Estructurado*

**Autor:** Samuel David Fontalvo Guzman**

**Palabras clave:** Inyección de agua de baja salinidad, métodos de recobro mejorado, modelos integrados de yacimiento, curvas de saturación facies-dependientes, composición iónica de agua inyectada.

**Descripción:**

Variantes de la técnica EOR de inyección de agua de baja salinidad han emergido recientemente. En este proceso, la salinidad del agua inyectada es considerablemente baja, comparada con la salinidad de la formación. El cambio de mojabilidad del yacimiento hacia un estado mojado por agua y la presencia de minerales de arcilla son postulados como los factores más contribuyentes. En esta tesis, se evalúa el rendimiento de la inyección de agua de baja salinidad bajo condiciones de yacimiento usando modelos integrados de yacimiento exhaustivos, a través del diseño de experimentos. Los principales énfasis de esta investigación son los efectos de las curvas de saturación, cambio de mojabilidad dependiente de las facies, composición iónica del agua inyectada y el efecto de diferentes fluidos.

Los modelos integrados de yacimientos son construidos usando información geológica y geofísica disponible. Se usaron dos modelos diferentes de fluidos con el propósito de evaluar el efecto de la inyección de agua de baja salinidad en crudos de alto y bajo API. Curvas de saturación fueron asignadas para cada tipo de roca y así modelar el efecto del cambio de mojabilidad para las diferentes litofacies. Se evaluó el impacto de diferentes composiciones de los iones del agua inyectada. Se realizaron varios diseños de experimentos evaluando los endpoints de las curvas de saturación. Posteriormente, se incluyeron parámetros de porosidad, permeabilidad, anisotropía, propiedades de los fluidos, tasas y presiones de inyección y producción y la concentración de sal inyectada.

Los factores de recobro con funciones de saturación dependientes de las litofacies estrechan el rango de posibles resultados y proveen un mejor estimado del factor de recobro. Los resultados proveen una perspectiva crítica de los factores que afectan la inyección de agua de baja salinidad en alto y bajo API y permiten diagnosticar y optimizar tales procesos.


---

* Trabajo de Grado

** Facultad de Ingenierías Fisicoquímicas. Escuela de Ingeniería de Petróleos.
Director Maika Karen Gambús Ordaz, PhD. Codirector Zulfiquar Reza PhD.

# Introduction

Today, new discoveries of giant oil reservoirs are rare, and the oil demand is increasing worldwide. Therefore, there is a growing interest in maximizing the recovery potential of the currently developed fields. Enhanced Oil Recovery (EOR) methods are the means to maximize the recovery by either increasing the recovery factor of a reservoir or decreasing the time to achieve the same recovery.

In the last decade, it has been confirmed injection of Low Salinity Water (LSW) improves oil recovery. In low salinity water injection (LSWI), water with considerably reduced salinity compared to seawater (in the salinity range up to 10 Kppm) is injected into the oil reservoir (Webb et al, 2005; Zhang et al, 2007). This effectively shifts the average wettability of the system toward a more water-wet system. Additionally, this technique is considered cheap compared to other EOR methods. It requires low capital investment, as well as, the operational costs are low. Besides, its implementation is easier than other EOR techniques.

The mechanisms behind the improvement of the oil recovery by low salinity water injection (LSWI) are not yet well understood. There have been several hypotheses confirmed by experimental results (Tang & Morrow, 1999; McGuire et al, 2005; Lager et al, 2006; Lee et al, 2010; Austad et al, 2005) but it still lacks a consensus. However, there is an accord that LSWI is affected by multiple mechanisms. Current screening criteria for this EOR technique heavily rely on our understanding based on published data and limited experimental results.

Several companies including BP, ExxonMobil and Saudi Aramco have evaluated and implemented LSWI in their field development plans. The workflows used to evaluate and develop

LSWI start with EOR screening, and include laboratory analyses, single-well and multi-well pilots as well as 3D simulation within each one of those stages.

In this thesis, 3D simulation of Low Salinity Water Injection, using state-of-the-art technologies, is performed considering relevant risks and uncertainties. The integrated reservoir simulation has several aspects. The process starts with integrated reservoir models construction using all available geological, geophysical, and other relevant subsurface data. This stage focuses on the reservoir architecture, facies modeling, and facies-dependent petrophysical modeling. The subsequent process involves construction of fluid, rock, and rock-fluid interaction models. The next stage incorporates well completion information and the development strategies for the investigated scenarios.

Injection of low salinity water effectively alters the wettability of the system. Thus, rock-fluid interaction functions like relative permeability and capillary functions are needed for both the low and high salinity conditions. Realistic scaling factors between the low- and high-salinity saturation curves (relative permeability and capillary pressure) as a function of salinity were employed based on published literature.

Lithofacies-dependent saturation functions were assigned to capture the effect of the presence of clay minerals. This allows modeling the variation of low-salinity effect from coarse sand to shale formations and appropriately capturing their contributions to overall wettability change. This study evaluates efficacy of the LSWI on low and high API crude oil fluids. The technologies used throughout the thesis include PETREL, ECLIPSE and INTERSECT.

# 1. Objectives

The main objective of this study is to assess the implementation of Low Salinity Water Injection, using state-of-the-art technologies, considering risks and uncertainties.

The specific objectives of this study are as follows:

- to evaluate performance of Low Salinity Water Injection (LSWI) EOR process using state-of-the-art tools,
- to identify the main controls of LSWI,
- to ascertain the effect of facies-dependent saturation functions in LSWI performance, and
- to inquire how brine speciation affects LSWI performance.

## 1.1 Organization of Thesis

In Chapter 2, a literature review of low salinity water injection is done. The topics include some generalities of LSWI, the mechanisms behind LSWI and the screening for LSWI. Also, some experimental and field cases are presented.

In Chapter 3 is presented the reservoir static model construction, the facies model, the petrophysical model, the fluid model, the rock-physics saturation functions and the development strategy. Some features of the low salinity modeling with ECLIPSE and INTERSECT are also stated in this chapter.

Chapter 4 presents the evaluation of the impact of the saturation functions by Design of Experiments (DoE). First, the effect of low salinity scaling function is ascertained. A two-tier DoE for endpoint scaling is performed to find out the most impactful endpoints and the main operational variables behind this process. The same workflow for the last two-tier DoE is applied to the rock-

type dependent saturation functions to inquire the impact of lithofacies mimicking wettability change in LSWI.

Chapter 5 presents the study for the brine speciation effect on LSWI, through design of experiments. Brine speciation of water injection must be done in order to accurately model the effects of each brine on LSWI. In brine speciation, we introduce the presence of other salt ions in the aqueous phase than simply sodium chloride.

Chapter 6 discuss the main differences in the LSWI response between the high and low API. This comparison is done based on the evaluation of LSWI for saturation functions and for the brine speciation.

Chapter 7 gives a discussion of the evaluation of LSWI, as well as the limits for this EOR technique. Some recommendations are also stated for further works.

Finally, in Chapter 8 it is presented the most salient conclusions of the work performed throughout the thesis and the references used.

# 2. Low Salinity Water Injection

Low Salinity Water Injection (LSWI) is an Enhanced Oil Recovery (EOR) method where the salinity of the injected water is considerably decreased, compared to high-salinity conventional waterflooding. Extensive literature review has demonstrated the efficiency of LSWI in reducing the residual oil saturation by improvement in microscopic sweep efficiency. LSWI advantages include ease of implementation, compared to other EOR techniques, availability and affordability of water. This technique also offers benefits such as mitigation of reservoir scaling and souring risks. Additionally, this process requires lower capital investment than alternative EOR processes, and the operational costs are low (Walid & Sepehrnoori, 2017).

Clearly, there are several mechanisms behind LSWI, which have been discussed by the scientific community. Nonetheless, there is a lack of consensus about what is the predominant mechanism driving the effect of LSWI. It is known that low salinity water (LSW) alters the established chemical equilibrium among crude oil, brine and rock, changing the wettability of the system. LSW induces a change towards a more water-wet condition, and this is due to chemical reactions at the rock-fluid interface (Rotondi et al. 2014). This chemical effect produced when injecting low salinity water is what makes this process to be classified as an EOR process.

LSWI consists in the injection of low salinity water through an injector well that displaces the oil within the reservoir and push it towards the producer well, as shown in Figure 1. LSWI can be applied in any development stage of a reservoir. However, most of the literature cases have been implemented as EOR processes. Some companies, like BP, include LSWI when assessing

development strategies for either fields which have water flooding as secondaries recoveries or fields that are suitable for water flooding to be implemented.

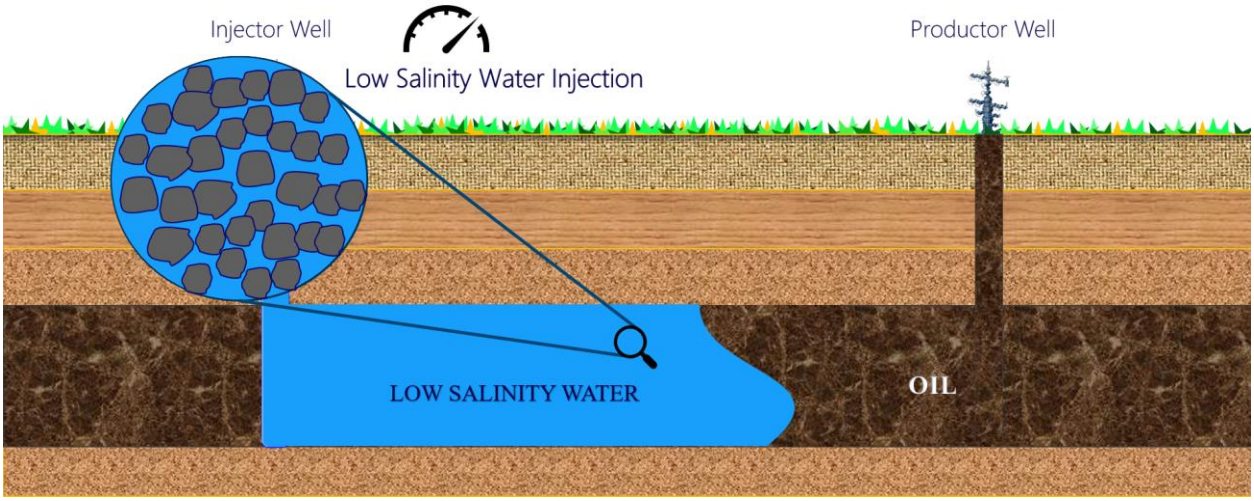


*Figure 1: Schematic of Low Salinity Water Injection.*

## 2.1 Generalities

### Salinity

The increase in oil recovery depends on the salinity of the brine injected. There is an upper and lower threshold to achieve good results. In the literature, salinity concentration between 1,000 – 2,000 ppm obtained the best results for oil recovery (Webb et al, 2005). Nevertheless, good results have been achieved with salinity concentrations up to 8,000 ppm. Beyond this limit there is not a notable difference in the effects of high and low salinity water injection. And below the lower limit, the improvement of oil recovery is minimum. The threshold value of the salt concentration is a balance between improvement of oil recovery by low salinity water injection and prevention of formation damage due to swelling and/or deflocculation of salinity sensitive clays present in sandstone rocks (Romanuka et al, 2012). Sorop et al. (2013) stated that the wettability change, which is the responsible for the improvement of oil recovery, is achieved below

a threshold level, believed to be around 5,000 ppm. If the salinity is further reduced to very low values, which in their case was 1000 ppm, this may lead to clay swelling and/or deflocculation, which may plug rock pores.

Webb et al. (2005) observed low salinity effect on oil recovery at salinities in the range of 2,000-3,000 ppm. Several core flood experiments were conducted by Zhang et al. (2007) to investigate the effect of low salinity brine on improving the oil recovery of Berea sandstone cores for both secondary and tertiary modes. Results were promising for the salinity level of 1,500 ppm NaCl. However, the use of 8,000 ppm NaCl had no effect on oil recovery, as the reduction in the brine salinity level seemed insufficient.

**Relative Permeability Curves**

The main effect of LSWI is a wettability change in the reservoir. The wettability of the system is dictated by the rock saturation functions like relative permeability and capillary pressure curves.

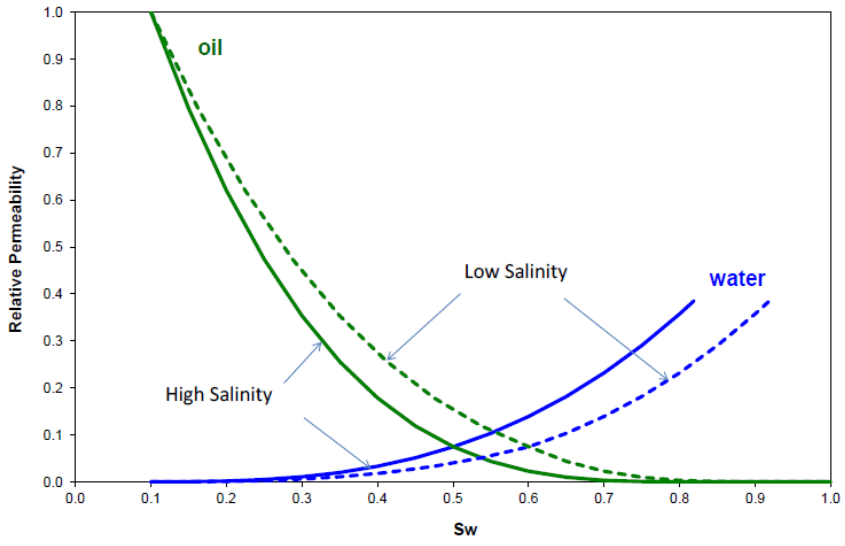


*Figure 2: High and low salinity relative permeability curves. Source: Adapted from Brodie & Jerauld (2014).*

The high-salinity and low-salinity relative permeability curves are illustrated in Figure 2. The continuous set of curves are for high salinity. The dotted set of curves are for low salinity. The change from the high to the low salinity curves represents the wettability shift toward a more water-wet system.

Brodie & Jerauld (2014) assigned the use of the high salinity curves when the concentration of NaCl in the aqueous phase exceeds 10,000 ppm. Below 3000 ppm, the low-salinity curves is used. The relative permeability at intermediate brine concentrations is linearly interpolated between the high- and low-salinity tables.

**Mixing of waters**

The literature suggests that the connate water in the pore space is displaced by the injected water. However, the two types of water mix to some degree so that the displacement is not piston-like. There can be diffusion in dead-end pore spaces. (Jerauld et al, 2008).

Jerauld et al. (2008) assume that connate water is displaced by injected water with some degree of mixing, based on what Sorbie et al. (1987) reported. Sorbie et al. (1987) said “clear banking of connate water was observed in both high and low permeability layers”.

Both at the laboratory and field scales, mixing is important and influences the interpretation and predictions of flood performance. Numerical dispersion appears to approximate physical dispersion well for the model he worked. (Jerauld et al, 2008)

**Fractional Flow**

Regarding the Buckley-Leverett solution, for high-salinity (ordinary), the solution consists of a shock front and a spreading wave, while the low-salinity solution consists of two fronts, one

corresponding to the transition between low and high salinity, and a second corresponding to the transition between high water saturation and connate at high salinity. The illustration of the displacement profile in the reservoir is shown in Figure 3. It should be noted that the ordinary Buckley-Leverett front speed is faster and particularly, breakthrough of high salinity water must occur earlier in the ordinary flood than in a low-salinity flood.

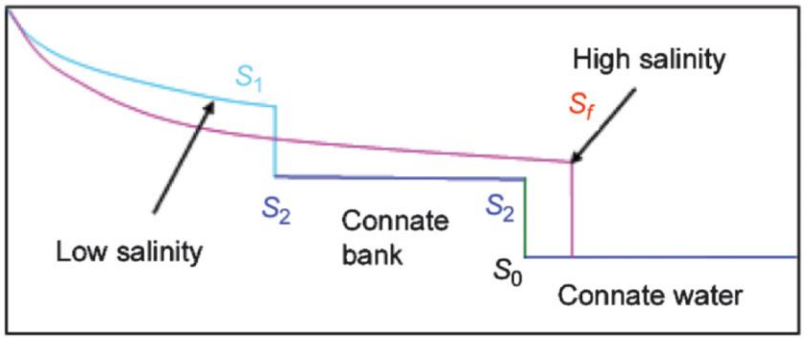


*Figure 3: Saturation profile of high salinity vs low salinity. Source: Adapted from Jerauld (2008).*

## 2.2 Mechanisms

There are several mechanisms that researchers have attributed the low salinity effect. In the literature, there is a lack of consensus on a single underlining mechanism for incremental oil recovery caused by low salinity water injection in both sandstone and carbonate rocks. However, no single suggested mechanism has been accepted as the main mechanism for low salinity effect (Walid & Sepehrnoori, 2017).

Tang & Morrow (1999) suggested a mechanism based on fine migration, implying that oil-wet clay particles are detached from the pore surface when in contact with low salinity water, increasing oil mobility. McGuire et al. (2005) suggested an alkaline/flooding behavior, caused by a pH increase. Lager et al. (2006) and Lee et al. (2010), suggested the Multiple-Ion-Exchange (MIE) process as a mechanism. MIE suggest that multivalent cations in the brine film at clay

surfaces are bonded to polar compounds of the oil phase, promoting initial oil-wetness on rock surfaces. The injection of low salinity brine causes ion exchange between ions from the invading brine and these complexes, leading to a more water-wet surface. Low salinity water expands the electrical double-layer established at the clay surface, weakening the bonds that hold the oil in contact with the rock. (Rotondi et al. 2014). Also, oil recovery due to LSWI was coincident with decrease in pressure drop, increase in pH, and fine migration. (Walid & Sepehrnoori, 2017).

Austad et al. (2005) have identified the effect of unexpectedly high oil recoveries upon injection of seawater into fractured chalk reservoirs can be attributable to the type and relative concentration of Potential Determining Ions (PDI), i.e. Mg+2, Ca+2, and (SO4)-2. It has been suggested that sulfate, which is abundantly present in seawater, will adsorb onto the positively charged sites on the chalk surface and thereby lower the positive surface charge. Because of a reduction in the electrostatic repulsion, excess Ca+2 will be localized closer to the chalk surface, where it may react with adsorbed oil polar compound, i.e. carboxylic acid.

Laboratory evidence supports two approaches to modify wettability of carbonate rocks under certain conditions: 1. increasing concentration of surface interacting ions, i.e. $(SO_4)^{-2}$, $(BO_3)^{-3}$ or $(PO_4)^{-3}$ in the injection brine or 2. lowering ionic strength of the injection brine. The results of the study performed by Romanuka et al (2012) demonstrate the oil recovery from several carbonate rock samples could be increased by lowering the ionic strength of the brine, possibly due to the wettability shift towards a more water-wet state. An enhanced oil recovery method based on this approach has some practical benefits as opposed to injection of brines containing elevated concentration of surface-interacting ions, i.e. $(SO_4)^{-2}$, $(BO_3)^{-3}$ or $(PO_4)^{-3}$. For instance, injecting high sulfate seawater into reservoirs which have formation water containing barium and strontium

increases the potential of scale formation in the production tubing and/or plugging of reservoir rock around the production well.

**2.2.1 Multiple-Ion Exchange.** Lager et al. (2006) proposed the main mechanism causing LSWI to increase oil recovery is due to cation exchange between the mineral surface and the invading brine. They state this mechanism explains why the low salinity production mechanism does not work when a core is acidized and fired because the cation exchange capacity of the clay minerals is destroyed. It explains the reason LSWI has no effect on mineral oil, as no polar compounds are present to strongly interact with the clay minerals.

Valocchi et al. (1981) carried out an experiment injecting fresh water into a brackish water aquifer. They noticed the concentration of $Ca^{+2}$ and $Mg^{+2}$ in different control wells were lower than the invading water and the connate brine. This indicates that $Mg^{+2}$ and $Ca^{+2}$ were strongly adsorbed by the rock matrix. Adsorption by cation exchange occurs when molecules containing quaternized nitrogen or heterocyclic ring replace exchangeable metal cations initially bound to clay surface. On an oil wet surface, multivalent cations at a clay surface will bond to polar compounds present in the oil phase (resin and asphaltene) forming organo-metallic complexes. These complexes promote oil-wetness in the reservoirs. During the injection of low salinity brine, multicomponent ionic exchange (MIE) will take place, removing organic polar compounds and organo-metallic complexes from the surface and replacing them with uncomplexed cations.

Because the mechanism proposed needs clay minerals for the cation exchange, Lager et al. (2006) stated the low salinity production mechanism does not seem to work on carbonate reservoirs. Conversely, several authors have explained the effectiveness of LSWI in carbonates. (Romanuka et al, 2012; Austad et al. 2005)

**2.2.2 Fine migration.** Core waterfloods were tested using Berea sandstone, observing the effect of mobile fine particles in the recovery with LSW. They established the following conditions necessary for increase in oil recovery with decrease in salinity: Adsorption from crude oil, the presence of potentially mobile fines and initial water saturation. Production of fines was observed leading to additional oil recovery. Observed recovery behavior is ascribed to partial stripping of mixed-wet fines from pore walls during waterflooding (Tang and Morrow, 1999).

Tang & Morrow (1999) noticed fines, mainly kaolinite, being eluted during low-salinity waterfloods on Berea core samples. They concluded fines mobilization resulted in exposure of underlying surfaces, which increased the water-wetness of the system. For oil-wet reservoirs, in the presence of high salinity brine, clays are undisturbed and retain their oil-wet nature, leading to poor displacement efficiency. When contacted with low-salinity water, clay particles detach from the pore surface, leading to the mobilization of oil with clays. The mechanism of fines migration was explained by the Deryaguin-Landau-Verwey-Overbeek (DLVO) theory of colloids. The permeability reduction occurs if the ionic strength of the injected brine is equal to or less than the critical flocculation concentration (CFC), which is strongly dependent on the relative concentration of divalent cations such as $Ca^{+2}$ and $Mg^{+2}$.

The double layer theory or DLVO theory describes the force between charged surfaces interacting through a liquid medium. It combines the effects of Van der Waals attraction and electrostatic repulsion. Low salinity brine reduces clay-clay attraction by expansion of the electric double layer, resulting in more water-wet on clay surfaces. Thus, more oil is detached. (Sheng, 2014; Dang et al. 2015)

Several studies have shown that kaolinite is wetted by crude oil (Sincock and Black 1988; Sutanto et al. 1990; Fassi-Fihri et al. 1995; Rueslåtten et al. 1994; Jerauld and Rathmell 1997).

The components of crude oil are thought to be ionically adsorbed, particularly to clays because they have a large surface area. Then, with increasing kaolinite content, oil recovery increases. (Jerauld et al, 2008)

Jerauld et al. (2008) shows a strong correlation between incremental oil recovery and kaolinite content. They address the impact of different kaolinite contents by assigning different relative permeability curves to each one. The behavior of the relative permeability curves with increasing clay content is showed in Figure 4.

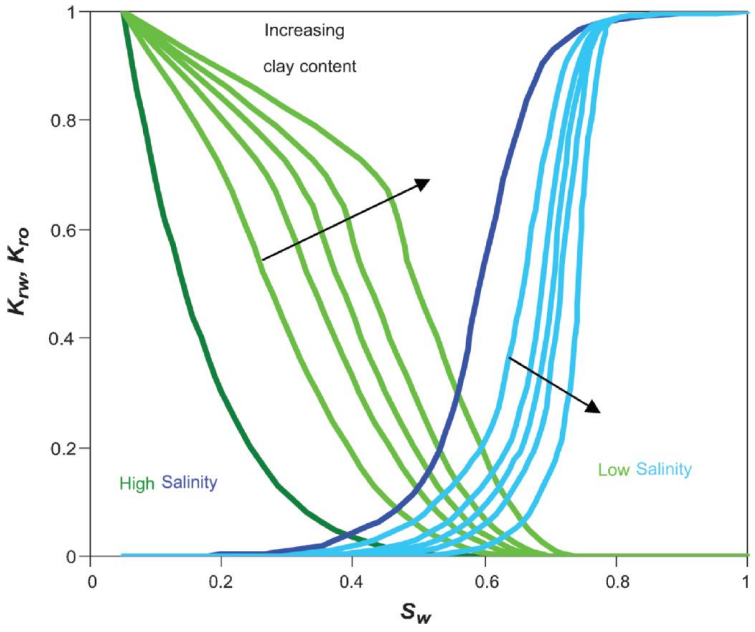


*Figure 4: Relative permeability curves with increasing clay content. Source: Adapted from Jerauld et al. (2008).*

Regarding the mechanisms promoting the improvement in oil recovery through low salinity, fine migration can contribute to the benefits of LSWI in some cases, but it is not the principal mechanism, because fine migration occurs if the ionic strength of the injected brine is less than the critical flocculation concentration. The critical flocculation concentration is strongly dependent on the relative concentration of divalent cations. (Dang et al, 2015)

In tests realized by Dang et al. (2015) from ten geological realizations with same clay distributions but with difference on their clay contents, the recovery factors tend to increase with an increase in clay contents, as shown in Figure 5. From this point of view, a preferred sandstone reservoir must contain enough clay in order to be considered for LSWI implementation.

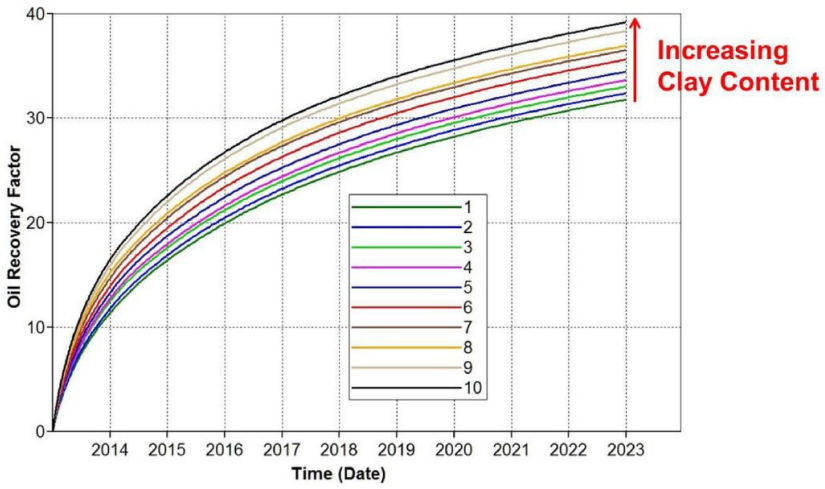


*Figure 5: Effect of clay content on LSWI recovery factor. Source: Dang et al (2015).*

Despite the results that suggest fine mobilization as the main mechanism, Lager et al. (2006) performed several core floods where the oil recovery was improved, and no fines migration or permeability reduction were observed. The results achieved by Al-Qattan et al. (2018) indicated no signs of clay swelling, or fines migration as indicated by the slightly decreasing pressure drop over the course of low salinity injection. However, the residual oil saturation was decreased about 3% with LSWI, through laboratory and by conducting a series of Single-Well Chemical Tracer Test (SWCTT) in Wara sandstone reservoir (Al-Qattan et al. 2018).

**2.2.3 pH increase.** A rise in pH has been observed when low-salinity processes are carried out. This pH increase could be explained by carbonate dissolution and/or cation exchange. However, Lager et al. (2006) argument that carbonate dissolution is relatively slow and depends on the amount of carbonate material present in the rock. If $CO_2$ is present in the reservoir, it will act as a pH buffer, then the change in pH to achieve an alkaline-like flooding is not enough. In several studies, while conducting low-salinity experiments the pH in the effluent current was increased. Therefore, it was suggested in LSWI, an alkaline-like flood was achieved, by generating of in-situ surfactants, changes in wettability and reduction in IFT. (Dang et al, 2015).

Nevertheless, LSWI achieved good results even with an initially low pH condition of about 6, with an increase until only 7.5 (Rivet 2009). Since the pH from tests carried out by Dang et al. (2018) was lower than what is required to achieve saponification and emulsification, the alkaline-like flooding pH mechanism may not work in LSWI. Nevertheless, these important chemical reactions must be carefully considered on modeling of the LSWI process as they could affect the ion exchange and wettability alteration. (Dang et al. 2018)

**2.2.4 Salting-in effect.** RezaeiDoust et al. (2009) presents the idea of a "salting-in" effect in which a decrease in salinity can increase the solubility of organic materials in the aqueous phase, resulting in an additional oil recovery. However, this simple explanation cannot explain the dependence of clay, mineral composition, and pH increase in LSW. (Dang et al. 2015)

## 2.3 Screening of LSWI

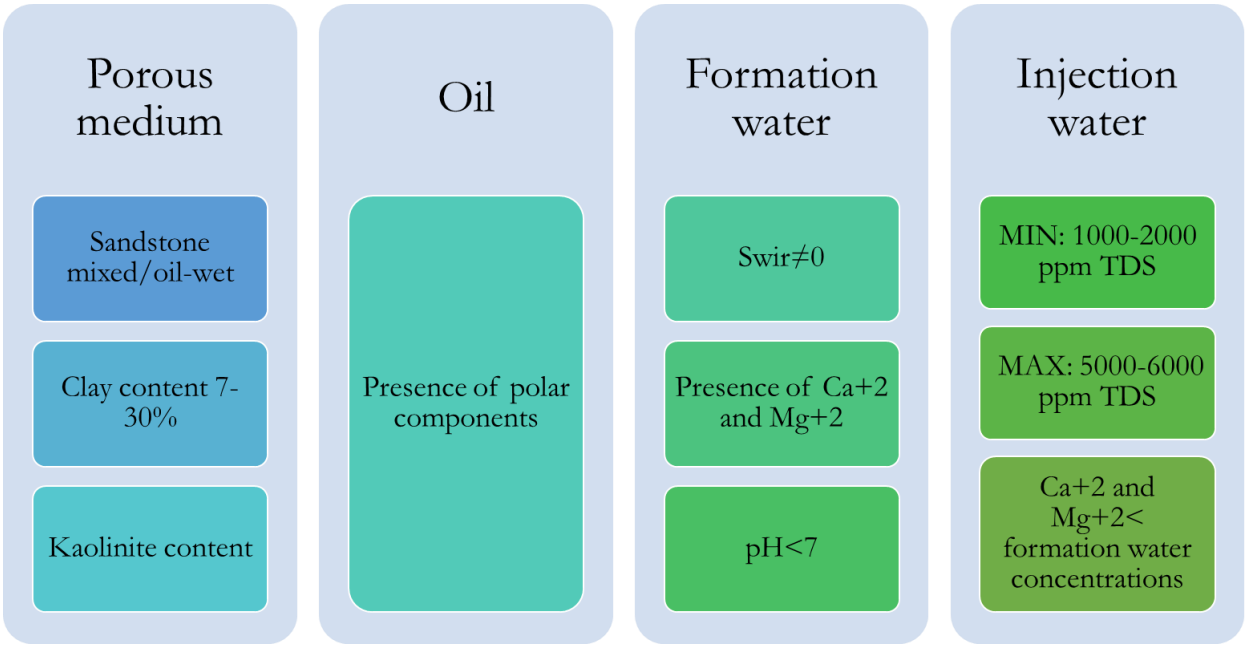


*Figure 6: Screening of Low salinity water injection EOR processes.*

As shown in Figure 6, the consensus in the industry about the screening for LSWI processes is the presence of clay content and initial oil-wet like condition. The composition of formation water is found an important factor for LSWI screening because, as noted from various corefloodings, LSWI has no effect when divalent ions such as calcium or magnesium do not exist in the formation water. Thus, reservoirs that contain calcite or magnesite minerals could be suitable candidates for LSWI, since these minerals are the source of calcium and magnesium for ion exchange and wettability alteration.

LSWI application is unlimited by reservoir depth and temperature, like chemical EOR processes. LSWI and hybrid LSWI have been successfully applied for both light oil and heavy oil reservoirs (Dang et al, 2015).

Also, the evaluation of LSWI should be considered with surface facilities. The candidate field should be implementing waterflooding or should be a candidate for it, with good sweep efficiency, because LSWI improves mainly the microscopic sweep efficiency (Sorop et al, 2013).

## 2.4 Laboratory Experiments

The most discussed and earliest laboratory experiments were performed by Tang & Morrow (1999). These core waterfloods were tested using Berea sandstone, observing the effect of mobile fine particles in the oil recovery with LSW. They established the following conditions necessary for increase in oil recovery with decrease in salinity: Adsorption from crude oil, the presence of potentially mobile fines and initial water saturation.

Callegaro et al. (2015) carried out laboratory tests, single-well chemical tracer tests and sector scale simulation, achieving promising results. Core flooding experiments were conducted by Zhang et al. (2007) to investigate the effect of low salinity brine on improving the oil recovery of Berea sandstone cores oil for both secondary and tertiary modes. Results were promising for the salinity level of 1500 ppm NaCl; however, the use of 8000 ppm NaCl had no effect on oil recovery, as the reduction in the brine salinity level seemed insufficient.

Al-Qattan et al. (2018) injected 700 ppm Total Disolved Solids (TDS) low salinity water in core floods, recovering 11.3% of the waterflood residual oil. Together with HPAM polymer flooding, LSWI recovered 12.4% of the waterflood residual oil saturation. Also, the results indicated no signs of clay swelling, or fines migration as indicated by the slightly decreasing pressure drop over the course of low salinity injection.

## 2.5 Field Experience

Several projects have been developed around the world, either single-well, pilot or sector model scales. The first field were LSWI was carried out was in the Omar and Sijan field, where for operational reasons they should decrease the salinity of the injected water achieving good results (Vledder et al. 2010, Mahani et al. 2011).

Webb et al. (2004) performed a log-inject-log field test to identify the effectiveness of LSWI within the near well region of a reservoir. This technique is based on running multiple passes of pulsed neutron capture logs after injection of two or more different brines, which have measurable differences in capture cross section. This technique aims for determining the residual oil saturation after the process, evaluating the efficiency of the process. They carried out a field LSWI trial in a clastic reservoir with high permeabilities and good porosity reaching remaining oil saturations between 30-50% higher compared to high salinity waterflood.

Al-Qattan et al. (2018) investigated the efficacy of low salinity water injection and low-salinity polymer injection by conducting a series of single-well chemical tracer test (SWCTT) in Wara sandstone reservoir. The results show a reduction in the residual oil saturation of 3% with low-salinity water injection, and a reduction in the residual oil saturation of 4% with Low-salinity polymer injection.

Other LSWI projects comprehend, an inter-well field trial in the BP-offshore Endicott field (2008-2009) in the Alaskan North Slope (Seccombe et al. 2010); River basin of Wyoming in United States (Robertson 2007, Thyne & Gamage 2011); A sector model at Clair field in the United Kingdom (Robbana et al. 2012, Mair 2010); Norwegian Continental Shelf fields (Skrettinglan et al. 2010) did not show significant reduction in oil saturation due to the high presence of plagioclase

feldspar; the giant offshore El-Morgan field in Gulf of Suez (GUPCO) with a full field deployment plan (Darhim et al. 2013).

# 3. Numerical Modeling of Low Salinity Water Injection

This chapter discusses the numerical investigation of low salinity water injection (LSWI) performed in this thesis. Most numerical investigation performed employs state-of-the-art reservoir simulators, ECLIPSE and INTERSECT from Schlumberger, which allow the simulation of chemical Enhanced Oil Recovery, as well as, modeling the brine speciation.

In the following, this chapter introduces the base model setup, various aspects of modeling: facies modeling, petrophysical modeling, fluid and rock-physics modeling, and the development strategy.

## 3.1 Model setup

In the models investigated throughout this thesis, the reservoir architecture consists of three producing zones with a baffle between the top two zones. Models use Cartesian grid with a total of 117,304 grid cells, composed of 44 × 43 × 62 cells in X, Y and Z directions, respectively (Figure 7). The study area is about 440m × 430m, with the total reservoir thickness 30.50m. The lateral dimension of the grid cells is 10m, while the average thickness is 0.48m. The criteria for the grid cell width selection was based on the kind of EOR process to simulate.

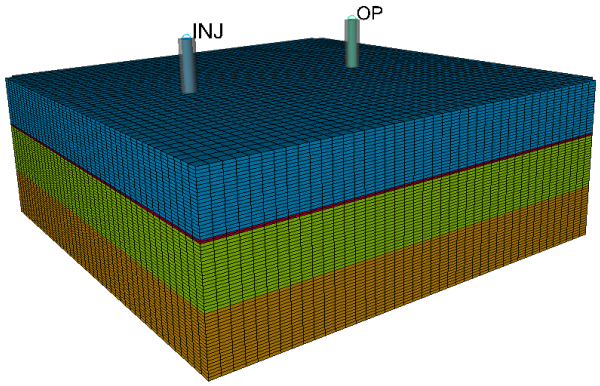


*Figure 7: 3D model structure showing the four zones.*

The depth of the top layer is 2600m. There is an aquifer in the bottom of the model.

The injector well is completed in the lower zone, between 2612 m and 2630 m. The producer well is completed in the upper zone between 2600 m and 2618 m. Figure 8 shows the well completions.

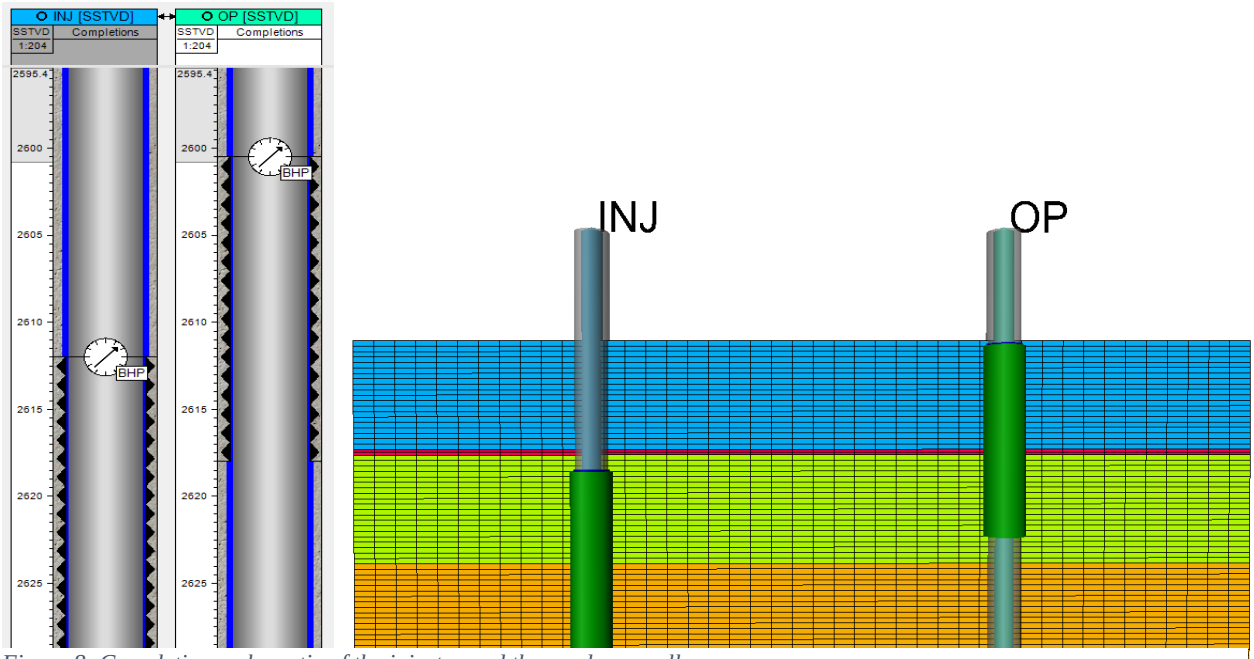


*Figure 8: Completions schematic of the injector and the producer wells.*

## 3.2 Facies Modeling

The facies model is composed by four different rock-types: Coarse sand, sand, fine sand and shale, as shown in Figure 9. From top to bottom, the first zone has the following facies distribution:

Sand (35%), fine sand (25%), coarse sand (10%) and shale (30%). The second zone acts like a seal, composed mainly with fine sand (15%) and shale (85%). The third zone was modeled with fluvial channels (30%), composed by sand and coarse sand, adaptive channels (20%), composed by sand and fine sand and aeolian sand dune (20%), composed by fine sand. The fourth and final zone has the same composition than the first zone, with different distribution of the rock-types. Table 1 shows the final facies distribution in each zone.

Table 1.

*Facies percentage for each zone.*

| Zone | Facies | (%) |
|---|---|---|
| 1 | Coarse Sand | 11.8 |
| | Sand | 30.5 |
| | Fine Sand | 25.6 |
| | Shale | 32 |
| 2 | Fine Sand | 12.9 |
| | Shale | 87.1 |
| 3 | Coarse Sand | 23.4 |
| | Sand | 26.6 |
| | Fine Sand | 19 |
| | Shale | 31 |
| 4 | Coarse Sand | 31.3 |
| | Sand | 24.2 |
| | Fine Sand | 11.8 |
| | Shale | 32.8 |

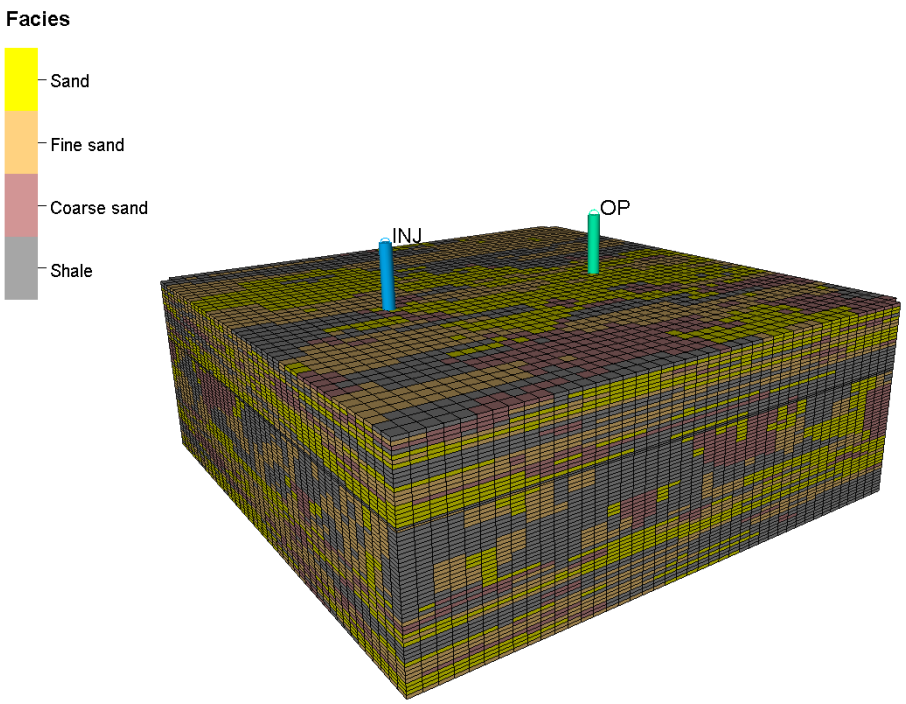


*Figure 9: Facies distribution of the base model.*

## 3.3 Petrophysical Modeling

**3.3.1 Porosity.** The distribution of porosity is constructed using Sequential Gaussian Simulation for each zone. Resulting porosity distribution follows a normal distribution with the parameters stated in Table 2. Figure 10 illustrates the average porosity maps for the top, baffle, third and bottom zones.

Table 2.

*Parameters for the porosity distribution of the base model.*

| Zone | Facies | Porosity Range (%) | | | Avg. Porosity (%) |
|---|---|---|---|---|---|
| 1 | Coarse Sand | 10 | - | 30 | 19 |
| | Sand | 8 | - | 25 | 17 |
| | Fine Sand | 5 | - | 21 | 13 |
| | Shale | 0.5 | - | 9 | 5 |
| 2 | Fine Sand | 5 | - | 15 | 9 |
| | Shale | 0.5 | - | 9 | 5 |
| 3 | Coarse Sand | 9 | - | 29 | 21 |
| | Sand | 8 | - | 25 | 19 |

| | | | | | |
|---|---|---|---|---|---|
| | Fine Sand | 5 | - | 18 | 10 |
| | Shale | 0.5 | - | 9 | 5 |
| 4 | Coarse Sand | 9 | - | 25 | 18 |
| | Sand | 7 | - | 22 | 15 |
| | Fine Sand | 5 | - | 20 | 12 |
| | Shale | 0.5 | - | 8 | 4.5 |

The top zone has an average porosity of 12.3%. The baffle zone has low porosity, with a mean of 6.4%. This is due to the facies present in the baffle zone. The third zone has an average porosity of 12.6% and the bottom zone has a mean porosity of 11.02%. Figure 11 shows the histogram of porosity for the base model.

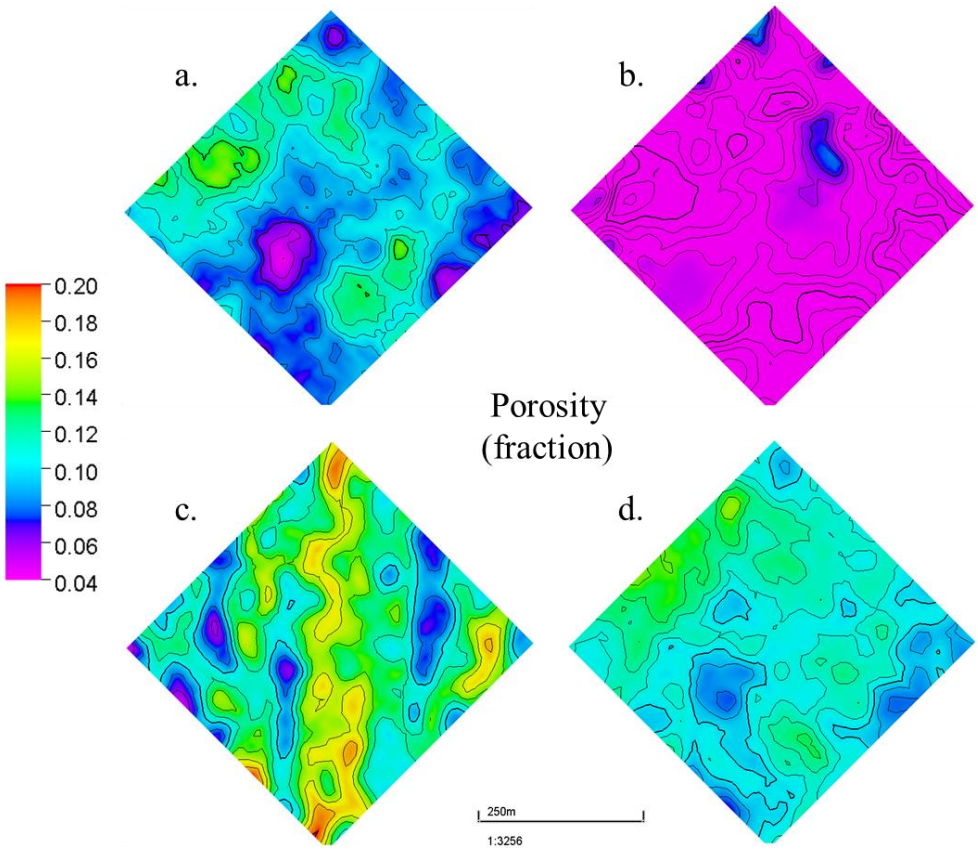


*Figure 10: Areal view of average porosity for the top (a), baffle (b), third (c) and bottom (d) zones for the base model.*

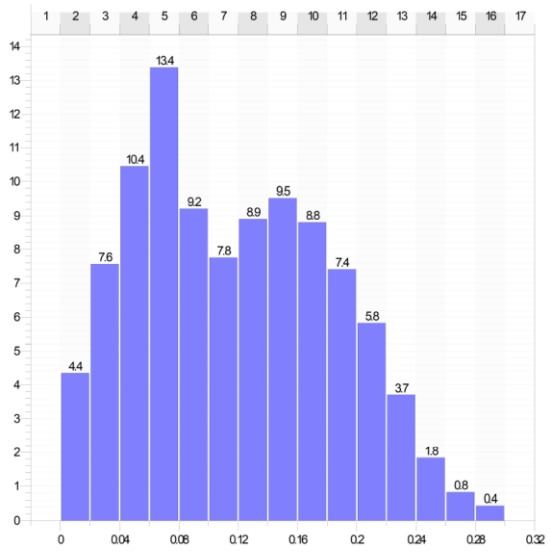


*Figure 11: Histogram of porosity for the base model.*

**3.3.2 Permeability.** The permeability model is constructed using Sequential Gaussian Simulation with collocated co-kriging with porosity as the secondary variable. Resulting permeability distribution follows log-normal distributions with the parameters stated in Table 3. Figure 12 illustrates the average permeability maps for the top, baffle, third and bottom zones.

Table 3.

*Parameters for permeability distribution of the base model.*

| Zone | Permeability (mD) | | | Avg. Perm (mD) |
|---|---|---|---|---|
| 1 | 0.1 | - | 1000 | 19.4 |
| 2 | 0.05 | - | 1 | 0.2 |
| 3 | 0.1 | - | 1000 | 19.4 |
| 4 | 0.1 | - | 1000 | 19.4 |

The distribution of permeability in the top (first), third and bottom (fourth) zone has values between 0.1 to 1000 mD, with an average of 19.4 mD. The baffle has low permeability values, ranging between 0.05 to 1 mD, with an average 0.2 mD. This baffle captures realistic vertical communication in a reservoir.

Lateral permeability is isotropic. However, vertical permeability anisotropy, kv/kh, is 0.1. In other words, vertical permeability is 10% of the permeability in the horizontal direction, to assure a realistic vertical flow behavior.

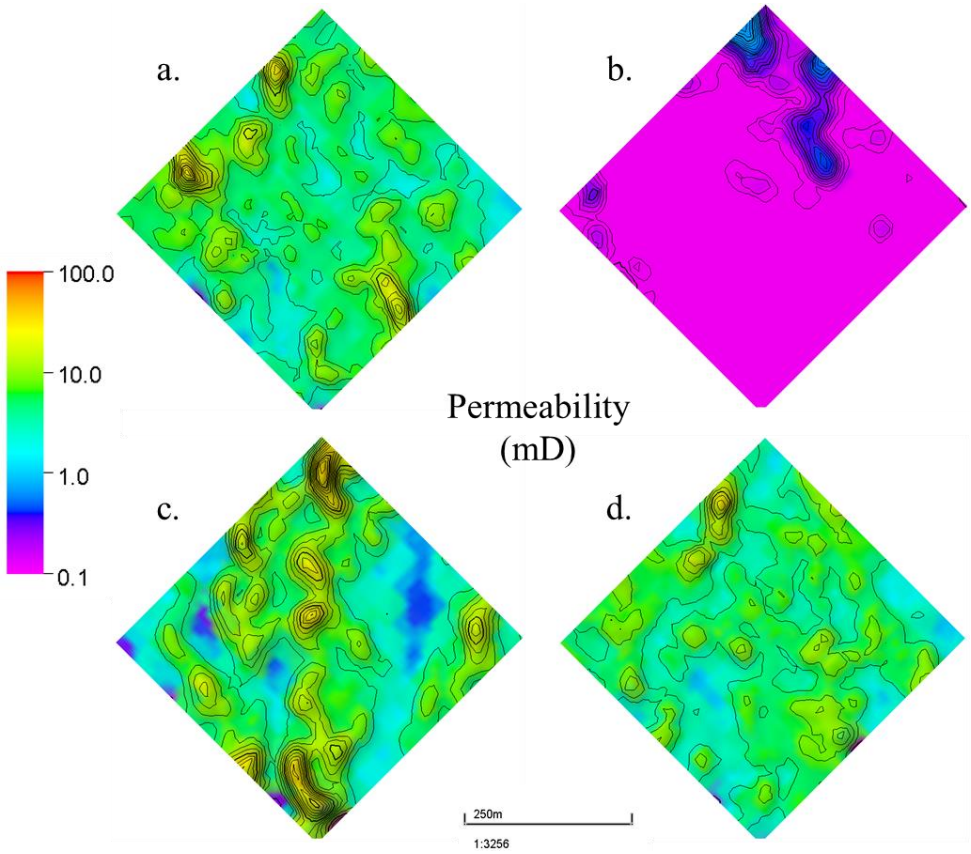


*Figure 12: Areal view of average permeability (mD) for the top (a), baffle (b), third (c) and bottom (d) zones for the base model.*

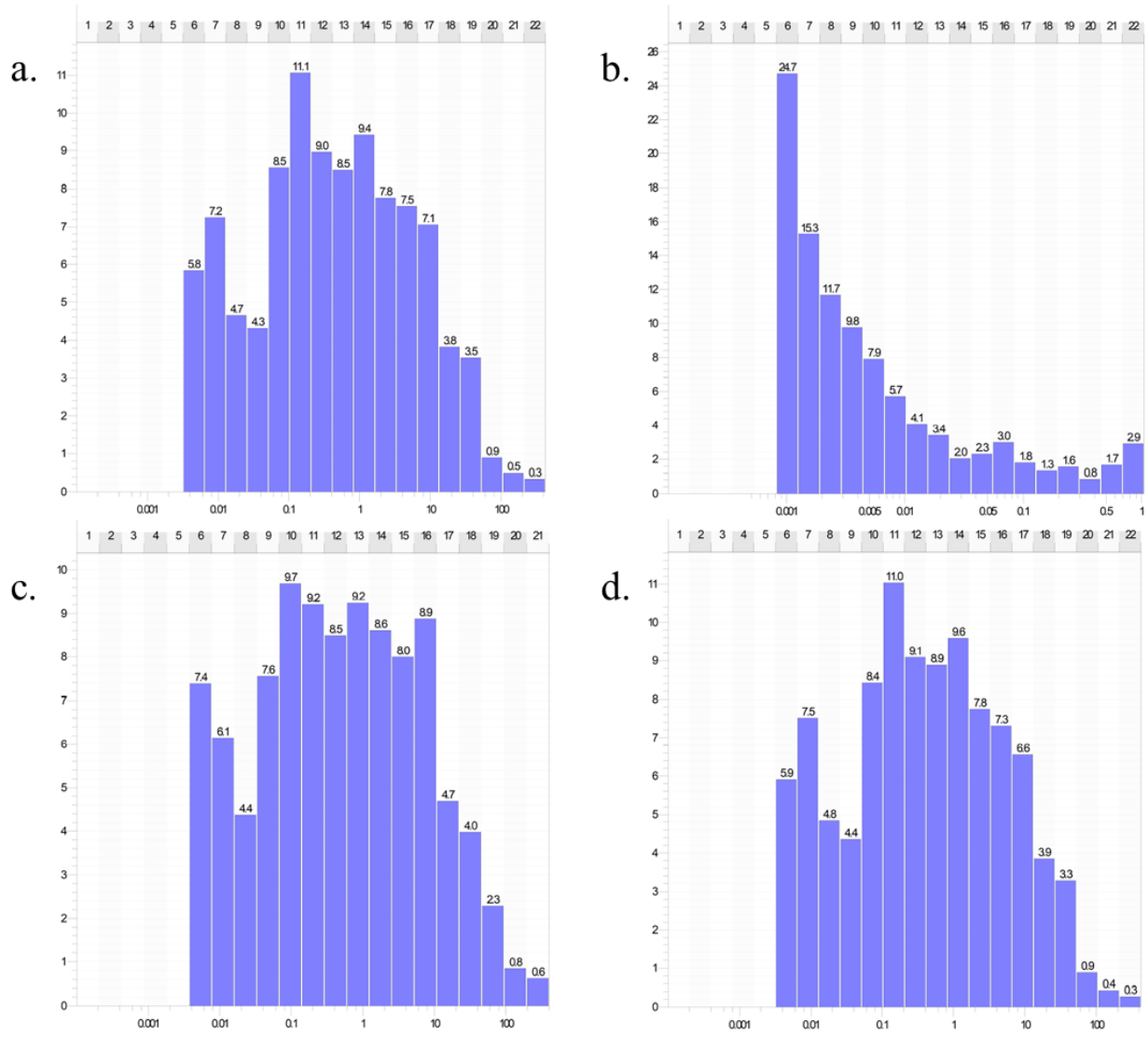


*Figure 13: Histogram of permeability in X direction for each zone corresponding to the top (a), baffle (b), third (c) and bottom (d) zones for the base case.*

## 3.4 Fluid Modeling

Throughout all the investigation, two different fluid models were used: Low API and High API. This was done with the aim to investigate what is the impact of LSWI in each one of these fluids.

In the design of experiments, that will be explained in following chapters, when changing the fluid API it can either produce gas or not. This represents a problem in the moment of setting

up the base case, because initial conditions like the solution gas oil ratio should not be specified in the low API case, however, in the high API case it is required. Also, some endpoints for saturation functions are required just for the high API case. In this order of ideas, setting up just one fluid API does not allow to model properly the design of experiments, as well as, limit the extend of the uncertainty, giving a narrow approach. Therefore, the whole study will be done for two different fluid models: the low and high API. This will give us a wider insight of the evaluation of LSWI. The temperature was set 76 ºC assuming an temperature gradient of 0.018 ºC/m (1 ºF/100 ft), and also compared by the literature review for Low salinity EOR projects.

The light oil crude has 40 ºAPI and the bubble point pressure is 160 bar. The gas density used has an specific gravity of 0.7; The black oil crude has 26 ºAPI and the bubble point pressure is 30 bar. The gas density has an specific gravity of 0.7.

PVT tables for water were created from Massachusetts Institute of Technology (MIT) data about thermodinamical properties of the water with salinity concentration variations. This data was used to interpolate the values of compressibility (Cw), water formation volumetric factor (Bw) and viscosity ($\mu_w$). Salt concentration values range from 0.0 ppm to 120,000 ppm.

In the thermodinamical properties of the water was not data for formation volumetric factor (Bw) directly correlated with salt concentration. Then, the formation volumetric factor was inferred from the definition of compressibility:

$$C = -\frac{1}{V}\frac{dV}{dP} \quad (1)$$

and,

(2)

$$B_w = \frac{V_r}{V_{sc}}$$

The derivative of the  (2 gives,

$$\frac{dB}{dP} = \frac{1}{V_{sc}}\frac{dV_r}{dP} - \frac{V_r}{{V_{sc}}^2}\frac{dV_{sc}}{dP} \quad (3)$$

The second term of the right side of the Equation 3 can be neglected, because the change in volume of  at surface conditions is almost zero. Thus, the derivative of the Equation 2, is approximately,

$$\frac{dB}{dP} = \frac{V_r}{V_{sc} * V_r}\frac{dV_r}{dP} \quad (4)$$

Relating Equation 1 and Equation 4, it can be get an expression of compressibility in terms of formation volumetric factor, thus:

$$C = -\frac{1}{B}\frac{dB}{dP} \quad (5)$$

Solving the Equation 5, can be get the next expression:

$$B_2 = B_1 * e^{-C\,(P_2 - P_1)} \quad (6)$$

Given the pressure (P=1 bar) for the compressibility tables with increasing salinity, the formation volumetric factor $B_1$ is equal to 1. Therefore, using $P_2$ as the reference pressure for the PVTWSALT table, the Equation 6 is reduced to,

$$B_2 = e^{-C\,(P_{ref} - 1)} \quad (7)$$

For ECLIPSE, the PVTWSALT table supplies the water PVT data in which the brine option is active. The table consists in 5 columns of data: the first column is the salt concentration. Its values should increase monotonically down the column. The second column is the water formation volume factor. For this column, ECLIPSE remarks that values should be level or decreasing down the column. The third is the water compressibility as a function of salt concentration. The fourth is the water viscosity as a function of salt concentration. The last column is the water viscosibility as function of salt concentration. The water viscosibility is set to zero, assuming that the derivative of the viscosity with respect to pressure is neglected.

Analyzing the data from MIT (Figure 14) and the correlation between compressibility and formation volume factor (Equation 7) it can be concluded that water formation volume factor should increase with increasing salt concentration, as shown in Figure 15. In other words, with increasing salt concentration, the water compressibility decreases. Then, with decreasing the water compressibility, the water formation volume factor increases. Therefore, the remark done for the second column by ECLIPSE was omitted.

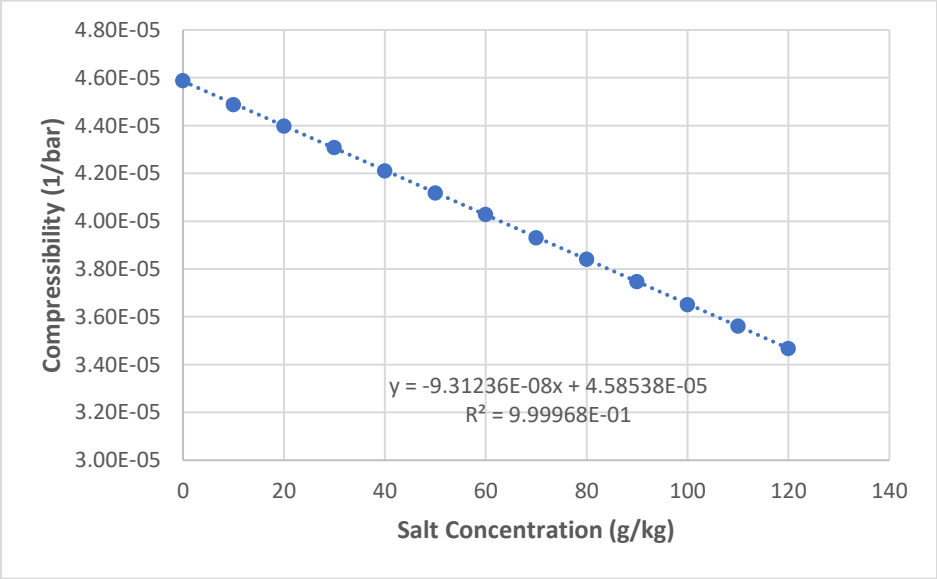


*Figure 14: Isothermal compressibility of water vs salt concentration.*

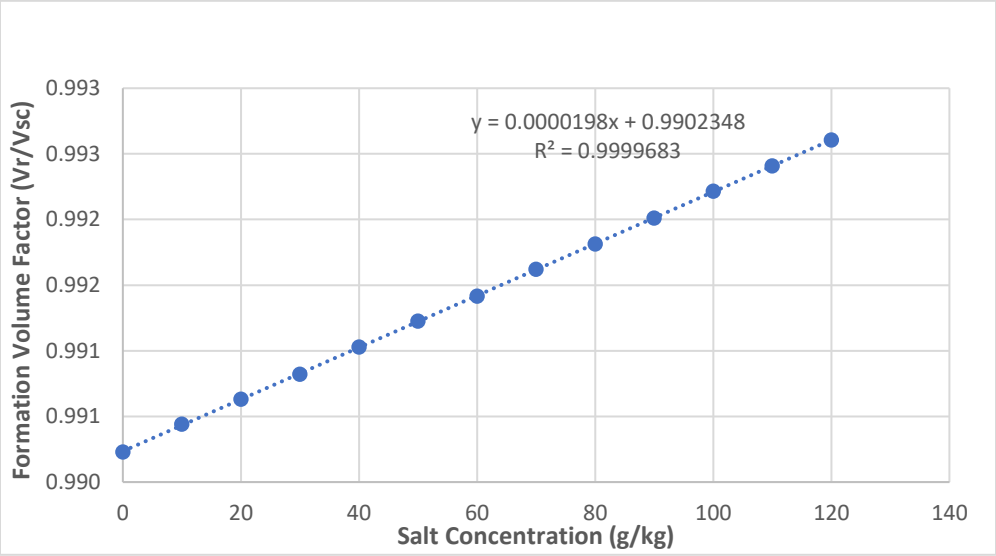


*Figure 15: Formation volume factor vs. salt concentration.*

The equation for viscosibility is:

$$C_v = \frac{1}{\mu}\frac{d\mu}{dP} \cong 0 \quad (8)$$

Solving the Equation 8, it can be inferred that the viscosity at $P_1$ is equal to the viscosity at $P_2$, as follow:

$$\mu \,@\, P_1 = \mu \,@\, P_2 \quad (9)$$

With this approach, the viscosity data from MIT was used directly, and the values are summarized in the Figure 16.

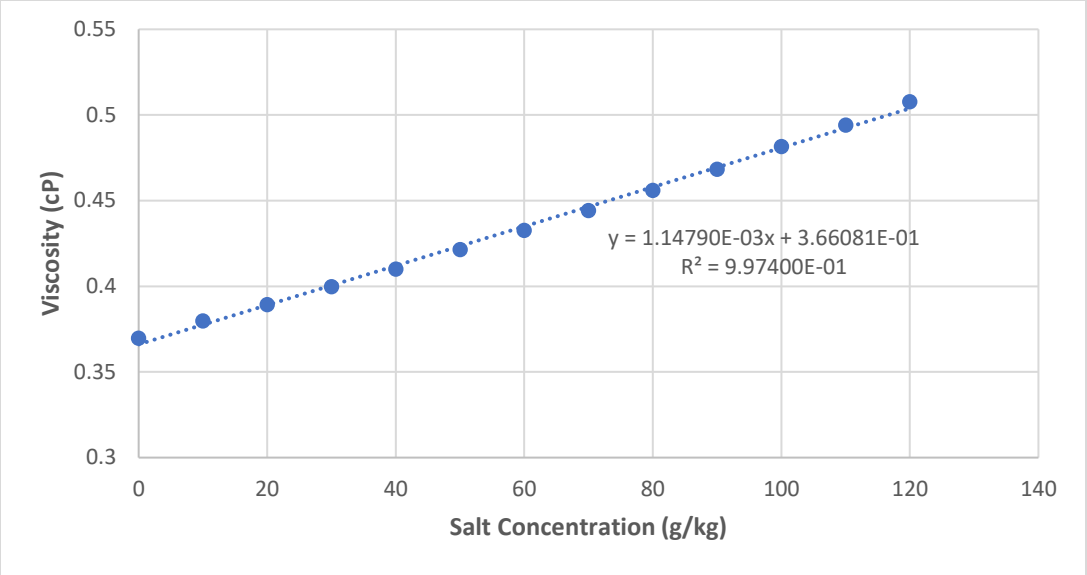


*Figure 16: Viscosity vs. salt concentration.*

### 3.5 Rock-Physics Modeling

The main effect of LSWI is a shifting of the wettability of the system to a more water-wet state, which improves the oil recovery. There were created two different sets of relative permeability functions. The first set is for high salinity and the second set is for low salinity. The simulator calculates the saturation function interpolating between the high and low salinity functions depending on the salt concentration. For this interpolation the salinity weithing factors are used. The salinity weighting factors table provides the weighting factors for relative permeability and capillary pressure with salinity increase. In ECLIPSE this table is referred to as LSFNC within the Props section, while in INTERSECT is called LowSaltWeightingTable within the Rock node.

The values assigned to the saturation functions for the base case were got in the literature from different data from laboratory and simulations (Jerauld et al, 2008; Callegaro et al, 2015). Values chosen comply with the screening criteria of an oil-wet reservoir. Nonetheless, in the

uncertainty and characterization (Chapter 3) the endpoints are shifted to other values to find out the effect in the oil and gas recovery. In Figure 17 is plotted the relative permeability curves for the high and low salinity. The blue set of curves is for high-salinity, which is characterized for an oil wettability. The red set of curves is for low-salinity, which has a shifting to a more water-wet behavior.

When the curves change toward a more water-wet behavior, the oil relative permeability to water at critical water saturation turns higher, the water relative permeability at residual oil saturation shifts lower, the critical water saturation increases, as well as the residual oil saturation gets lower. The oil relative permeability to gas does not affects the simulation because the low salinity weighting factors just affect the oil-water saturation functions. For gas, the high salinity gas-oil relative permeability curves are used.

It should be noted that the intersection between each set of curves usually reflects the wettability of the system. A water saturation of 0.5 is the cutoff value. Below 0.5, the system is more oil-wet. Increasing water saturation above 0.5 it turns more water-wet. Around 0.5, it is known as an intermediate wettability. However, reservoirs are heterogeneus and there are several parameters that affect the wettability of a system.

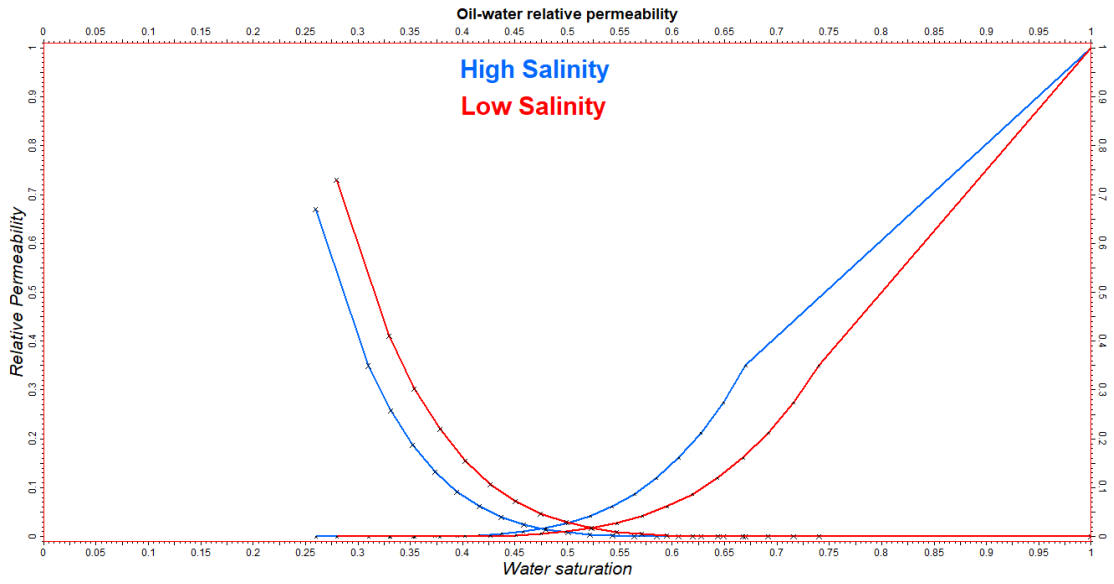


*Figure 17: Relative permeability curves for high and low salinity.*

The imbibition capillary pressure curves shown in Figure 18 are for high salinity (blue curve) and low salinity (red curve). It should be noted that decreasing the salt concentration of the injecting water, increases the capillary pressure.

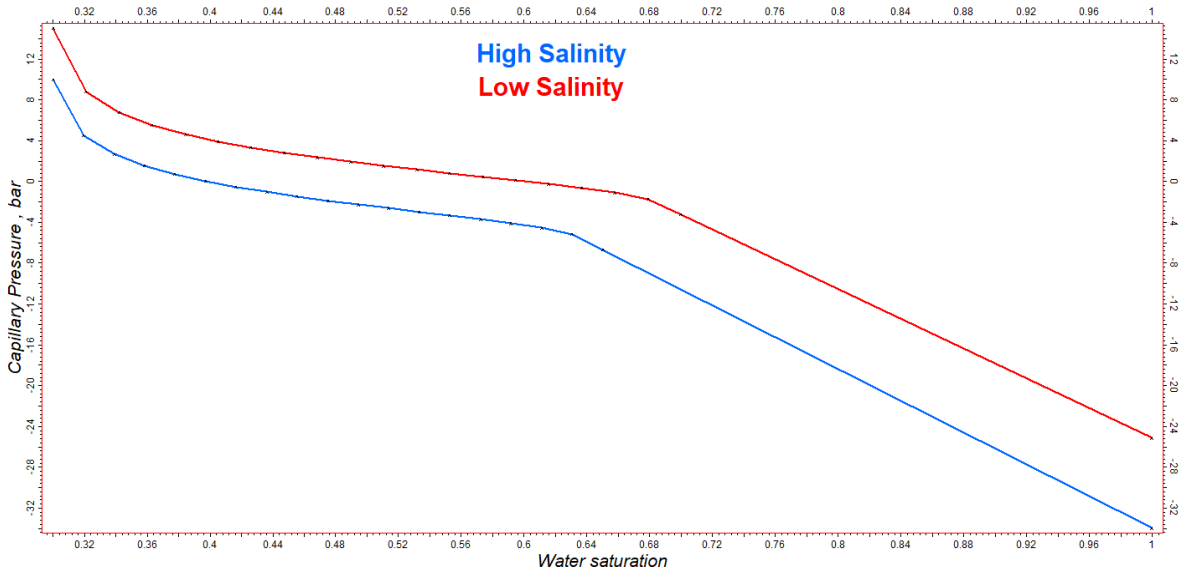


*Figure 18: Capillary pressure curves for high and low salinity.*

### 3.6 Development Strategy

In the base case, the constraints for the producer are a bottom hole pressure of 10 bar with a reservoir volume rate of 500 m^3/d. For the injector, the reservoir rate is 100 m^3/d and a bottom hole pressure of 410 bar. The bottom hole pressure for the injector was calculated below the fracture gradient. The fracture gradient was assumed to be 0.85 psi/ft.

The brine injected is related to the water phase. Although in the literature brine concentration in the range of 1000 ppm to 8000 ppm shows an increase in the recovery factor, in this study brine concentration is varied from 1,000 ppm to 20,000 ppm to research the effect of saturation functions and from 2,000 ppm to about 80,000 ppm to research the effect of brine speciation. This ranges are expanded with the aim to ascertain the impact of different brine concentrations. The brine concentration is specified as WSALT in ECLIPSE and as the FluidSourceExternal node in INTERSECT within the field management strategy. For INTERSECT the composition of each specie should be specified. It is important to note that in ECLIPSE 100, to simulate LSWI processes it is allowed with the single brine model option. While INTERSECT allows the multi-brine speciation and has a wider speciation than ECLIPSE.

The evaluation period for this study starts on January 2020 and finish until December 2030, encompassing a total of 10 years, starting the injection and the production since the first day.

## 4. Effect of saturation functions

Rock-physics saturation functions are the mean of modeling Low Salinity Water Injection (LSWI) effect. This is due to the change in wettability toward a more water wet system. Scaling

factors represent the change from a high saline water to the low salinity water. In this chapter it is evaluated the effect of the rock-physics saturation functions on LSWI performance. First, the scaling function for LSWI are evaluated to find out the capillary pressure and relative permeability effect. Second, the endpoints of the saturation functions are assessed to determine the most impactful endpoints. Finally, rock-physics saturation functions are assigned to different facies to determine the effect on the LSWI performance.

## 4.1 Low Salinity Function Scaling

The low salinity function scaling (LSFNC) provides the weighting factors for the interpolation between the high and low salinity function. This weighting factors are directly related to the injected salt concentration. This function scaling is used for both relative permeability and capillary pressure curves. This scaling allows to model whether a process is trending to the low or high salinity curves.

In ECLIPSE, LSWI simulation is activated with LOWSALT. Then, the LSFNC keyword should be included with the scaling factors. Basically, this keyword is set to input the weighting factors for the low-salinity saturation functions as a function of the salt concentration. These coefficients are used in calculating the saturation endpoints, the water and oil relative permeabilities and the water-oil capillary pressure. (ECLIPSE Reference Manual, 2018)

Each table consists of the following columns of data: 1. Salt concentration. These values decrease monotonically. 2. Weighting factor F1 for the low-salinity saturation endpoints and the relative permeabilities interpolation. These values range between 0 to 1, decreasing. 3. Weighting factor F2 for the low-salinity capillary pressure interpolation. These values range between 0 and 1 and decrease monotonically. The values used for the base case are specified in Table 4:

Table 4.

*LSFNC for the base case.*

| LSALTFNC | | |
|---|---|---|
| 0.01 | 0.65 | 0.65 |
| 3 | 0.45 | 0.45 |
| 30 | 0.25 | 0.25 |

**4.1.1 Design of Experiments.** Three uncertainty and characterization assessments will be performed. First, for relative permeability weighting factor F1; Second, for capillary pressure weighting factor F2; Third, for both weighting factors together. Besides, the salt concentration values of the scaling function will be part of the DoE. The variables SCL, SCM and SCH correspond to the salt concentration low, intermediate and high respectively, as shown in Table 5. The values used for these variables are shown in Table 6. The scaling function was designed to evaluate the relative permeability and the capillary pressure weighting factors separately and together, using the values specified in the Table 5. These weighting factors values shown in Table 5 represent the minimum change in the saturation functions (MIN), the maximum change in the saturation functions (MAX) and somewhere in the MIN-MAX interval (BASE).

Table 5.

*LSFNC for the uncertainty, using relative permeability and capillary pressure separately and together.*

| | MIN | | | BASE | | | MAX | | |
|---|---|---|---|---|---|---|---|---|---|
| RELATIVE PERMEABILITY | LSALTFNC | | | LSALTFNC | | | LSALTFNC | | |
| | SCL | 0.3 | 1 | SCL | 0.65 | 1 | SCL | 1 | 1 |
| | SCM | 0.1 | 1 | SCM | 0.45 | 1 | SCM | 0.8 | 1 |
| | SCH | 0.01 | 1 | SCH | 0.25 | 1 | SCH | 0.5 | 1 |
| CAPILLARY PRESSURE | LSALTFNC | | | LSALTFNC | | | LSALTFNC | | |
| | SCL | 1 | 0.3 | | 1 | 0.65 | SCL | 1 | 1 |
| | SCM | 1 | 0.1 | | 1 | 0.45 | SCM | 1 | 0.8 |
| | SCH | 1 | 0.01 | | 1 | 0.25 | SCH | 1 | 0.5 |
| REL PERM & CAP PRES | LSALTFNC | | | LSALTFNC | | | LSALTFNC | | |
| | SCL | 0.3 | 0.3 | SCL | 0.65 | 0.65 | SCL | 1 | 1 |
| | SCM | 0.1 | 0.1 | SCM | 0.45 | 0.45 | SCM | 0.8 | 0.8 |

| | | | | | | | | | |
|---|---|---|---|---|---|---|---|---|---|
| | SCH | 0.01 | 0.01 | SCH | 0.25 | 0.25 | SCH | 0.5 | 0.5 |

These uncertainties were realized alongside the saturation function tables, i.e. three different sets of saturation functions for low and high salinity were created. Other variable included was the salt concentration of the injecting water. The uncertainty was performed separately for Low-API and High-API, because the influence of the PVT model and the presence of gas could affect the analysis of the results, which was explained in Chapter 3.4.

Two different sampling methods were used: The Plackett-Burman method, which evaluate the extreme cases, and the Latin-hypercube sampling, which evaluate different random values. The Plackett-Burman method design a matrix with the minimum and maximum values for all the variables where each combination of levels for any pair of values appears the same number of times, throughout all the experimental runs. The Latin-hypercube sampling method uses equi-probable 'bins' for random sampling. This ensure a more even distributions of values within each variable. The number of bins (for each variable) is the same as the number of samples (in each loop). Therefore, Latyn-hypercube method allows to test values within the minimum and maximum values. With these well-structured data matrices, DoE delivers accurate results even when the matrix that is analyzed is quite small.

Finally, the DoE variables for the low salinity scaling function is shown in Table 3.

Table 6.

*Uncertain variables for the DoE with endpoints.*

| Uncertain Variables | Keyword | Base Value | Range | |
|---|---|---|---|---|
| | | | Min | Max |
| Low salinity scaling function | LSFNC | 2 | 1 | 3 |
| Saturation Functions | SF | 2 | 1 | 3 |
| Salt Concentration-Injection | WSALT | 5 | 1 | 20 |

| | | | | |
|---|---|---|---|---|
| Salt conc scaling function low | SCL | 0.01 | 0 | 0.05 |
| Salt conc scaling function medium | SCM | 3 | 2 | 5 |
| Salt conc scaling function high | SCH | 30 | 20 | 40 |

**4.1.2 Results and Analysis.** The results of the DoE for the relative permeability weighting factor F1 are shown in Figure 19. The results of the DoE for the capillary pressure weighting factor F2 are shown in Figure 20. The results of the DoE for the relative permeability weighting factor F1 together with capillary pressure weighting factor F2 of the LSFNC are shown in Figure 21.

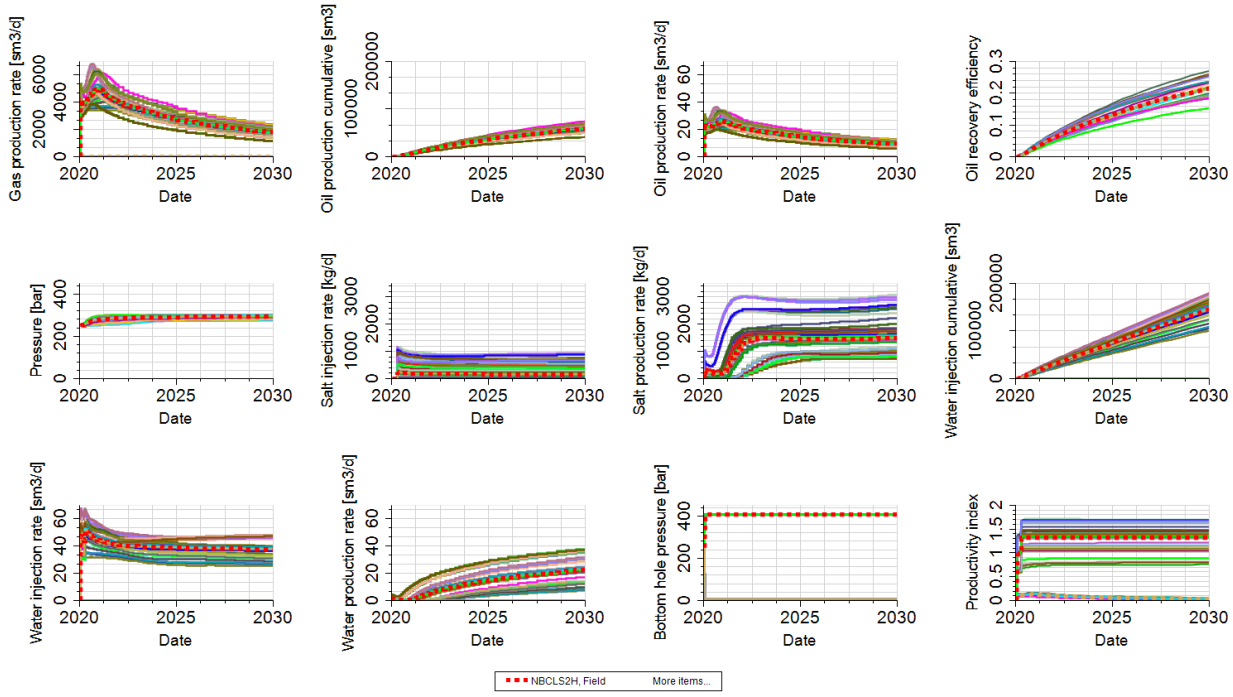


*Figure 19: Results of the DoE for the relative permeability weighting factor F1 LSFNC.*

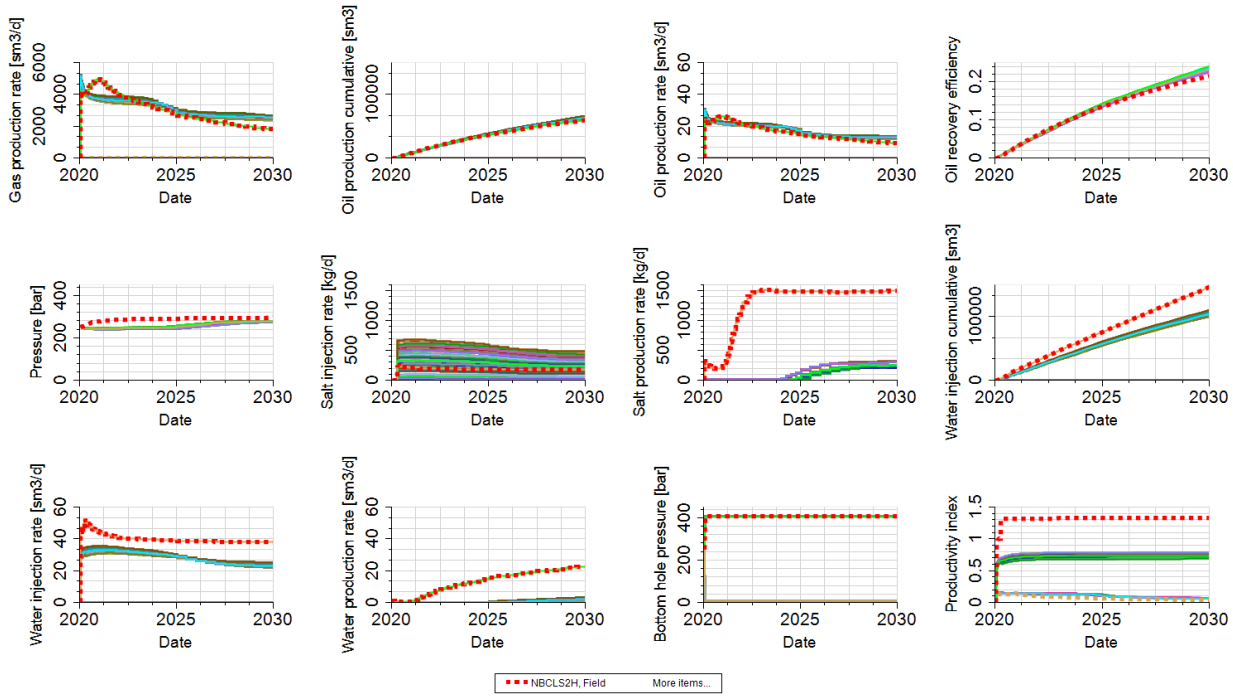


*Figure 20: Results of the DoE for the capillary pressure weighting factor F2 LSFNC.*

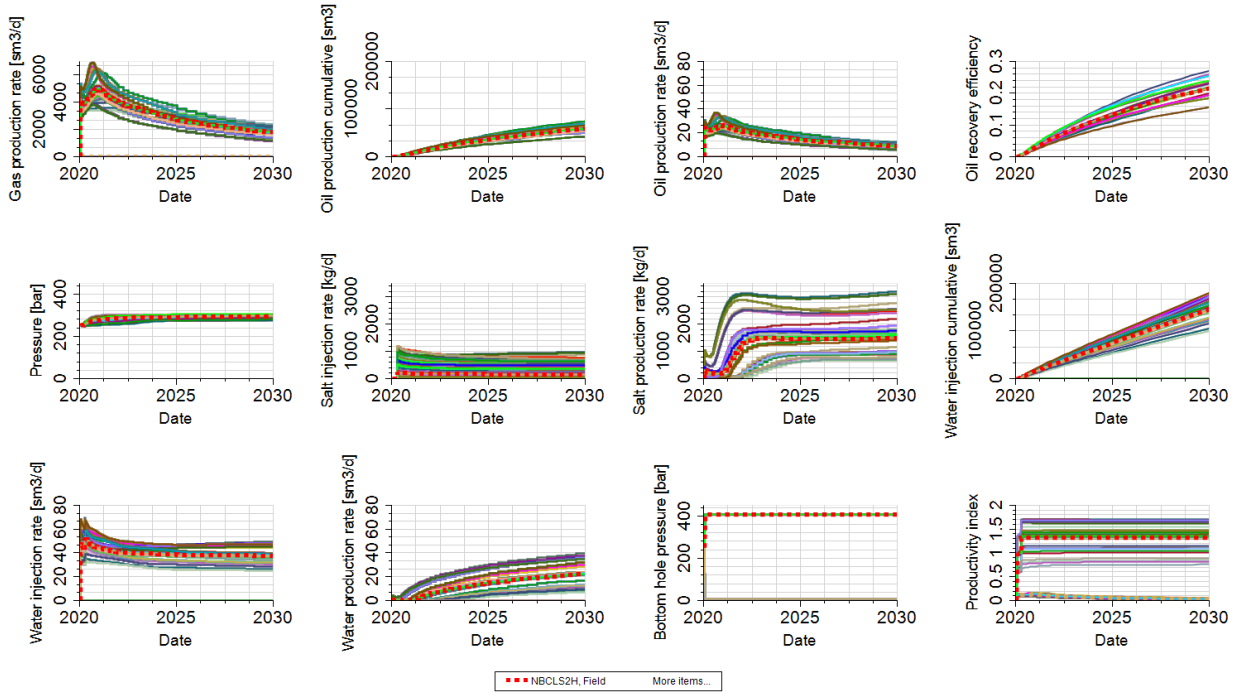


*Figure 21: Results of the DoE for the relative permeability weighting factor F1 together with capillary pressure weighting factor F2 LSFNC.*

The response variables analyzed in this thesis are cumulative oil (CUMOIL), cumulative gas (CUMGAS), cumulative water (CUMWAT), recovery factor (RF), water cut (WC), and cumulative oil, gas, water (OGW). Comparing the results of the scaling function for the design of experiments performed for high and low API it can be observed that between the relative permeability weighting factors and the capillary pressure weighting factors, the second have lesser impact in the low salinity saturation function scaling. The capillary pressure weighting factors have slightly higher impact in the cumulative oil and the recovery factor for low API, however the predominant impact is achieved with relative permeability weighting factors. Nonetheless, when analyzing the scaling function with relative permeability and capillary pressure weighting factors, the effect is larger than for the relative permeability or capillary pressure weighting factors alone, as can be observed in Figures 22 and 23.

The results of LSFNC providing relative permeability weighting factors (Figure19), are very different from the results obtained from the LSFNC providing capillary pressure weighting factors (Figure 20). Particularly, in Figure 20, it can be observed the distancing of the uncertainty cases from the base case.

Although the results for relative permeability weighting factors and the results for the relative permeability and capillary pressure together seem to be similar, in the graphs presented in Figures 22 and 23 it is shown an increase when the relative permeability and capillary pressure weighting factors are used, compared to the relative permeability weighting factors alone.

Therefore, in the next design of experiments the low salinity scaling function will be used with the relative permeability and capillary pressure weighting factors combined.

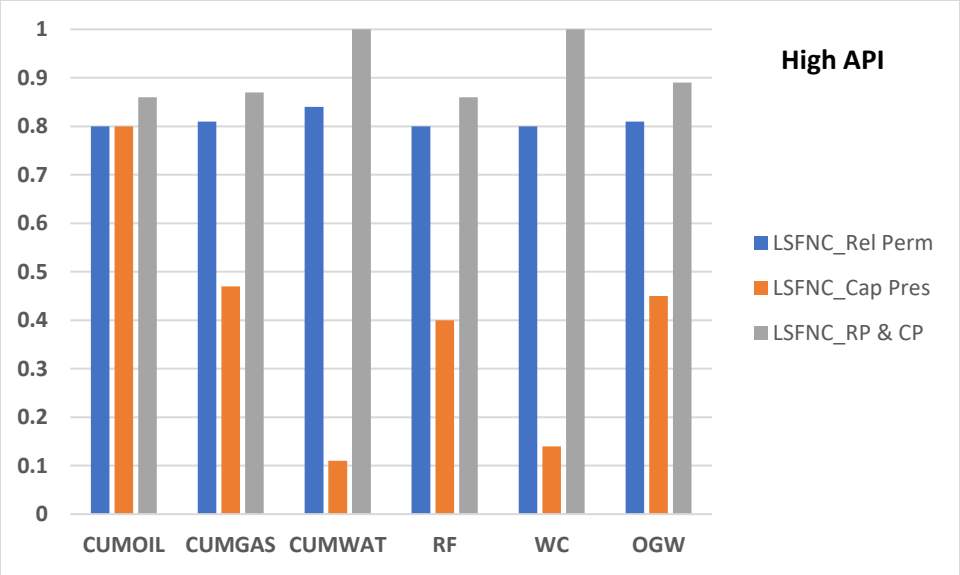


*Figure 22: Objective functions vs. Impact of LSFNC for high API.*

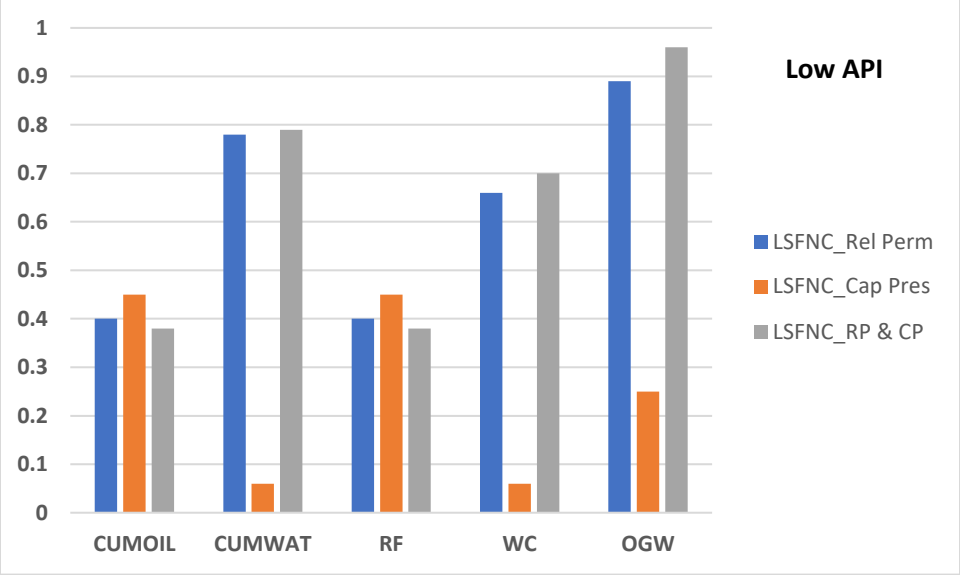


*Figure 23: Objective functions vs. Impact of LSFNC for low API.*

The saturation functions are very important in the modeling of low salinity as well as the low salinity scaling function. These variables have the larger impact within this uncertainty. The effect of other variables is low.

From Figures 24 to 27 it can be observed the single term and cross term effects of each of the variables used in the recovery factor and water cut. The recovery factor and water cut were chosen like representative of the effect of each variable on other functions. The effect on the other objective functions stated before are shown in the Appendix A.

The salt concentration for the injection water and the salt concentration for the scaling function are less impactful for low API (Figures 24 and 25) than they are for the high API (Figures 26 and 27). However, the most affecting variables in both low and high API are the saturation functions and the low salinity scaling function.

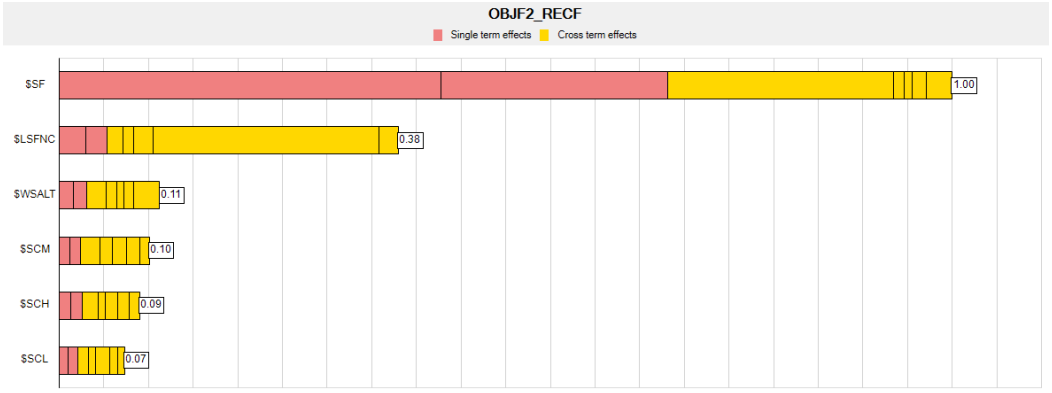


*Figure 24: Impact on recovery factor vs. variables of uncertainty. Rel perm/capillary pressure scaling - Low API – DoE.*

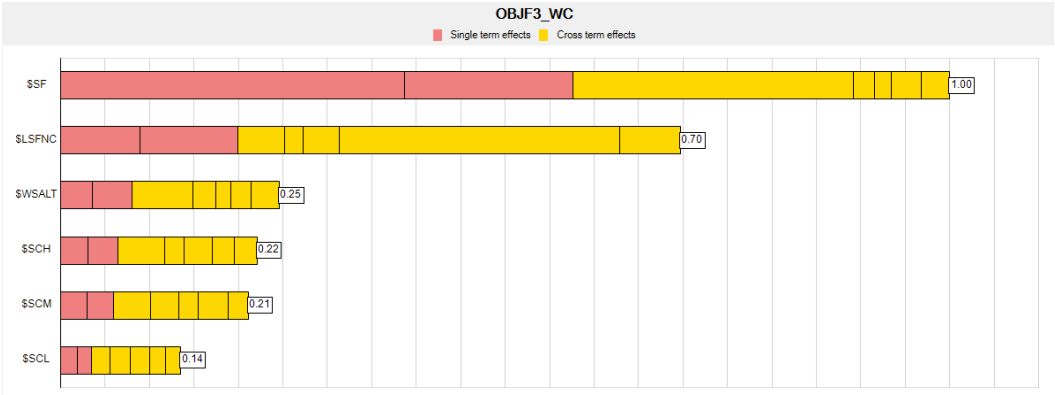


*Figure 25: Impact on water cut vs. variables of uncertainty. Rel perm/capillary pressure scaling - Low API – DoE.*

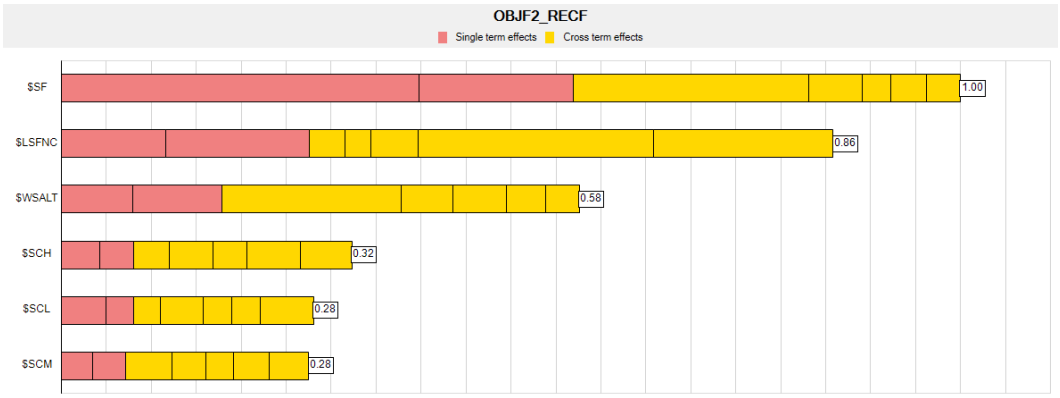


*Figure 26: Impact on recovery factor vs. variables of uncertainty. Rel perm/capillary pressure scaling - High API – DoE.*

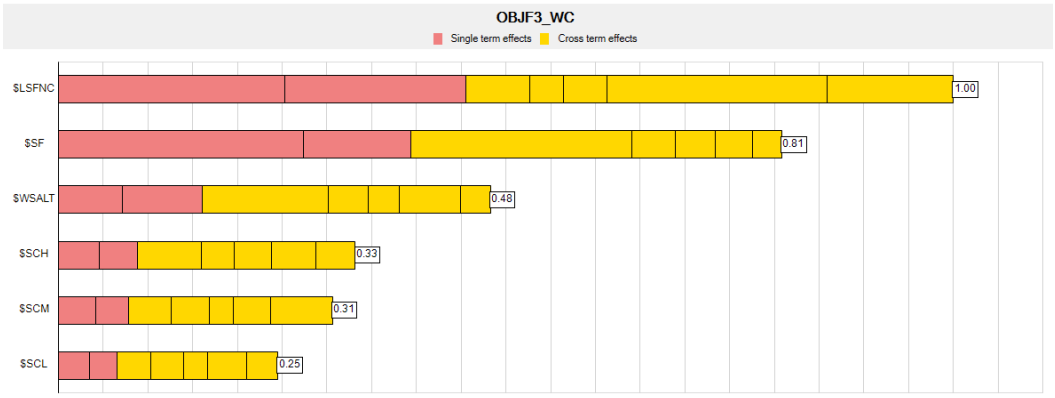


*Figure 27: Impact on water cut vs. variables of uncertainty. Rel perm/capillary pressure scaling - High API – DoE.*

## 4.2 Saturation Functions Endpoint Scaling

After performing the uncertainty with the saturation functions scaling, the next question was what are the most impactful endpoints? and what is the overall effect of endpoint scaling over the Low Salinity Water Injection (LSWI)? To address these questions, it was performed a new Design of Experiments (DoE) having into account the saturation function endpoints and, also including all the saturation function scaling variables from the last DoE. An uncertainty for high API was performed, mainly because the high API includes the endpoints for gas. Then, the results of the endpoint scaling for high API can be applied to the low API, without using the gas endpoints.

The endpoints are specified both for high and low salinity, i.e. relative permeability and capillary pressure endpoints are set for high and low salinity. The objective is to quantify the impact of high and low salinity endpoints separately. Figure 28 shows the main differences in the saturation functions curves and its endpoints between high and low salinity. Also, shows the difference of the endpoints for high and low salinity by color. The low salinity saturation function endpoints are preceded with the suffix 'L'.

Based in literature review, going from high to low salinity, the critical and connate water saturation tends to increase, the residual oil saturation tends to decrease, the relative permeability to oil at critical water saturation tends to increase, the relative permeability to the water at residual oil saturation tends to decrease, the relative permeability to gas, in spite there is a slightly change, tends to increase. Also, the maximum capillary pressure tends to increase.

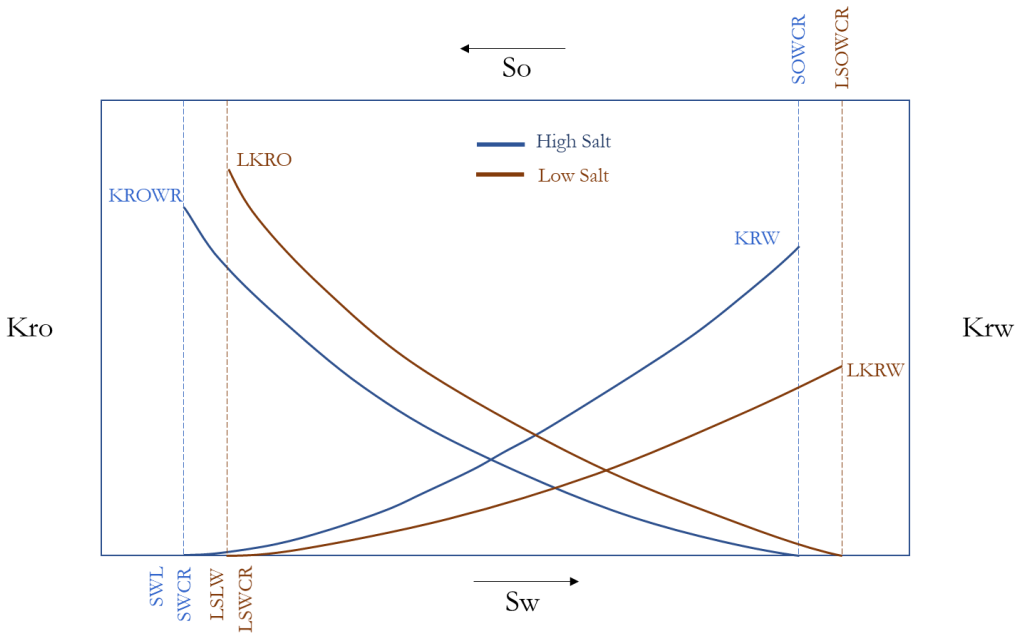


*Figure 28: Water-oil relative permeability curves with endpoints.*

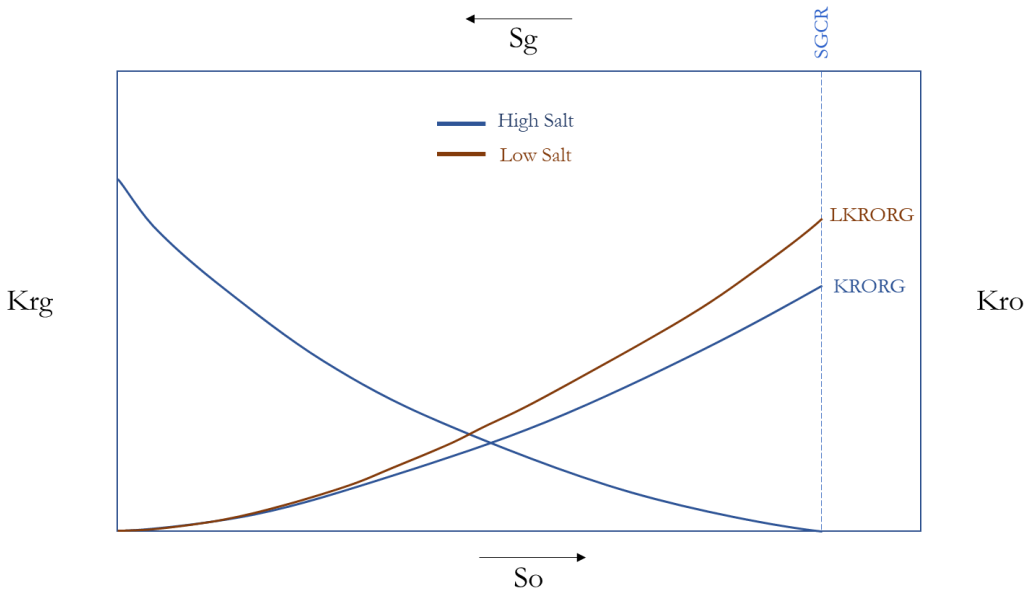


*Figure 29: Oil-gas relative permeability curves with endpoints.*

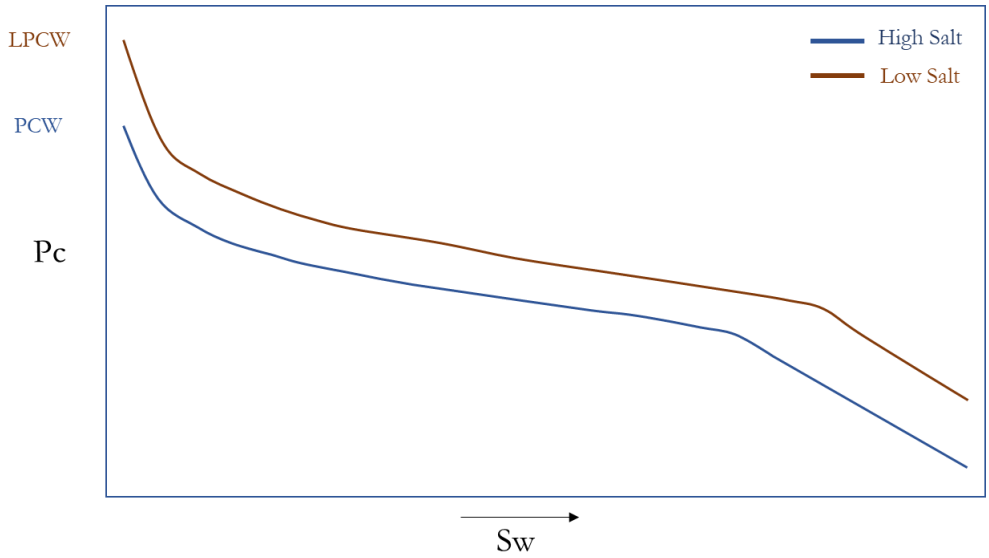


*Figure 30: Capillary pressure curves for high and low salinity and its endpoints.*

**4.2.1 Methodology.** A two-tier Design of Experiments (DoE) are performed. First-tier uncertainty characterization (DoE) focused on all possible relative-permeability and capillary-pressure related endpoints and other parameterization for both low- and high-salinity saturation curves and their scaling. Then, the most impactful variables of the first-stage DoE are combined with other reservoir and operational uncertain variables to perform the overall uncertainty assessment of LSWI. Uncertain variables explored include parameterizations for porosity, permeability, anisotropy, fluid properties, production and injection rates and pressures and salinity of the injected water.

**4.2.2 Design of Experiments with Endpoint variables.** The uncertainty and characterization for the saturation function endpoints was done using the variables from the last design of experiments of the low salinity scaling function (LSFNC) and adding all the possible endpoints as new variables. Table 7 shows the variables and its base values and the minimum and maximum values.

The values for the LSFNC and saturation functions are integers because they are included files. Also, the endpoint values are multiplier factors.

Table 7.

*Uncertain variables for DoE with endpoint scaling.*

| Uncertain Variables | Keyword | Base Value | Range | |
|---|---|---|---|---|
| | | | Min | Max |
| Low salinity scaling function | LSFNC | 2 | 1 | 3 |
| Saturation Functions | SF | 2 | 1 | 3 |
| Salt Concentration-Injection | WSALT | 5 | 1 | 20 |
| Salt conc scaling function low | SCL | 0.01 | 0 | 0.05 |
| Salt conc scaling function medium | SCM | 3 | 2 | 5 |
| Salt conc scaling function high | SCH | 30 | 20 | 40 |
| Kro at critical water | KROWR | 1 | 0.9 | 1.2 |
| Krw at residual oil | KRWR | 1 | 0.8 | 1.2 |
| Kro at critical gas | KRORG | 1 | 0.8 | 1.2 |

| | | | | |
|---|---|---|---|---|
| Maximum oil relative permeability (low salinity) | LKRO | 1 | 0.9 | 1.1 |
| Oil relative permeability at critical gas saturation (Low salinity) | LKRORG | 1 | 0.75 | 1.2 |
| Maximum water relative permeability (Low salinity) | LKRW | 1 | 0.75 | 1.2 |
| Critical oil-in-water saturation (Low salinity) | LSOWCR | 1 | 0.5 | 2 |
| Critical water saturation (Low salinity) | LSWCR | 1 | 0.5 | 1.5 |
| Critical gas saturation | SGCR | 1 | 0 | 1.5 |
| Maximum gas saturation | SGU | 1 | 0.97 | 1.05 |
| Connate water saturation | SWL | 1 | 0 | 1.5 |
| Maximum water saturation | SWU | 1 | 0.85 | 1.05 |
| Maximum capillary pressure water | PCW | 1 | 0 | 2 |
| Scaled maximum water capillary pressure (low salinity) | LPCW | 1 | 0.17 | 2 |

**4.2.3 Results and Analysis.** A correlation analysis is performed to evaluate the most positive or negative impactful variables. The results are shown in Figure 31.

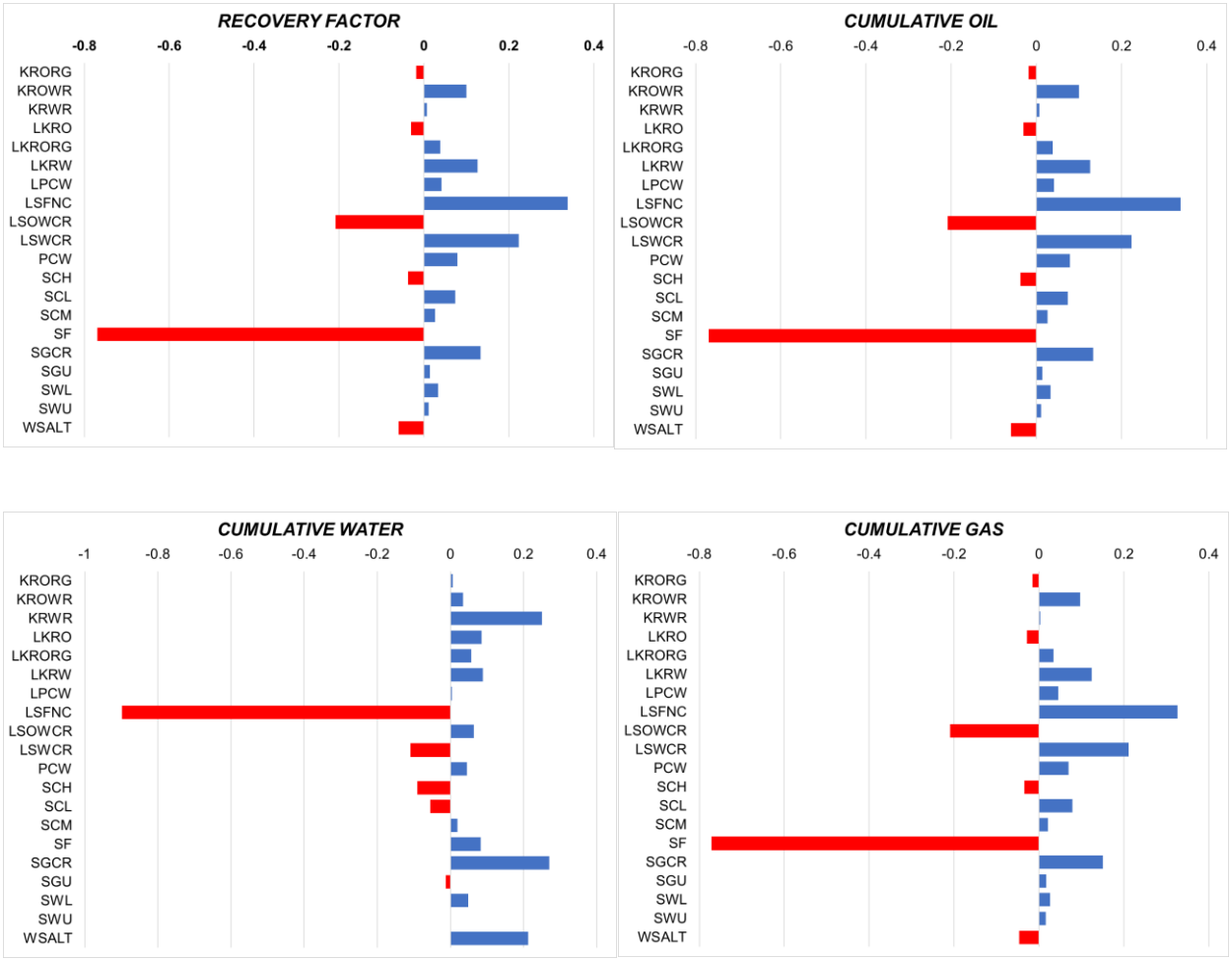

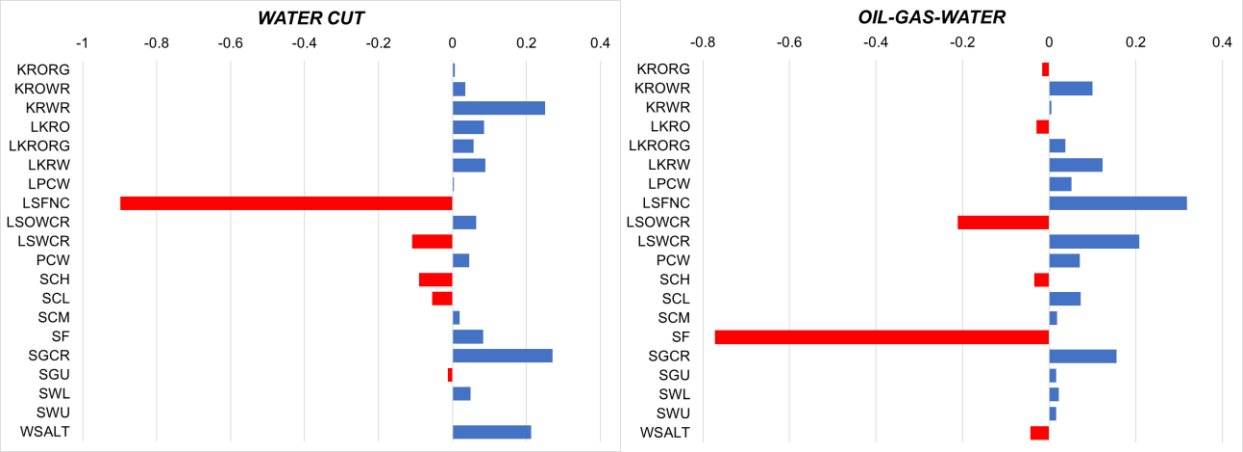


*Figure 31: Impact of each uncertain variable on the objective functions.*

The most impactful variables, either positively and negatively, with more than 5% of impact were the salt concentration (WSALT), the saturation function scaling (LSFNC), and the low salt concentration within the saturation function scaling (SCL), the saturation functions (SF). The most impactful endpoints were Kro at critical water (KROWR), maximum water relative permeability (LKRW), critical oil-in-water saturation for low salinity (LSOWCR), critical water saturation for low salinity (LSWCR), the maximum water capillary pressure (PCW) and the critical gas saturation (SGCR).

With the most impactful endpoints it is possible to infer that the setup of the low salinity saturation functions endpoints is of relevant importance, especially with the relative permeability curves. The most relevant endpoints were those of the low salinity saturation curves. The importance of the high salinity saturation curves endpoints is less than 5%. Therefore, the change brought about by the low salinity water injection toward a water-wet state is more important than the original wettability of the system, despite the starting point should be representing an oil-wet or intermediate-wet.

Based on the analysis presented, the variables with less than 5% of impact were left outside for the next uncertainty, except that directly related with the impactful variables.

**4.2.4 Design of Experiments with Parameterizations for Porosity, Permeability, Anisotropy, Fluid Properties, Production and Injection Rates and Pressures.** This uncertainty and characterization was done using the variables from the last uncertainty using endpoint scaling and adding new parameters as fluid properties, injection and production constrains, static reservoir properties like porosity, permeability in horizontal and vertical directions and initial water saturation. Table 8 shows the variables, the base, minimum and maximum values.

The values for the LSFNC and saturation functions are integers because they are included files. Also, the endpoint values are multiplier factors. Gas endpoints stated in Table 8 are for the high API uncertainty. However, those endpoints were not used for the low API uncertainty.

Table 8.

*Uncertain variables for DoE with operational, fluid and additional parametrization.*

| Uncertain Variables | Keyword | Base Value | Range | |
|---|---|---|---|---|
| | | | Min | Max |
| API gravity of the oil | API | 40 | 30 | 50 |
| Bubble Point - Saturation Pressure | SATP | 160 | 130 | 210 |
| Bottom Hole Pressure for the injector | BHPI | 410 | 300 | 475 |
| Bottom Hole Pressure for the producer | BHPP | 10 | 5 | 30 |
| Injection rate | IRATE | 100 | 30 | 250 |
| Production rate | PRATE | 500 | 300 | 650 |
| Low salinity scaling function | LSFNC | 2 | 1 | 3 |
| Saturation Functions | SF | 2 | 1 | 3 |
| Salt conc scaling function low | SCL | 0.01 | 0 | 0.05 |
| Salt conc scaling function medium | SCM | 3 | 2 | 5 |
| Salt conc scaling function high | SCH | 30 | 20 | 40 |
| Salt Concentration-Injection | WSALT | 5 | 1 | 20 |
| Initial reservoir pressure | INITRESP | 1 | 0.95 | 1.05 |
| Kro at critical water | KRORW | 1 | 0.9 | 1.2 |
| Vertical Permeability | KVKH | 0.1 | 0.01 | 1 |
| Permeability Y axis | KYKX | 1 | 0.25 | 4 |

| | | | | |
|---|---|---|---|---|
| Maximum water relative permeability (Low salinity) | LKRW | 1 | 0.75 | 1.2 |
| Scaled maximum water capillary pressure (low salinity) | LPCW | 1 | 0.17 | 2 |
| Critical oil-in-water saturation (Low salinity) | LSOWCR | 1 | 0.25 | 1.2 |
| Critical water saturation (Low salinity) | LSWCR | 1 | 0.51 | 1.1 |
| Maximum capillary pressure water | PCW | 1 | 0 | 2 |
| Porosity | PORO | 1 | 0.5 | 1.5 |
| Initial Formation Salt Concentration | SALT | 1 | 0.5 | 1.5 |
| Critical gas saturation | SGCR | 1 | 0 | 1.2 |
| Initial reservoir water saturation | SWAT | 1 | 0.7 | 1.1 |
| Permeability X axis | PERMX | 1 | 0.1 | 10 |

**4.2.5 Results and analysis.** Figure 32 shows the results of this DoE. A correlation analysis unveils the most impactful variables in the uncertainty where the horizontal permeability in X, the porosity, the injection rate, the initial water saturation and the low salinity scaling function.

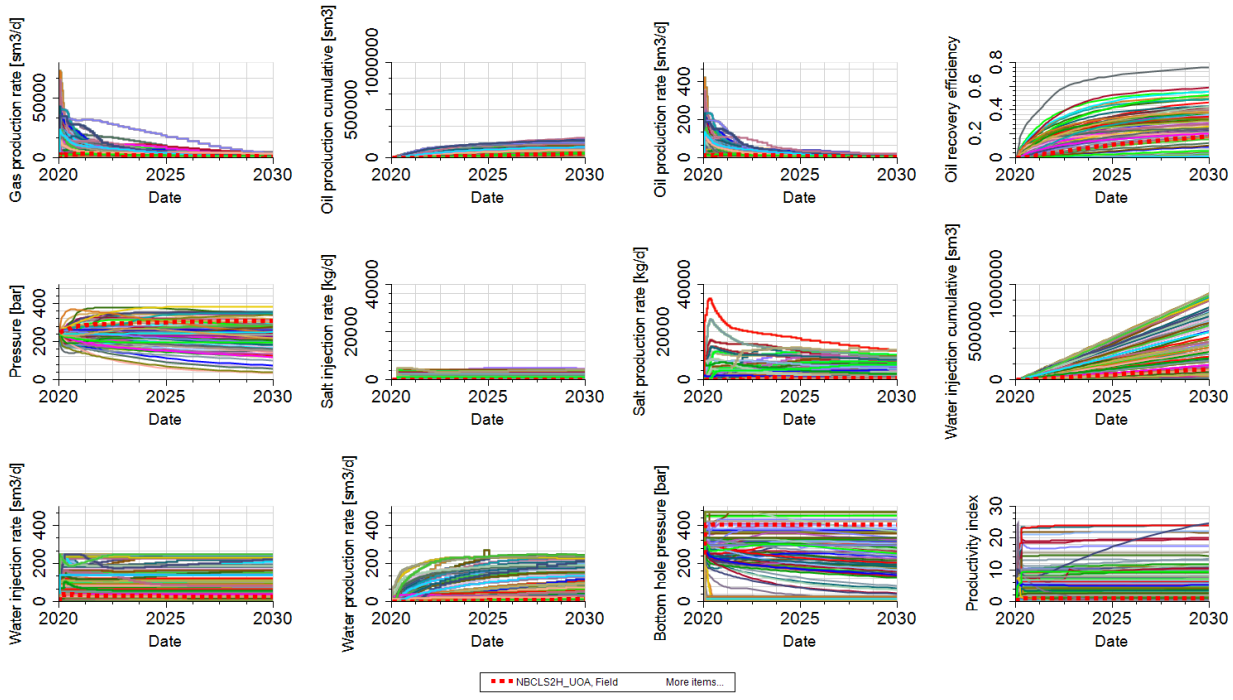


*Figure 32: Results of uncertainty with endpoint scaling and another parametrization.*

The effects of each uncertain variable to the response variables was found out through a sensitivity analysis, establishing a cutoff value of 80% of importance to reduce the number of

relevant variables. The most important variables affecting the recovery factor are the horizontal permeability in X, porosity, injection rate and initial water saturation; for water cut, the most important variables are the porosity, horizontal permeability in X direction, the saturation functions, low salinity scaling function, initial water saturation and permeability in Y direction; for cumulative oil, the most relevant variables are the horizontal permeability in X direction, injection rate, vertical permeability and initial water saturation; for cumulative gas, the most relevant parameters are the horizontal permeability in X and Y direction; for cumulative water, the most important variables are the injection rate and the permeability in X and Y direction. The impact of all the variables in the recovery factor, water cut, and cumulative gas are shown in Figure 33.

It can be inferred that the modeling of static reservoir properties like horizontal permeability, porosity and with a lesser extend the anisotropy, must be done with a geological and petrophysical accuracy to get a successful insight of the effectiveness of LSWI. Also, the initial water saturation is of relevant importance, mainly because the saturation functions, that are the responsible for the low salinity effect, are directly affected by the initial water saturation. Thus, with increasing the initial water saturation the low salinity effect is decreased.

The low salinity scaling function continues being important. Operational parameters related to the water injection like injection rate and bottom hole pressure are also relevant in the development of LSWI projects. Besides, the API density of the bearing fluid affects the success of LSWI project. The fluid effect on LSWI will be discussed later in chapter 6.

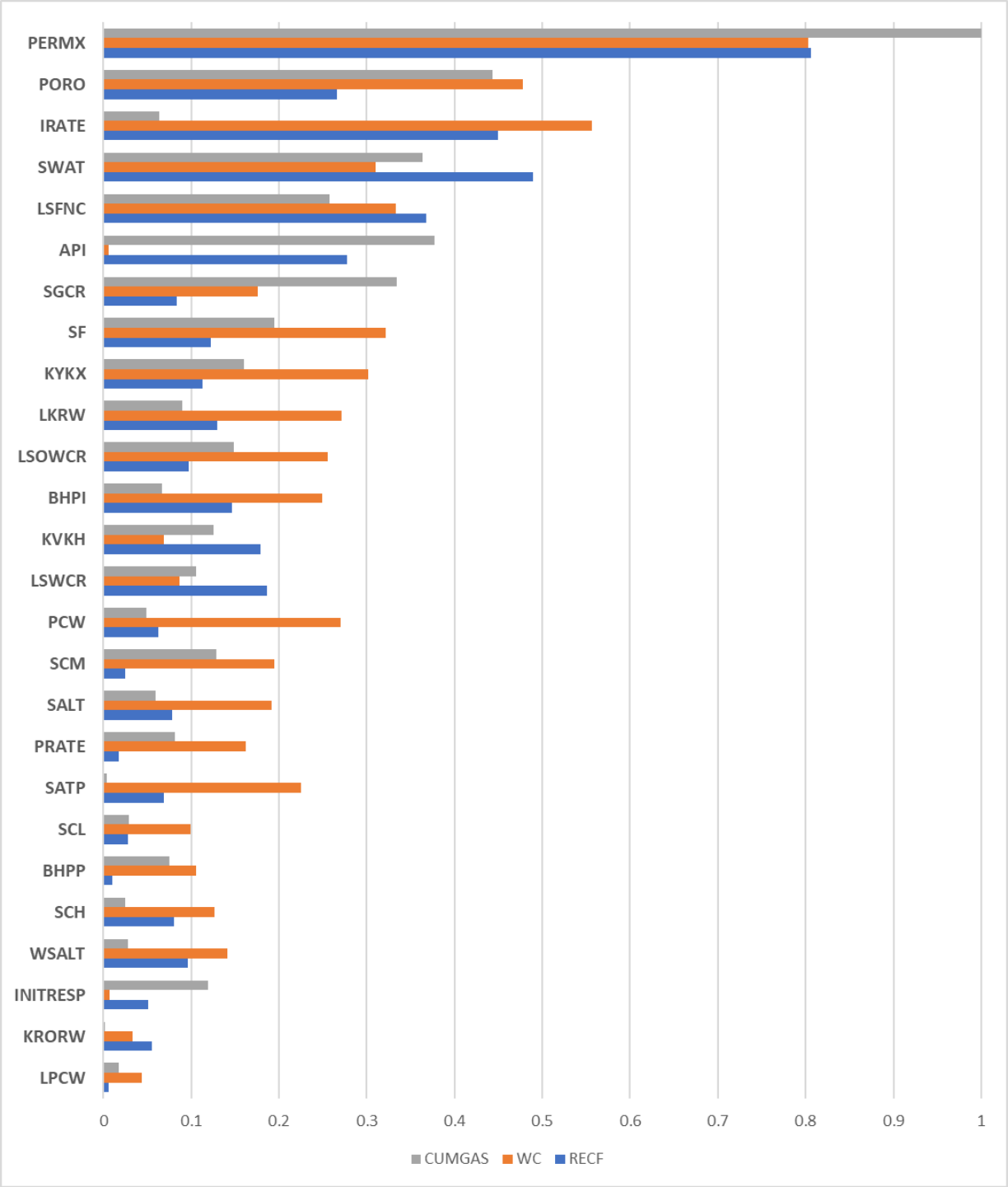


*Figure 33: Effect of uncertain variables in the recovery factor, water cut and cumulative gas for the DoE.*

### 4.3 Rock-Type Saturation Functions

As it was stated by the literature review, Low Salinity Water Injection (LSWI) evaluation uses rock-physics saturation functions for high and low salinity to reflect the change of wettability of all the system toward a more water-wet state. One of the driving mechanisms for this wettability change is the presence of clay minerals, that also stands within the LSWI screening. Reservoir simulations for LSWI project evaluation uses one set of saturation functions (relative permeability and capillary pressure) for high and low salinity. However, the assignment of rock-physics saturation functions to different rock-types has not been investigated. So far, in this thesis it has been provided one set of saturation functions to all the reservoir to model the change of the wettability, no distinguishing between the facies. Therefore, lithofacies-dependent saturation functions were assigned to capture the effect of the presence of clay minerals. This allows modeling the variation of low-salinity effect from coarse sand to shale formations and appropriately capturing their contributions to overall wettability change. The data to build the rock saturation functions for the base case is shown in Table 9. The values for the uncertainty and the criteria to select those values is described in the methodology.

Table 9.

*Parameters for building the lithofacies saturation functions.*

| SANDSTONE | | | | FINE SANDSTONE | | | |
|---|---|---|---|---|---|---|---|
| **HIGH SAL** | | **LOW SAL** | | **HIGH SAL** | | **LOW SAL** | |
| ***Relative permeabilites*** | | | | ***Relative permeabilites*** | | | |
| **Krw@Sorw** | 0.55 | **Krw@Sorw** | 0.45 | **Krw@Sorw** | 0.45 | **Krw@Sorw** | 0.35 |
| **Krw@S=1** | 0.85 | **Krw@S=1** | 0.8 | **Krw@S=1** | 0.8 | **Krw@S=1** | 0.7 |
| **Swi** | 0.15 | **Swi** | 0.17 | **Swi** | 0.2 | **Swi** | 0.22 |
| **Swcr** | 0.2 | **Swcr** | 0.22 | **Swcr** | 0.25 | **Swcr** | 0.27 |
| **Nw** | 3 | **Nw** | 3 | **Nw** | 3.5 | **Nw** | 3.5 |
| **Kro@Somax** | 0.85 | **Kro@Somax** | 0.9 | **Kro@Somax** | 0.75 | **Kro@Somax** | 0.85 |

| | | | |
|---|---|---|---|
| **Sor** | 0.3 | **Sor** | 0.25 |
| **Sorg** | 0 | **Sorg** | 0 |
| **No/w** | 4 | **No/w** | 4 |
| **No/g** | 2 | **No/g** | 2 |
| **Krg@Swmin** | 0.9 | **Krg@Swmin** | 0.85 |
| **Sgc** | 0.05 | **Sgc** | 0.05 |
| **Ng** | 2 | **Ng** | 2 |
| **Krorg@Sgcr** | 0.35 | **Krorg@Sgcr** | 0.4 |

| | | | |
|---|---|---|---|
| **Sor** | 0.32 | **Sor** | 0.27 |
| **Sorg** | 0 | **Sorg** | 0 |
| **No/w** | 4.5 | **No/w** | 4.5 |
| **No/g** | 3 | **No/g** | 3 |
| **Krg@Swmin** | 0.85 | **Krg@Swmin** | 0.7 |
| **Sgc** | 0.05 | **Sgc** | 0.05 |
| **Ng** | 3 | **Ng** | 3 |
| **Krorg@Sgcr** | 0.45 | **Krorg@Sgcr** | 0.5 |

| ***Capillary Pressure*** | | | |
|---|---|---|---|
| **SwPc=0** | 0.45 | **SwPc=0** | 0.5 |
| **Max Pc (bar)** | 5 | **Max Pc (bar)** | 10 |
| **Bro/Cor ao** | 1000 | **Bro/Cor ao** | 1000 |
| **Bro/Cor aw** | 350 | **Bro/Cor aw** | 350 |

| ***Capillary Pressure*** | | | |
|---|---|---|---|
| **SwPc=0** | 0.55 | **SwPc=0** | 0.6 |
| **Max Pc (bar)** | 50 | **Max Pc (bar)** | 70 |
| **Bro/Cor ao** | 1000 | **Bro/Cor ao** | 1000 |
| **Bro/Cor aw** | 600 | **Bro/Cor aw** | 600 |

## COARSE SANDSTONE

| **HIGH SAL** | | **LOW SAL** | |
|---|---|---|---|
| ***Relative permeabilites*** | | | |
| **Krw@Sorw** | 0.6 | **Krw@Sorw** | 0.5 |
| **Krw@S=1** | 0.9 | **Krw@S=1** | 0.8 |
| **Swi** | 0.1 | **Swi** | 0.12 |
| **Swcr** | 0.2 | **Swcr** | 0.23 |
| **Nw** | 3 | **Nw** | 3 |
| **Kro@Somax** | 0.9 | **Kro@Somax** | 0.95 |
| **Sor** | 0.3 | **Sor** | 0.25 |
| **Sorg** | 0 | **Sorg** | 0 |
| **No/w** | 4 | **No/w** | 4 |
| **No/g** | 2 | **No/g** | 2 |
| **Krg@Swmin** | 0.95 | **Krg@Swmin** | 0.9 |
| **Sgc** | 0.05 | **Sgc** | 0.05 |
| **Ng** | 2 | **Ng** | 2 |
| **Krorg@Sgcr** | 0.2 | **Krorg@Sgcr** | 0.25 |
| ***Capillary Pressure*** | | | |
| **SwPc=0** | 0.4 | **SwPc=0** | 0.45 |
| **Max Pc (bar)** | 2 | **Max Pc (bar)** | 4 |
| **Bro/Cor ao** | 1000 | **Bro/Cor ao** | 1000 |

## SHALE

| **HIGH SAL** | | **LOW SAL** | |
|---|---|---|---|
| ***Relative permeabilites*** | | | |
| **Krw@Sorw** | 0.4 | **Krw@Sorw** | 0.3 |
| **Krw@S=1** | 0.7 | **Krw@S=1** | 0.6 |
| **Swi** | 0.25 | **Swi** | 0.3 |
| **Swcr** | 0.3 | **Swcr** | 0.35 |
| **Nw** | 4 | **Nw** | 4 |
| **Kro@Somax** | 0.65 | **Kro@Somax** | 0.75 |
| **Sor** | 0.35 | **Sor** | 0.25 |
| **Sorg** | 0 | **Sorg** | 0 |
| **No/w** | 5 | **No/w** | 5 |
| **No/g** | 3 | **No/g** | 3 |
| **Krg@Swmin** | 0.75 | **Krg@Swmin** | 0.65 |
| **Sgc** | 0.05 | **Sgc** | 0.05 |
| **Ng** | 3 | **Ng** | 3 |
| **Krorg@Sgcr** | 0.55 | **Krorg@Sgcr** | 0.6 |
| ***Capillary Pressure*** | | | |
| **SwPc=0** | 0.6 | **SwPc=0** | 0.65 |
| **Max Pc (bar)** | 98 | **Max Pc (bar)** | 120 |
| **Bro/Cor ao** | 500 | **Bro/Cor ao** | 500 |

| | | | | | | | |
|---|---|---|---|---|---|---|---|
| **Bro/Cor aw** | 150 | **Bro/Cor aw** | 150 | **Bro/Cor aw** | 350 | **Bro/Cor aw** | 350 |

**4.3.1 Methodology.** A two-tier DoE were performed. First-tier uncertainty characterization (DoE) focused on all possible relative-permeability and capillary-pressure related endpoints and other parameterization for both low- and high-salinity saturation curves and their scaling. Then, all the variables of the first-stage DoE were combined with other reservoir and operational variables to perform the overall uncertainty assessment of LSWI. Uncertain variables explored include parameterizations for porosity, permeability, anisotropy, fluid properties, production and injection rates and pressures and salinity of the injected water.

**4.3.2 Design of Experiments.** The methodology used for the creation of the minimum, base and maximum values of the rock-physics saturation functions is based in the change of wettability. The minimum set of saturation function curves has the less change of wettability. The maximum set of saturation function curves has the larger change of wettability. While the base set of saturation function curves represents a balance between the wettability change of the minimum and the maximum saturation function sets.

For relative permeability curves, when increasing from the minimum to the maximum saturation function curves scenarios, the high salinity relative permeability curves move from right to left toward a more oil-wet state, simulating the original wettability of the formation before the low salinity water injection. Also, when increasing from the minimum to the maximum saturation function curves scenarios, the low salinity relative permeability curves move from left to right toward a more water-wet state, simulating the wettability change after applying the low salinity water injection. This implies, for the best scenario, the critical water saturation is increased for the high salinity saturation functions and decreased for the low salinity saturation functions, the residual oil saturation is increased for the high salinity saturation functions and decreased for the low salinity saturation functions. The relative permeability to oil is higher for the low salinity

curves than for the high salinity. This effect makes wider from the worst to best scenario. The relative permeability to water decreases from high to low salinity. This effect is larger from the worst to best scenario.

The sets of relative permeability curves for the uncertainty is designed to have the largest wettability change for shale (Figure 37) and the lowest wettability change for coarse sandstone (Figure 34). The sandstone and fine sandstone effects are between the coarse sandstone and shale effects, proportionally distributed, as shown in Figures 34 to 37. This saturation functions were built from the data contained in Tables 10 to 13.

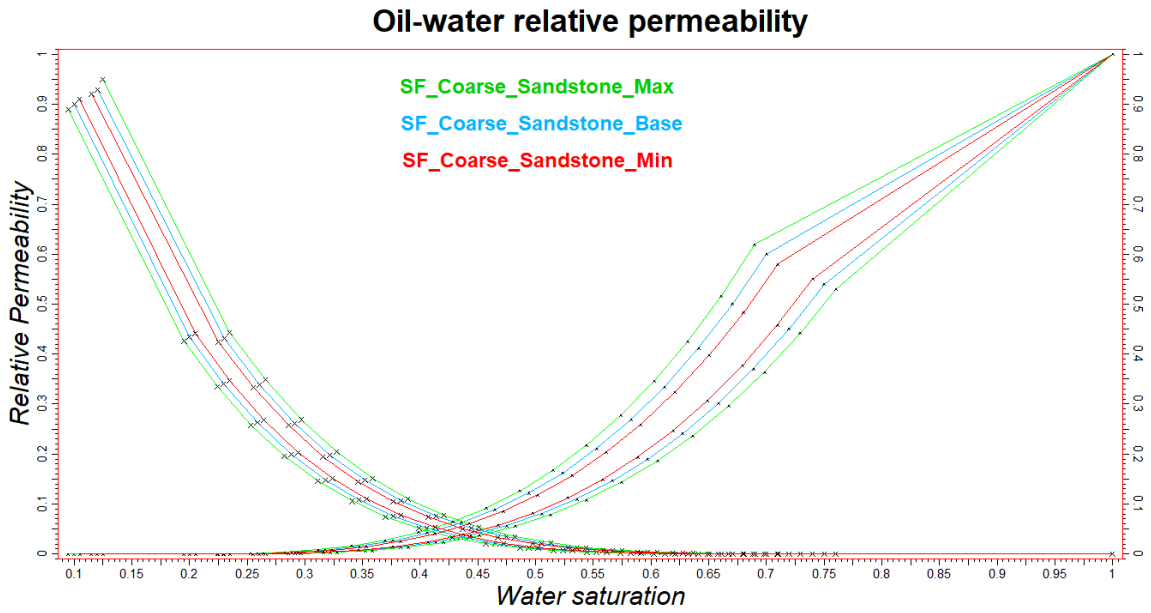


*Figure 34: High and low relative permeability curves for coarse sandstone for the rock-type saturation functions dependent DoE.*

Table 10.

*High and low relative permeability parameters for coarse sandstone for the rock-type saturation functions dependent DoE.*

## COARSE SANDSTONE

| | Min | | Base | | Max | |
|---|---|---|---|---|---|---|
| | **High Sal** | **Low Sal** | **High Sal** | **Low Sal** | **High Sal** | **Low Sal** |

| ***Relative permeabilites*** | | | | | | |
|---|---|---|---|---|---|---|
| **Krw@Sorw** | 0.58 | 0.55 | 0.6 | 0.54 | 0.62 | 0.53 |
| **Krw@S=1** | 1 | 1 | 1 | 1 | 1 | 1 |
| **Swi** | 0.105 | 0.115 | 0.1 | 0.12 | 0.095 | 0.125 |
| **Swcr** | 0.205 | 0.225 | 0.2 | 0.23 | 0.195 | 0.235 |
| **Nw** | 3 | 3 | 3 | 3 | 3 | 3 |
| **Kro@Somax** | 0.91 | 0.92 | 0.9 | 0.93 | 0.89 | 0.95 |
| **Sor** | 0.29 | 0.26 | 0.3 | 0.25 | 0.31 | 0.24 |
| **Sorg** | 0 | 0 | 0 | 0 | 0 | 0 |
| **No/w** | 4 | 4 | 4 | 4 | 4 | 4 |
| **No/g** | 2 | 2 | 2 | 2 | 2 | 2 |
| **Krg@Swmin** | 0.96 | 0.91 | 0.95 | 0.9 | 0.96 | 0.91 |
| **Sgc** | 0.04 | 0.04 | 0.05 | 0.05 | 0.06 | 0.06 |
| **Ng** | 2 | 2 | 2 | 2 | 2 | 2 |
| **Krorg@Sgcr** | 0.195 | 0.245 | 0.2 | 0.25 | 0.205 | 0.255 |

| ***Capillary Pressure*** | | | | | | |
|---|---|---|---|---|---|---|
| **SwPc=0** | 0.4 | 0.45 | 0.4 | 0.45 | 0.4 | 0.45 |
| **Max Pc (bar)** | 1 | 3 | 2 | 4 | 4 | 8 |
| **Bro/Cor ao** | 1000 | 1000 | 1000 | 1000 | 1000 | 1000 |
| **Bro/Cor aw** | 150 | 150 | 150 | 150 | 150 | 150 |

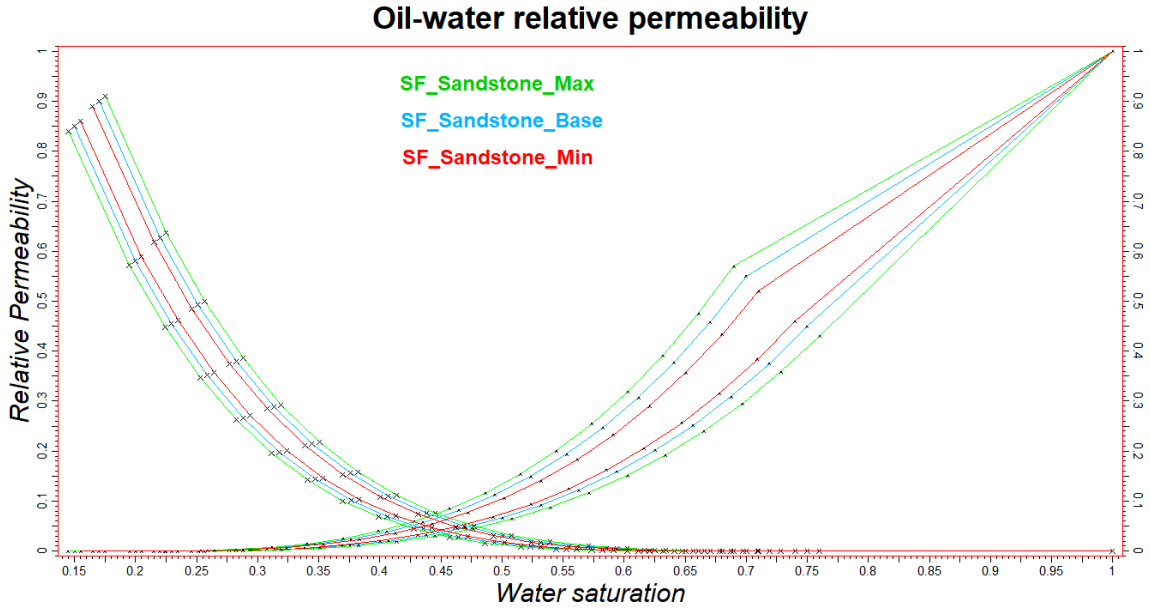


*Figure 35: High and low relative permeability curves for sandstone for the rock-type saturation functions dependent DoE.*

Table 11.

*High and low relative permeability parameters for sandstone for the rock-type saturation functions dependent DoE.*

## SANDSTONE

| | Min | | Base | | Max | |
|---|---|---|---|---|---|---|
| | **High Sal** | **Low Sal** | **High Sal** | **Low Sal** | **High Sal** | **Low Sal** |
| ***Relative permeabilites*** | | | | | | |
| **Krw@Sorw** | 0.52 | 0.46 | 0.55 | 0.45 | 0.57 | 0.43 |
| **Krw@S=1** | 1 | 1 | 1 | 1 | 1 | 1 |
| **Swi** | 0.155 | 0.165 | 0.15 | 0.17 | 0.145 | 0.175 |
| **Swcr** | 0.205 | 0.215 | 0.2 | 0.22 | 0.195 | 0.225 |
| **Nw** | 3 | 3 | 3 | 3 | 3 | 3 |
| **Kro@Somax** | 0.86 | 0.89 | 0.85 | 0.9 | 0.84 | 0.91 |
| **Sor** | 0.29 | 0.26 | 0.3 | 0.25 | 0.31 | 0.24 |
| **Sorg** | 0 | 0 | 0 | 0 | 0 | 0 |
| **No/w** | 4 | 4 | 4 | 4 | 4 | 4 |
| **No/g** | 2 | 2 | 2 | 2 | 2 | 2 |
| **Krg@Swmin** | 0.91 | 0.86 | 0.9 | 0.85 | 0.89 | 0.84 |
| **Sgc** | 0.06 | 0.06 | 0.05 | 0.05 | 0.07 | 0.07 |
| **Ng** | 2 | 2 | 2 | 2 | 2 | 2 |
| **Krorg@Sgcr** | 0.34 | 0.39 | 0.35 | 0.4 | 0.36 | 0.41 |
| ***Capillary Pressure*** | | | | | | |
| **SwPc=0** | 0.45 | 0.5 | 0.45 | 0.5 | 0.45 | 0.5 |
| **Max Pc (bar)** | 3 | 8 | 5 | 10 | 7 | 12 |
| **Bro/Cor ao** | 1000 | 1000 | 1000 | 1000 | 1000 | 1000 |
| **Bro/Cor aw** | 350 | 350 | 350 | 350 | 350 | 350 |

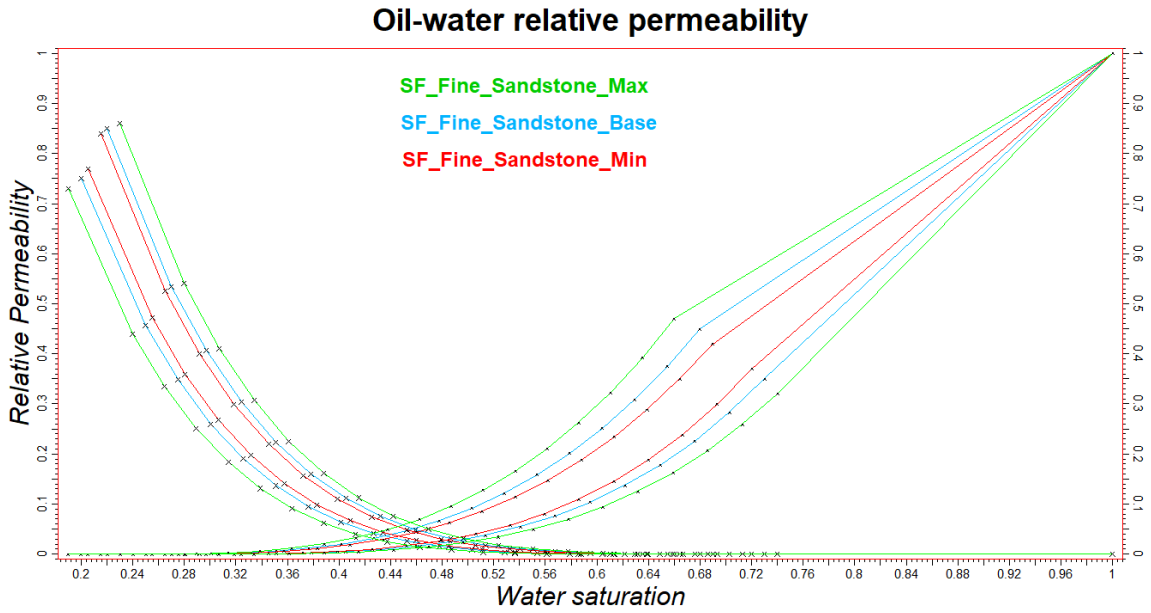


*Figure 36: High and low relative permeability curves for fine sandstone for the rock-type saturation functions dependent DoE.*

Table 12.

*High and low relative permeability parameters for fine sandstone for the rock-type saturation functions dependent DoE.*

## FINE SANDSTONE

| | Min | | Base | | Max | |
|---|---|---|---|---|---|---|
| | **High Sal** | **Low Sal** | **High Sal** | **Low Sal** | **High Sal** | **Low Sal** |
| ***Relative permeabilites*** | | | | | | |
| **Krw@Sorw** | 0.42 | 0.37 | 0.45 | 0.35 | 0.47 | 0.32 |
| **Krw@S=1** | 1 | 1 | 1 | 1 | 1 | 1 |
| **Swi** | 0.205 | 0.215 | 0.2 | 0.22 | 0.19 | 0.23 |
| **Swcr** | 0.255 | 0.265 | 0.25 | 0.27 | 0.24 | 0.28 |
| **Nw** | 3.5 | 3.5 | 3.5 | 3.5 | 3.5 | 3.5 |
| **Kro@Somax** | 0.77 | 0.84 | 0.75 | 0.85 | 0.73 | 0.86 |
| **Sor** | 0.31 | 0.28 | 0.32 | 0.27 | 0.34 | 0.26 |
| **Sorg** | 0 | 0 | 0 | 0 | 0 | 0 |
| **No/w** | 4.5 | 4.5 | 4.5 | 4.5 | 4.5 | 4.5 |
| **No/g** | 3 | 3 | 3 | 3 | 3 | 3 |
| **Krg@Swmin** | 0.86 | 0.71 | 0.85 | 0.7 | 0.84 | 0.69 |
| **Sgc** | 0.04 | 0.04 | 0.05 | 0.05 | 0.07 | 0.07 |
| **Ng** | 3 | 3 | 3 | 3 | 3 | 3 |
| **Krorg@Sgcr** | 0.44 | 0.49 | 0.45 | 0.5 | 0.46 | 0.51 |

| ***Capillary Pressure*** | | | | | | |
|---|---|---|---|---|---|---|
| **SwPc=0** | 0.55 | 0.6 | 0.55 | 0.6 | 0.55 | 0.6 |
| **Max Pc (bar)** | 40 | 60 | 50 | 70 | 60 | 80 |
| **Bro/Cor ao** | 1000 | 1000 | 1000 | 1000 | 1000 | 1000 |
| **Bro/Cor aw** | 600 | 600 | 600 | 600 | 600 | 600 |

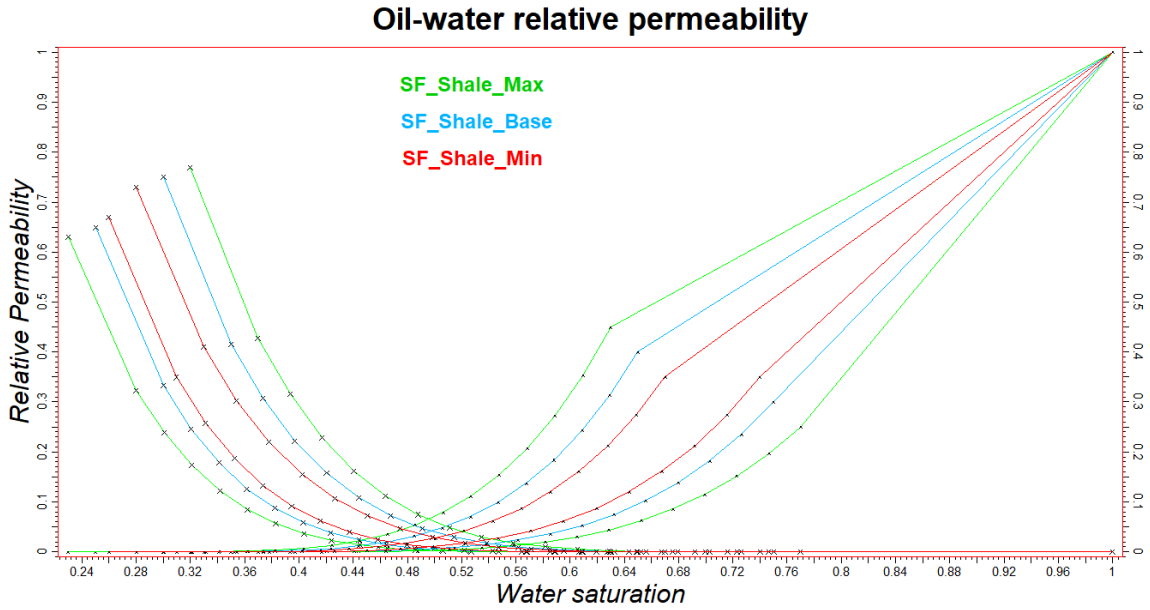


*Figure 37: High and low relative permeability curves for shale for the rock-type saturation functions dependent DoE.*

Table 13.

*High and low relative permeability parameters for shale for the rock-type saturation functions dependent DoE.*

## SHALE

| | **Min** | | **Base** | | **Max** | |
|---|---|---|---|---|---|---|
| | **High Sal** | **Low Sal** | **High Sal** | **Low Sal** | **High Sal** | **Low Sal** |
| ***Relative permeabilites*** | | | | | | |
| **Krw@Sorw** | 0.35 | 0.35 | 0.4 | 0.3 | 0.45 | 0.25 |
| **Krw@S=1** | 1 | 1 | 1 | 1 | 1 | 1 |
| **Swi** | 0.26 | 0.28 | 0.25 | 0.3 | 0.23 | 0.32 |
| **Swcr** | 0.31 | 0.33 | 0.3 | 0.35 | 0.28 | 0.37 |
| **Nw** | 4 | 4 | 4 | 4 | 4 | 4 |
| **Kro@Somax** | 0.67 | 0.73 | 0.65 | 0.75 | 0.63 | 0.77 |
| **Sor** | 0.33 | 0.26 | 0.35 | 0.25 | 0.37 | 0.23 |

| | | | | | | |
|---|---|---|---|---|---|---|
| **Sorg** | 0 | 0 | 0 | 0 | 0 | 0 |
| **No/w** | 5 | 5 | 5 | 5 | 5 | 5 |
| **No/g** | 3 | 3 | 3 | 3 | 3 | 3 |
| **Krg@Swmin** | 0.76 | 0.66 | 0.75 | 0.65 | 0.73 | 0.63 |
| **Sgc** | 0.04 | 0.04 | 0.05 | 0.05 | 0.07 | 0.07 |
| **Ng** | 3 | 3 | 3 | 3 | 3 | 3 |
| **Krorg@Sgcr** | 0.53 | 0.58 | 0.55 | 0.6 | 0.57 | 0.61 |
| ***Capillary Pressure*** | | | | | | |
| **SwPc=0** | 0.6 | 0.65 | 0.6 | 0.65 | 0.6 | 0.65 |
| **Max Pc (bar)** | 80 | 100 | 98 | 110 | 105 | 120 |
| **Bro/Cor ao** | 500 | 500 | 500 | 500 | 500 | 500 |
| **Bro/Cor aw** | 350 | 350 | 350 | 350 | 350 | 350 |

Finally, all the uncertain variables used in the design of experiments are shown in Table 14.

The values for the LSFNC and SF are integers because they are included files. Also, the endpoint values are multiplier factors. It should be noted that the gas endpoints stated in Table 14 are for the high API uncertainty. However, those endpoints were not used for the low API uncertainty.

Besides, the multiplier factor for the critical water saturation also refers to the initial water saturation and the multiplier factor for the critical gas saturation refers also to the initial gas saturation.

Table 14.

*Uncertain variables used in the rock-type design of experiments for endpoint scaling.*

| **Uncertain Variables** | **Keyword** | **Base Value** | **Range** | |
|---|---|---|---|---|
| | | | **Min** | **Max** |
| Krg max (Maximum relative permeability to gas) | KRG | 1 | 0.95 | 1.05 |
| Kro at critical gas | KRORG | 1 | 0.95 | 1.05 |
| Kro at critical water | KRORW | 1 | 0.95 | 1.05 |
| Krw max | KRW | 1 | 0.95 | 1.05 |
| Krw at residual oil | KRWR | 1 | 0.95 | 1.05 |

| | | | | |
|---|---|---|---|---|
| Oil relative permeability at critical gas saturation (Low salinity) | LKRORG | 1 | 0.95 | 1.05 |
| Oil relative permeability at critical water saturation (Low salinity) (Oil-wet) | LKRORW | 1 | 0.95 | 1.05 |
| Maximum water relative permeability (Low salinity) | LKRW | 1 | 0.95 | 1.05 |
| Water relative permeability at critical oil saturation (Low salinity) (Oil-wet) | LKRWR | 1 | 0.95 | 1.05 |
| Scaled maximum water capillary pressure (low salinity) | LPCW | 1 | 0.17 | 2 |
| Critical oil-in-water saturation (Low salinity) | LSOWCR | 1 | 0.75 | 1.05 |
| Critical water saturation (Low salinity) | LSWCR | 1 | 0.5 | 1.05 |
| Maximum capillary pressure water | PCW | 1 | 0 | 2 |
| Critical gas saturation | SGCR | 1 | 0 | 1.05 |
| Residual oil to water | SOWCR | 1 | 0.75 | 1.05 |
| Critical water saturation | SWCR | 1 | 0.5 | 1.05 |
| Saturation function for coarse sandstone | CSST | 2 | 1 | 3 |
| Saturation function for fine sandstone | FSST | 2 | 1 | 3 |
| Saturation function for sandstone | SST | 2 | 1 | 3 |
| Saturation function for shale | SHL | 2 | 1 | 3 |
| Salt Concentration-Injection | WSALT | 5 | 1 | 3 |
| Low salinity scaling function | LSFNC | 2 | 1 | 3 |
| Salt conc scaling function low | SCL | 0.01 | 0 | 0.05 |
| Salt conc scaling function medium | SCM | 3 | 2 | 5 |
| Salt conc scaling function high | SCH | 30 | 20 | 40 |

4.3.3 **Results and analysis.** The results of the uncertainty for endpoint scaling are shown in Figure 38. The results shown are for high API.

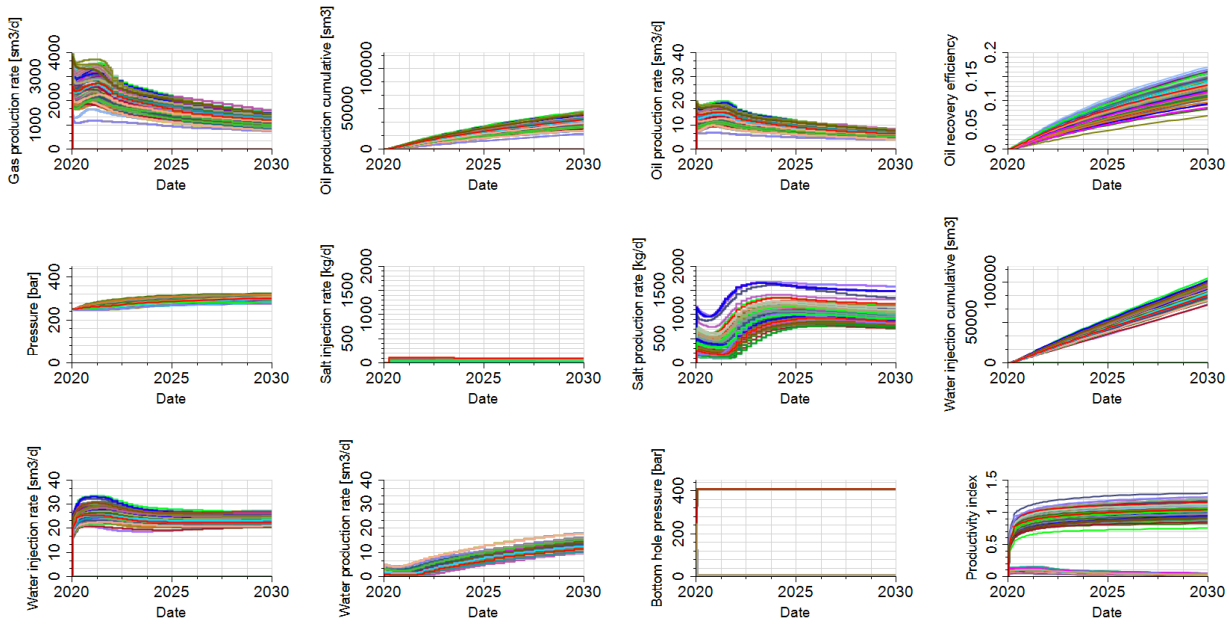


*Figure 38: Results of rock-type DoE for endpoint scaling.*

After performing an advanced sensitivity analysis, capturing the single-term effects and the cross-term effects, the endpoints with the largest impact are the critical water saturation and the residual oil saturation for the high salinity saturation function curves. The response variables established for this analysis were the cumulative oil, recovery factor, water cut, cumulative gas and cumulative water.

A correlation analysis was done, as shown in Figure 39. In this analysis, the most impactful endpoints are the critical water saturation and the residual oil saturation for high and low salinity. Also, the low salinity scaling function affected the uncertainty. This means the change of wettability, with the rock-type saturation functions dependence, is affected by the change in the water and oil saturation endpoints.

In previous design of experiments, the second-tier uncertainty was designed to get rid of the less impactful variables. The workflow used for the saturation function endpoint scaling without rock-type mimicking (section 4.2) will not be used since, in the advanced sensitivity analysis, all the variables have more than 10% impact in the uncertainty.

The discussion of the rock-type dependent saturation functions will be discussed in the next section.

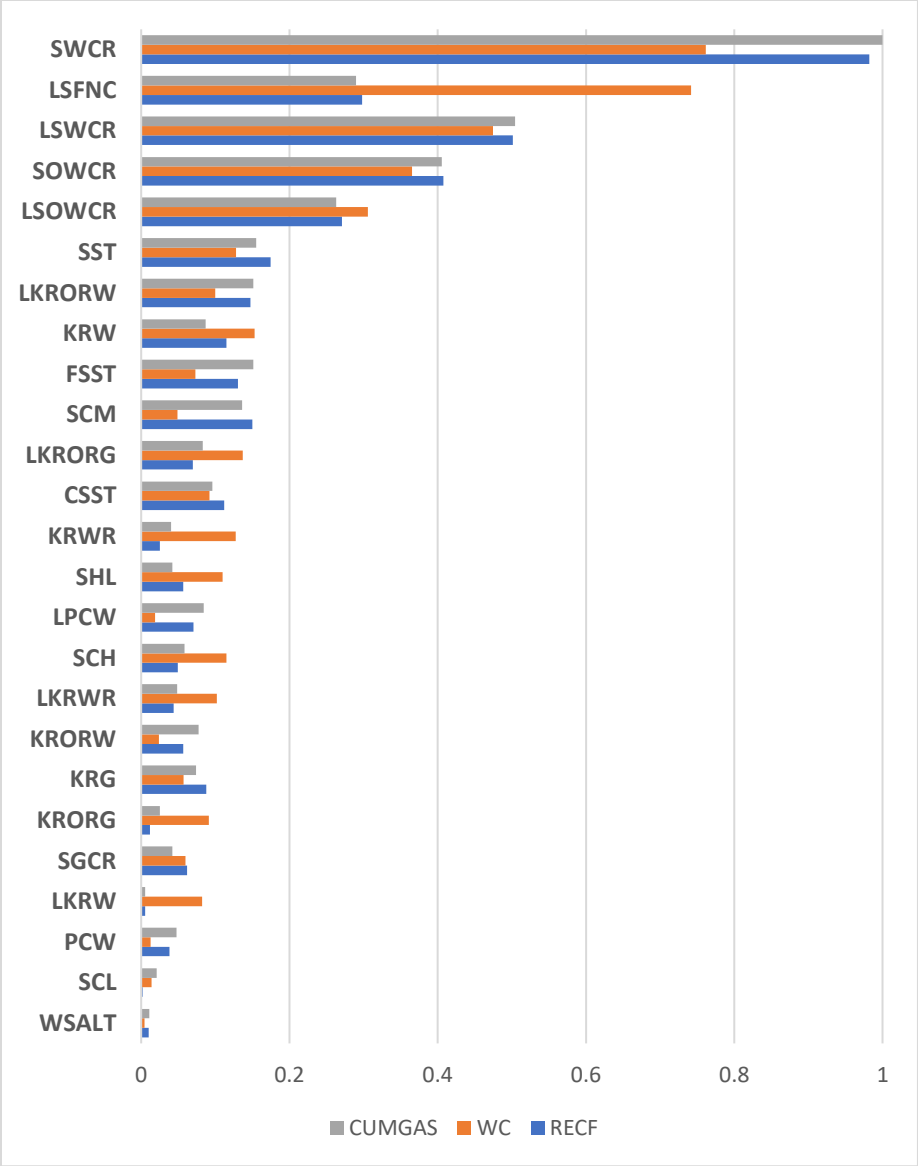


*Figure 39: Correlation analysis for uncertain variables vs effect in recovery factor, water cut and cumulative gas.*

### 4.3.4 Design of Experiments with Parameterizations for Porosity, Permeability, Anisotropy, Fluid Properties, Production and Injection Rates and Pressures.

This uncertainty and characterization was done using the variables from the last design of experiments with endpoint scaling and adding new parameters as fluid properties, injection and production constrains, static reservoir properties like porosity, horizontal permeability, anisotropy and initial water saturation. Table 15 shows the variables and its minimum, base and maximum values.

The values for the LSFNC and saturation functions are integers because they are included files. Also, the endpoint values are multiplier factors. The gas endpoints stated in Table 15 are for the high API uncertainty. However, those endpoints were not used for the low API uncertainty.

As in the last design of experiments, the multiplier factor for the critical water saturation also refers to the initial water saturation and the multiplier factor for the critical gas saturation refers also to the initial gas saturation.

Table 15.

*Uncertain variables for the DoE with another reservoir and operational parameters.*

| Uncertain Variables | Keyword | Base Value | Range | |
|---|---|---|---|---|
| | | | Min | Max |
| Krg max (Maximum relative permeability to gas) | KRG | 1 | 0.95 | 1.05 |
| Kro at critical gas | KRORG | 1 | 0.95 | 1.05 |
| Kro at critical water | KRORW | 1 | 0.95 | 1.05 |
| Krw max | KRW | 1 | 0.95 | 1.05 |
| Krw at residual oil | KRWR | 1 | 0.95 | 1.05 |
| Oil relative permeability at critical gas saturation (Low salinity) | LKRORG | 1 | 0.95 | 1.05 |
| Oil relative permeability at critical water saturation (Low salinity) (Oil-wet) | LKRORW | 1 | 0.95 | 1.05 |
| Maximum water relative permeability (Low salinity) | LKRW | 1 | 0.95 | 1.05 |
| Water relative permeability at critical oil saturation (Low salinity) (Oil-wet) | LKRWR | 1 | 0.95 | 1.05 |
| Scaled maximum water capillary pressure (low salinity) | LPCW | 1 | 0.17 | 2 |
| Critical oil-in-water saturation (Low salinity) | LSOWCR | 1 | 0.75 | 1.05 |

| | | | | |
|---|---|---|---|---|
| Critical water saturation (Low salinity) | LSWCR | 1 | 0.5 | 1.05 |
| Maximum capillary pressure water | PCW | 1 | 0 | 2 |
| Critical gas saturation | SGCR | 1 | 0 | 1.05 |
| Residual oil to water | SOWCR | 1 | 0.75 | 1.05 |
| Critical water saturation | SWCR | 1 | 0.5 | 1.05 |
| Saturation function for coarse sandstone | CSST | 2 | 1 | 3 |
| Saturation function for fine sandstone | FSST | 2 | 1 | 3 |
| Saturation function for sandstone | SST | 2 | 1 | 3 |
| Saturation function for shale | SHL | 2 | 1 | 3 |
| Salt Concentration-Injection | WSALT | 5 | 1 | 3 |
| Low salinity scaling function | LSFNC | 2 | 1 | 3 |
| Salt conc scaling function low | SCL | 0.01 | 0 | 0.05 |
| Salt conc scaling function medium | SCM | 3 | 2 | 5 |
| Salt conc scaling function high | SCH | 30 | 20 | 40 |
| API gravity of the oil | API | 40 | 30 | 50 |
| Bubble Point - Saturation Pressure | SATP | 160 | 130 | 210 |
| Bottom Hole Pressure for the injector | BHPI | 410 | 300 | 475 |
| Bottom Hole Pressure for the producer | BHPP | 10 | 5 | 30 |
| Injection rate | IRATE | 100 | 30 | 250 |
| Production rate | PRATE | 500 | 300 | 650 |
| Initial reservoir pressure | INITPRES | 1 | 0.95 | 1.05 |
| Vertical Permeability | KHKV | 0.1 | 0.01 | 1 |
| Permeability Y axis | KYKX | 1 | 0.25 | 4 |
| Permeability X axis | PERMX | 1 | 0.1 | 10 |
| Porosity | PORO | 1 | 0.5 | 1.5 |
| Initial Formation Salt Concentration | SALT | 1 | 0.5 | 1.5 |

**4.3.5 Results and analysis.** The results for the last rock-type DoE with additional parameters are shown in Figure 40.

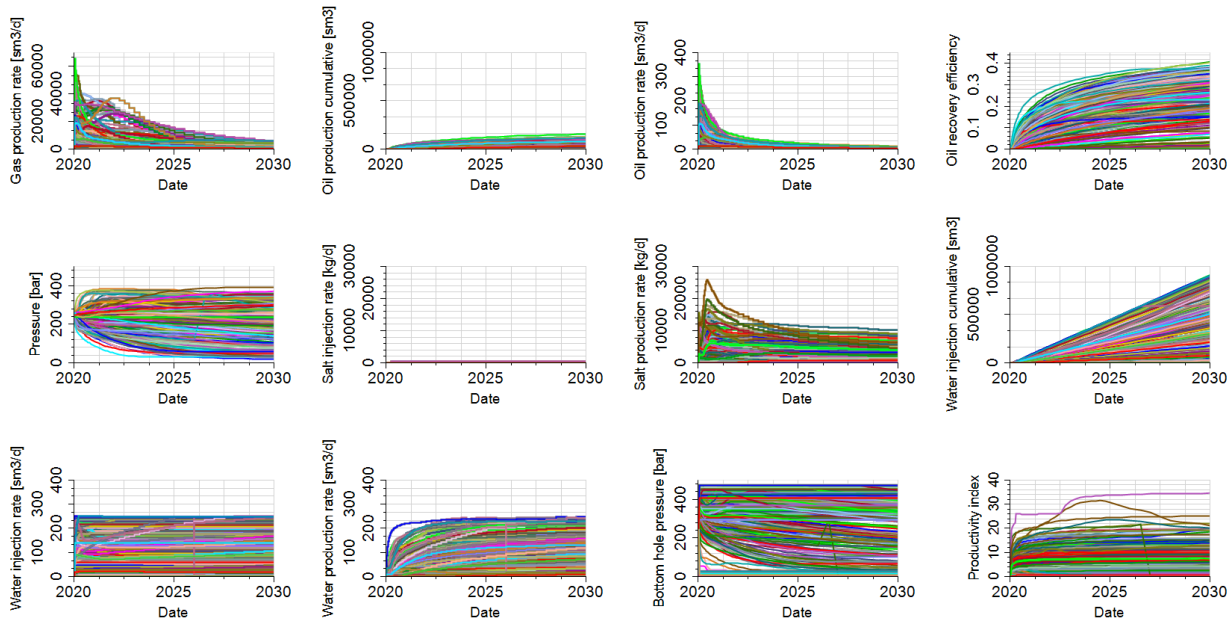


*Figure 40: Results of the rock-type DoE with additional reservoir and operational parameters.*

Performing an advanced sensitivity analysis, with single-term and cross-term effects of each uncertain variable, and establishing a cutoff value of 80%, we have that, for the recovery factor the most important variables are the horizontal permeability, porosity and API; for water cut, the most important variables are the porosity and horizontal permeability; for cumulative oil, the most relevant variables are the horizontal permeability in X, porosity, critical water saturation, low salinity scaling function, horizontal permeability in Y direction and injection rate; for cumulative gas, the most relevant parameters are the horizontal permeability in X and the API; for cumulative water, the most important variables are permeability in X direction, injection rate, bottom hole pressure of the injector and porosity.

The correlation analysis (Figure 41) shows the single-term effect of each uncertain variable in the recovery factor, the water cut and the cumulative gas. These objective functions were chosen because are representative of the others and the results are very similar.

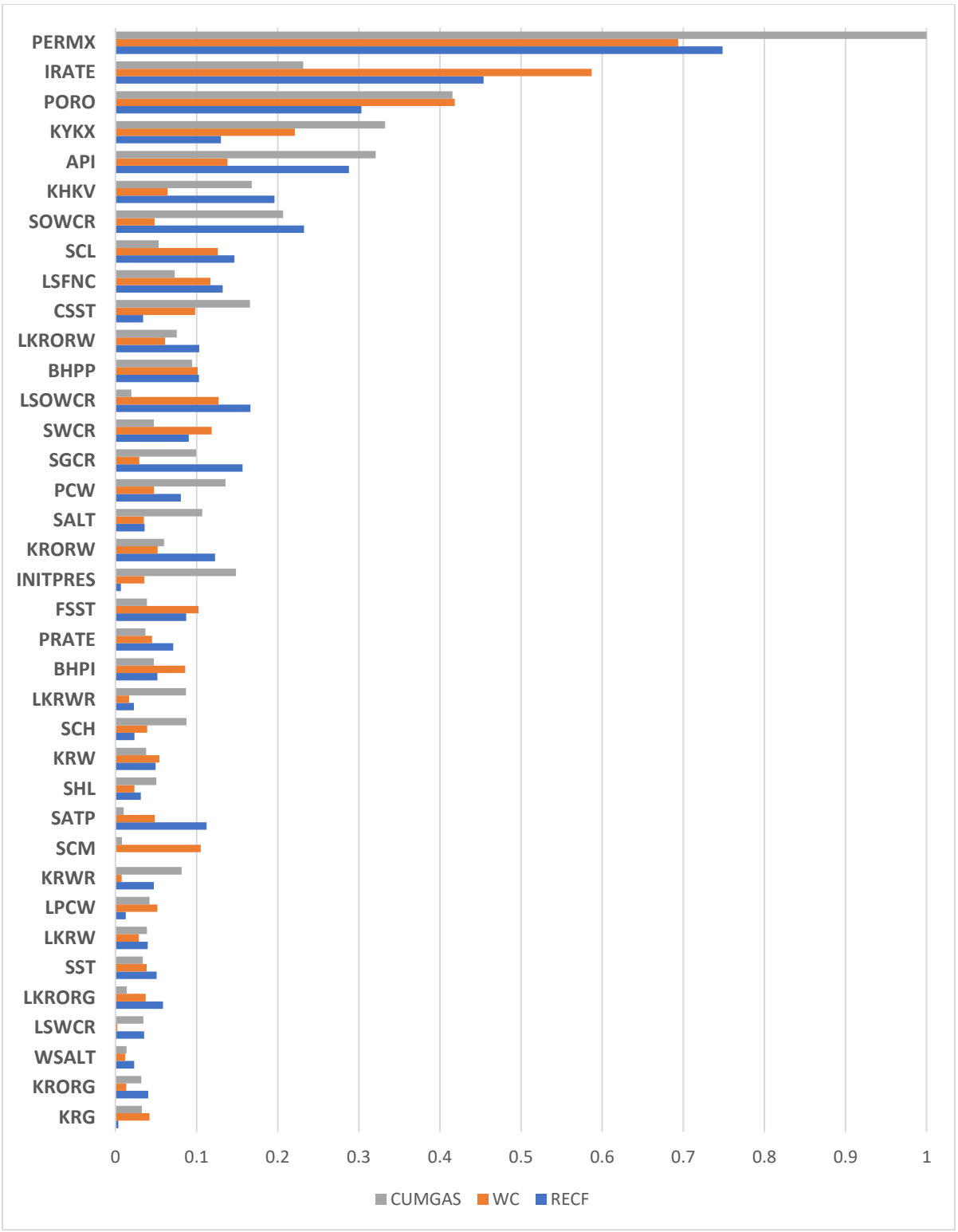


*Figure 41: Correlation analysis for the rock-type DoE for endpoint scaling.*

From this results, it is inferred that the modeling of static reservoir properties like horizontal permeability, lateral heterogeneity, porosity and with a lesser extend anisotropy, must include a comprehensive geological and petrophysical description to get a successful insight of the effectiveness of the implementation of LSWI.

Rock-type dependent saturation functions were not the most impactful variables in the advanced sensitivity analysis, neither the correlation analysis. However, when comparing the results achieved by the DoE with the rock-type dependent functions and the results from the DoE with one saturation function representing the wettability change for LSWI, the ranges of the results achieved with the lithofacies dependent saturation functions is narrow. In Figure 42 it is compared the results achieved with the Plackett-Burman and Latin-hypercube cases for the DoE with and without rock-type dependent saturation functions. The recovery factor varies from 0.07 to 0.17 for rock-type and from 0.10 to 0.27 when lithofacies effect is ignored. The water cut ranges from 0.27 to 0.65 for rock-type and from 0.11 to 0.72 when lithofacies effect is ignored. The cumulative gas goes from 3,659,044 to 8,707,006 sm3 for rock-type and from 5,221,284 to 1,380,000,000 sm3 when lithofacies effect is ignored. The cumulative oil varies from 19,911 to 48,132 sm3 using rock-type and from 28,204 to 74,799 sm3 when lithofacies effect is ignored. The cumulative water ranges from 17,467 to 44,104 sm3 with rock-type and from 5,679 to 105,322 when lithofacies effect is ignored.

Therefore, rock-type dependent saturation functions bring a more accurate approach to evaluate low salinity water injection projects narrowing the range of plausible results and providing a better estimate of the recovery factor, water cut, cumulative oil, water and gas.

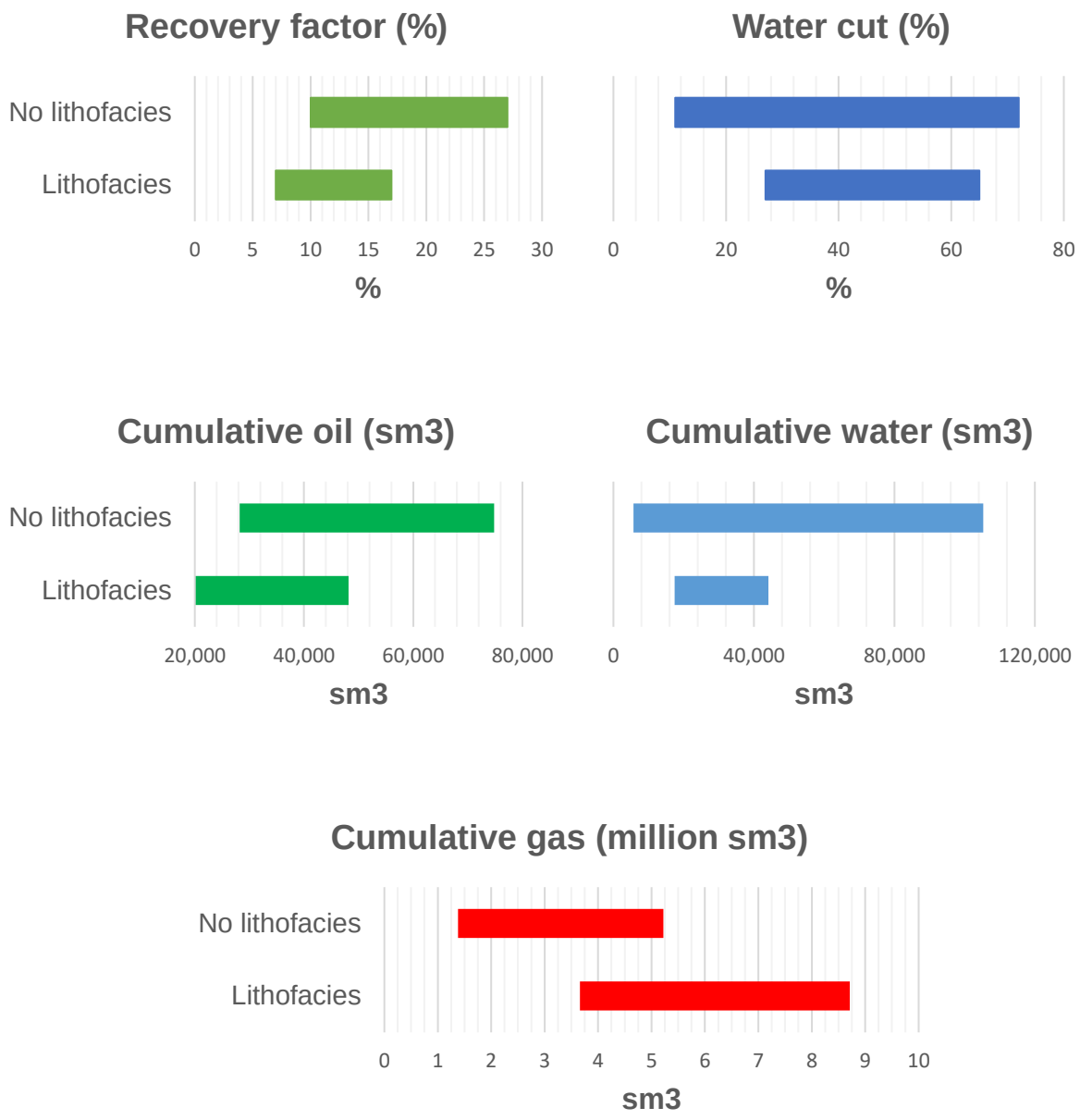


*Figure 42: Comparison of ranges when lithofacies effect is ignored and when it is used for different response variables.*

## 5. Effect of Brine Speciation

Decreasing considerably the salinity concentration of the injected water is the objective of the Low Salinity Water Injection (LSWI) processes. However, the salt concentration used so far lacks

brine speciation. Brine species of the injected water are among the parameters of LSWI screening. In the literature survey, some brine species seem to have a larger effect in the LSWI process than just injecting sodium chloride (NaCl). The injection of less concentration of calcium ($Ca^{+2}$) and magnesium ($Mg^{+2}$) cations, compared to the formation water concentration of these cations, is beneficial for the process.

Besides, as seen in the literature survey, the composition of formation water is also found an important factor for LSWI screening, because, as stated in the literature survey, LSWI has no effect when divalent ions such as calcium or magnesium do not exist in the formation water.

Brine speciation introduces the presence of other salt ions in the aqueous phase than simply sodium chloride. In the study of LSWI without brine speciation, it is overlooked the presence of other ions and the salinity of the water is based on equivalent sodium chloride concentration.

Therefore, the evaluation of the most impactful brine species is done through Design of Experiments (DoE). A two-tier design of experiments was carried out. First-tier uncertainty characterization (DoE) focused on all possible relative-permeability and capillary-pressure related endpoints and other parameterization for both low- and high-salinity saturation curves and their scaling. Then, all the variables of the first-stage DoE were combined with other reservoir and operational variables to perform the overall uncertainty assessment of LSWI. Uncertain variables explored include parameterizations for porosity, permeability, anisotropy, fluid properties, production and injection rates and pressures and salinity of the injected water.

The concentration of the brine species used was taken from the study developed by Rostami et al. (2019). In this laboratory study, four samples of synthetic brine were used. The formation water and seawater contain dissolved solids. The main dissolved solids are sodium chloride,

calcium chloride, magnesium chloride, sodium sulfate, and sodium bicarbonate. The dissolved salt concentration is expressed in parts per million on a mass basis (ppm).

The molar concentration in the water phase of each of the brine species can be specified through the component equivalent concentration. The equivalent concentration corresponds to the equivalent amount of electrical charges per volume each ionic specie contributes. For neutral species, the concentration input is treated as a molar concentration.

The mathematical definition of equivalent concentration of each component is given by the following equation:

$$Component\_Equiv\_Conc\ (kg\ mole/m^3) = \frac{Component\_Mass\_Conc\ (ppm)}{1000 * Molecular\_Weight} \quad (10)$$

The composition of brine species for sea water is shown in Table 16 (Rostami et al, 2019).

Table 16.

*Composition of sea water brine.*

| | SEA WATER BRINE | | |
|---|---|---|---|
| | **MW** | **CONCENTRATION (ppm)** | **EQUIV_CONC (kg-mole/m3)** |
| NACL | 58.44 | 28400 | 0.486 |
| CACO3 | 100.09 | 800 | 0.008 |
| MGCL2 | 95.21 | 6430 | 0.068 |
| CACL2 | 110.98 | 1380 | 0.012 |
| NA2SO4 | 142.04 | 4490 | 0.032 |
| NAHCO3 | 84.01 | 100 | 0.001 |
| ***TOTAL*** | | ***41600*** | |

The composition of the formation brine is specified in Table 17. These values were extrapolated from the sea water brine to achieve the salinity used for the formation brine throughout the thesis. This was done maintaining the same proportion of each component got from

the data and extrapolating to 220,000 ppm. This concentration was taken from the formation brine concentration from a North African giant brown field (Callegaro et al, 2015).

Table 17.

*Composition of the formation brine.*

| FORMATION BRINE | | | |
|---|---|---|---|
| | **MW** | **CONCENTRATION (ppm)** | **EQUIV_CONC (kg-mole/m3)** |
| NACL | 58.44 | 150,192.3 | 2.570 |
| CACO3 | 100.09 | 4,230.8 | 0.042 |
| MGCL2 | 95.21 | 34,004.8 | 0.357 |
| CACL2 | 110.98 | 7,298.1 | 0.066 |
| NA2SO4 | 142.04 | 23,745.2 | 0.167 |
| NAHCO3 | 84.01 | 528.8 | 0.006 |
| ***TOTAL*** | | ***220,000*** | |

For the injection water brine, the minimum values were extrapolated from the sea water brine to achieve the low-salinity range. The values used in the design of experiments are shown in Table 18. The minimum values are equivalent to the 0.5% of the sea water brine and the maximum values are equivalent to the double of the sea water brine concentrations. This range of values exceeds by far the range for low salinity to find out what is the impact of brine species to values of brine concentration below the formation brine concentration.

Table 18.

*Composition of the injection brine for the DoE.*

| INJECTION BRINE | | | |
|---|---|---|---|
| | **EQUIV_CONC (kg-mole/m3)** | | |
| | **Base** | **Max** | **Min** |
| NACL | 0.4860 | 0.9719 | 0.0243 |
| CACO3 | 0.0080 | 0.0160 | 0.0004 |
| MGCL2 | 0.0675 | 0.1351 | 0.0034 |
| CACL2 | 0.0124 | 0.0249 | 0.0006 |
| NA2SO4 | 0.0316 | 0.0632 | 0.0016 |
| NAHCO3 | 0.0012 | 0.0024 | 0.0001 |
| **Total (ppm)** | **41600** | **83200** | **2060** |

## 5.1 Design of Experiments Endpoint Scaling with Brine Speciation

This uncertainty and characterization follows the same workflow as the rock-physics saturation functions design of experiments for endpoint scaling, described in Chapter 4.3. The main difference is the injecting salt composition is divided in each specie to get an insight of the most impactful species in LSWI.

The rock-physics saturation functions included in this design of experiments are described in Chapter 4.3. These lithofacies dependent saturation functions reflects a realistic and accurate modeling of LSWI. Therefore, lithofacies dependent saturation functions will be used in this DoE.

Another variable included in this DoE is the splitting of the low salinity scaling function for each of the facies, to observe the most impactful scaling function in LSWI.

The values for the LSFNC and saturation functions are integers because they are as included files. Also, the endpoint values are multiplier factors. The gas endpoints stated in Table 19 are for the high API uncertainty. However, those endpoints were not used for the low API uncertainty.

Table 19.

*Uncertain variables for the brine speciation endpoint scaling DoE.*

| Uncertain Variables | Keyword | Base Value | Range | |
|---|---|---|---|---|
| | | | Min | Max |
| Krg max (Maximum relative permeability to gas) | KRG | 1 | 0.95 | 1.05 |
| Kro at critical gas | KRORG | 1 | 0.95 | 1.05 |
| Kro at critical water | KRORW | 1 | 0.95 | 1.05 |
| Krw max | KRW | 1 | 0.95 | 1.05 |
| Krw at residual oil | KRWR | 1 | 0.95 | 1.05 |
| Oil relative permeability at critical gas saturation (Low salinity) | LKRORG | 1 | 0.95 | 1.05 |

| | | | | |
|---|---|---|---|---|
| Oil relative permeability at critical water saturation (Low salinity) (Oil-wet) | LKRORW | 1 | 0.95 | 1.05 |
| Maximum water relative permeability (Low salinity) | LKRW | 1 | 0.95 | 1.05 |
| Water relative permeability at critical oil saturation (Low salinity) (Oil-wet) | LKRWR | 1 | 0.95 | 1.05 |
| Scaled maximum water capillary pressure (low salinity) | LPCW | 1 | 0.17 | 2 |
| Critical oil-in-water saturation (Low salinity) | LSOWCR | 1 | 0.75 | 1.05 |
| Critical water saturation (Low salinity) | LSWCR | 1 | 0.5 | 1.05 |
| Maximum capillary pressure water | PCW | 1 | 0 | 2 |
| Critical gas saturation | SGCR | 1 | 0 | 1.05 |
| Critical water saturation | SWCR | 1 | 0.5 | 1.05 |
| Saturation function for coarse sandstone | SFCST | 2 | 1 | 3 |
| Saturation function for fine sandstone | SFFST | 2 | 1 | 3 |
| Saturation function for sandstone | SFSST | 2 | 1 | 3 |
| Saturation function for shale | SFSH | 2 | 1 | 3 |
| Injection Salt Concentration - NaCl | NACL_IB | 0.486 | 0.024 | 0.972 |
| Injection Salt Concentration - CaCO3 | CACO3_IB | 0.008 | 0.000 | 0.016 |
| Injection Salt Concentration - MgCl2 | MGCL2_IB | 0.068 | 0.003 | 0.135 |
| Injection Salt Concentration - CaCl2 | CACL2_IB | 0.012 | 0.001 | 0.025 |
| Injection Salt Concentration - Na2SO4 | NA2SO4_IB | 0.032 | 0.002 | 0.063 |
| Injection Salt Concentration - NaHCO3 | NAHCO3_IB | 0.001 | 0.000 | 0.002 |
| Low salinity scaling function for coarse sandstone | LSFNCCST | 2 | 1 | 3 |
| Low salinity scaling function for fine sandstone | LSFNCFST | 2 | 1 | 3 |
| Low salinity scaling function for sandstone | LSFNCSST | 2 | 1 | 3 |
| Low salinity scaling function for shale | LSFNCSH | 2 | 1 | 3 |
| Salt conc scaling function low | SCL | 0.01 | 0 | 0.05 |
| Salt conc scaling function medium | SCM | 3 | 2 | 5 |
| Salt conc scaling function high | SCH | 30 | 20 | 40 |

## 5.2 Results and analysis

Performing a correlation analysis, the most relevant relative permeability endpoints are the critical water saturation for both high and low salinity, the residual oil saturation for low salinity, the relative permeability to water for high salinity and the critical gas saturation for high salinity. However, the maximum capillary pressure for high and low salinity are the most impactful. This

means the capillary pressure plays an important role when injecting salt species different than just sodium chloride.

The sodium sulfate, calcium carbonate and the calcium chloride are the most impactful species. Relating this to the literature survey, it seems potential determining ions, i.e. $(SO_4)^{-2}$, could affect LSWI performance. Calcium anions ($Ca^{+2}$) could influence the performance of LSWI. A most detailed explanation will be done in the analysis of the next DoE.

The correlation analysis is shown in Figure 43.

Regarding the impact of brine speciation in the lithofacies dependent saturation functions, the shale and coarse sandstone saturation functions are the most impactful. The most impactful low salinity scaling functions are for fine sandstone and shale. This showcase the importance of appropriately characterize the shale and fine-grained sandstones effect on LSWI.

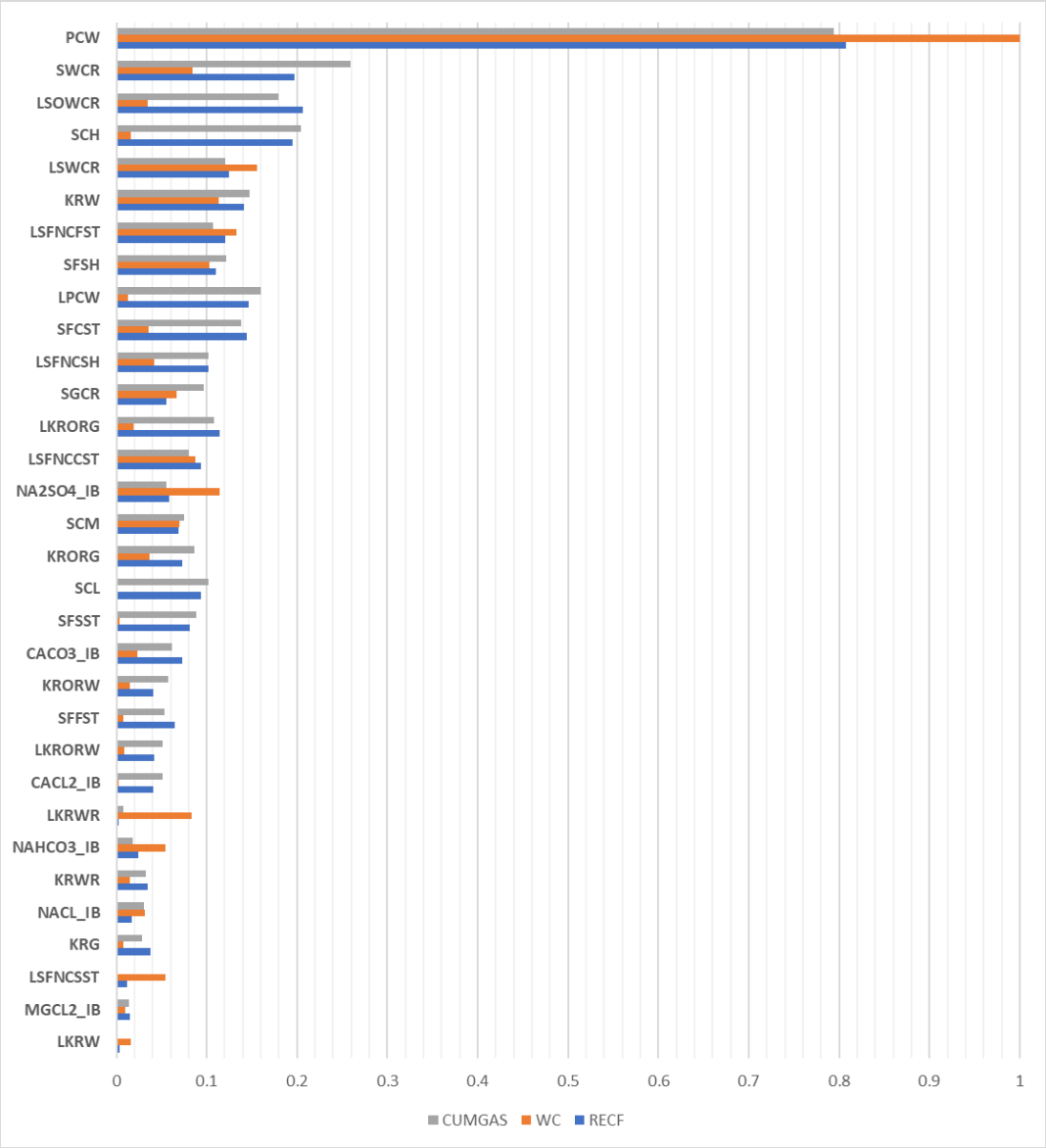


*Figure 43: Correlation analysis for the brine speciation DoE with endpoint scaling.*

## 5.3 Design of Experiments with Parameterizations for Porosity, Permeability, Anisotropy, Fluid Properties, Production and Injection Rates and Pressures.

This uncertainty and characterization follow the same workflow as the DoE with endpoint scaling and brine speciation and includes new parameters as fluid properties, injection and production constrains, static reservoir properties like porosity, permeability in horizontal and

vertical directions and initial water saturation. Table 20 shows the variables and its minimum, base and maximum values.

As the last DoE, the rock saturation functions, and the low salinity scaling function are lithofacies dependent to capture the effect of each facie in LSWI.

The values for the LSFNC and saturation functions are integers because they are included files. Also, the endpoint values are multiplier factors. The gas endpoints stated in Table 20 are for the high API uncertainty. However, those endpoints were not used for the low API uncertainty.

The multiplier factor for the critical water saturation refers to the critical and initial water saturation and the multiplier factor for the critical gas saturation refers also to the initial gas saturation.

Table 20.

*Uncertain variables for brine speciation DoE with another parameters.*

| Uncertain Variables | Keyword | Base Value | Range | |
|---|---|---|---|---|
| | | | Min | Max |
| Krg max (Maximum relative permeability to gas) | KRG | 1 | 0.95 | 1.05 |
| Kro at critical gas | KRORG | 1 | 0.95 | 1.05 |
| Kro at critical water | KRORW | 1 | 0.95 | 1.05 |
| Krw max | KRW | 1 | 0.95 | 1.05 |
| Krw at residual oil | KRWR | 1 | 0.95 | 1.05 |
| Oil relative permeability at critical gas saturation (Low salinity) | LKRORG | 1 | 0.95 | 1.05 |
| Oil relative permeability at critical water saturation (Low salinity) (Oil-wet) | LKRORW | 1 | 0.95 | 1.05 |
| Maximum water relative permeability (Low salinity) | LKRW | 1 | 0.95 | 1.05 |
| Water relative permeability at critical oil saturation (Low salinity) (Oil-wet) | LKRWR | 1 | 0.95 | 1.05 |
| Scaled maximum water capillary pressure (low salinity) | LPCW | 1 | 0.17 | 2 |
| Critical oil-in-water saturation (Low salinity) | LSOWCR | 1 | 0.75 | 1.05 |
| Critical water saturation (Low salinity) | LSWCR | 1 | 0.5 | 1.05 |

| | | | | |
|---|---|---|---|---|
| Maximum capillary pressure water | PCW | 1 | 0 | 2 |
| Critical gas saturation | SGCR | 1 | 0 | 1.05 |
| Critical water saturation | SWCR | 1 | 0.5 | 1.05 |
| Saturation function for coarse sandstone | SFCST | 2 | 1 | 3 |
| Saturation function for fine sandstone | SFFST | 2 | 1 | 3 |
| Saturation function for sandstone | SFSST | 2 | 1 | 3 |
| Saturation function for shale | SFSH | 2 | 1 | 3 |
| Injection Salt Concentration - NaCl | NACL_IB | 0.486 | 0.024 | 0.972 |
| Injection Salt Concentration - CaCO3 | CACO3_IB | 0.008 | 0.000 | 0.016 |
| Injection Salt Concentration - MgCl2 | MGCL2_IB | 0.068 | 0.003 | 0.135 |
| Injection Salt Concentration - CaCl2 | CACL2_IB | 0.012 | 0.001 | 0.025 |
| Injection Salt Concentration - Na2SO4 | NA2SO4_IB | 0.032 | 0.002 | 0.063 |
| Injection Salt Concentration - NaHCO3 | NAHCO3_IB | 0.001 | 0.000 | 0.002 |
| Low salinity scaling function for coarse sandstone | LSFNCCST | 2 | 1 | 3 |
| Low salinity scaling function for fine sandstone | LSFNCFST | 2 | 1 | 3 |
| Low salinity scaling function for sandstone | LSFNCSST | 2 | 1 | 3 |
| Low salinity scaling function for shale | LSFNCSH | 2 | 1 | 3 |
| Salt conc scaling function low | SCL | 0.01 | 0 | 0.05 |
| Salt conc scaling function medium | SCM | 3 | 2 | 5 |
| Salt conc scaling function high | SCH | 30 | 20 | 40 |
| Initial reservoir pressure | INITRESPRES | 1 | 0.95 | 1.05 |
| Vertical Permeability | KHKV | 0.1 | 0.01 | 1 |
| Permeability Y axis | KYKX | 1 | 0.25 | 4 |
| Permeability X axis | PERMX | 1 | 0.1 | 10 |
| Porosity | PORO | 1 | 0.5 | 1.5 |
| Bottom Hole Pressure for the injector | BHPI | 410 | 300 | 475 |
| Bottom Hole Pressure for the producer | BHPP | 10 | 5 | 30 |
| Injection rate | IRATE | 110 | 30 | 250 |
| Production rate | PRATE | 500 | 300 | 600 |
| API gravity of the oil | API | 40 | 30 | 50 |
| Bubble Point - Saturation Pressure | SATPRES | 160 | 130 | 200 |
| Formation brine concentration - CaCl2 | CACL2_FB | 2.570 | 0.129 | 5.140 |
| Formation brine concentration - CaCO3 | CACO3_FB | 0.042 | 0.002 | 0.085 |
| Formation brine concentration - MgCl2 | MGCL2_FB | 0.357 | 0.018 | 0.714 |
| Formation brine concentration - Na2SO4 | NA2SO4_FB | 0.066 | 0.003 | 0.132 |
| Formation brine concentration - NaCl | NACL_FB | 0.167 | 0.008 | 0.334 |
| Formation brine concentration - NaHCO3 | NAHCO3_FB | 0.006 | 0.000 | 0.013 |

## 5.4 Results and analysis

Performing a correlation analysis for this design of experiments, the most impactful reservoir static properties are the horizontal permeability in the X direction and the porosity. For the operational parameters, the most relevant are the injection rate and the bottom hole pressure of the injector. This indicates the injection rate and bottom hole pressure of the injector must be considered during the planning of a LSWI project, as well as, a sensitivity analysis must be done in order to determine the optimum rates and pressures to be used. Figure 44 shows the correlation analysis for the DoE with brine speciation, endpoint scaling and other parameters.

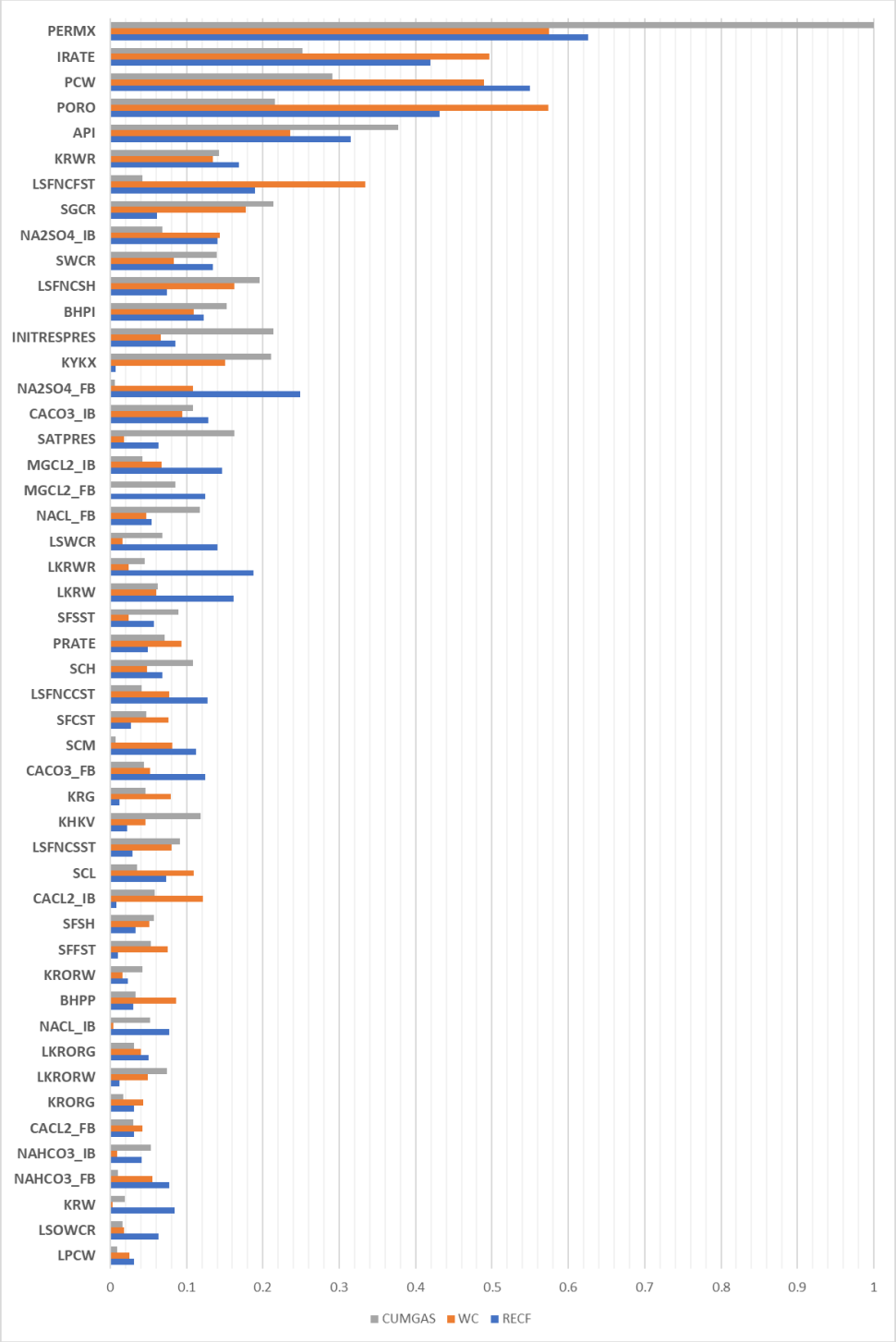


*Figure 44: Correlation analysis for brine speciation DoE with endpoint scaling and other parameters.*

Figure 45 shows three representative cases explaining the impact of sodium sulfate. The red curves represent the base case; the green curves represent the best scenario (case 36); the

yellow curves represent the worst scenario (case 127). The best scenario presents a better recovery factor and a lower water cut, also the breakthrough time is elongated; conversely, the worst scenario presents the lowest recovery factor and a high water cut. The base case has a similar trend to the worst scenario with a low recovery factor and a high water cut. Figure 45 also shows the concentrations of different brine species for these three cases. Comparing the concentrations of the species, sodium sulfate has the highest impact in the results, achieving a higher recovery factor and a lower water cut. With the concentration values it can be inferred that sodium sulfate concentration should be higher for the formation water than for the injection water in order to achieve beneficial results.

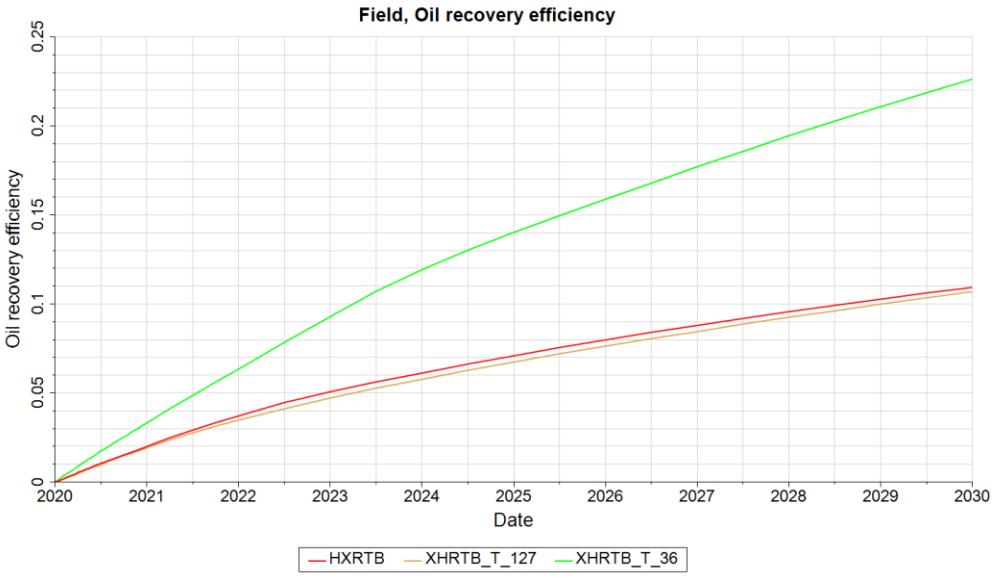

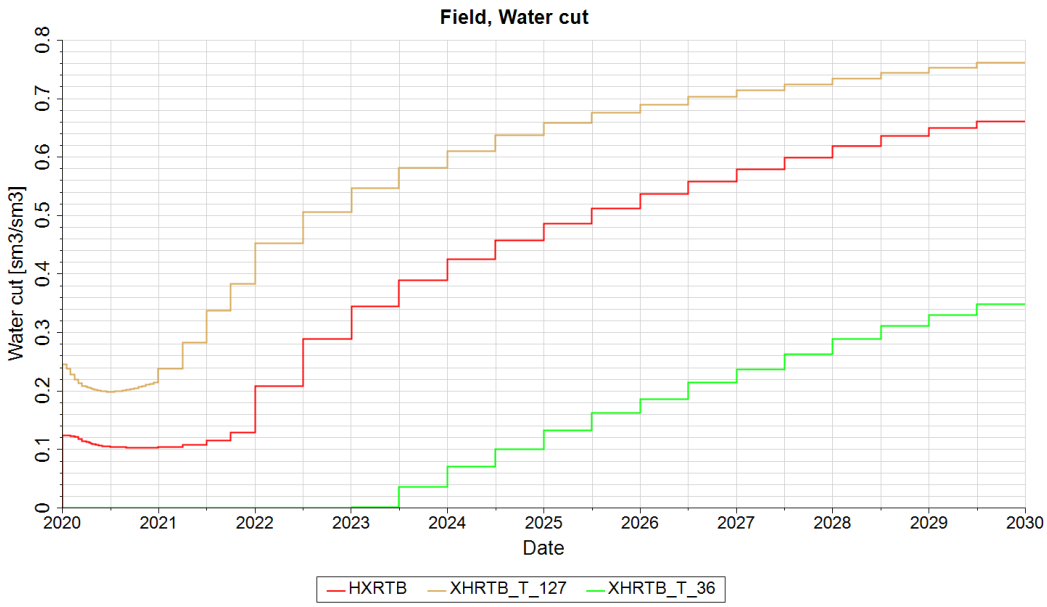


**Base Case**

| | Inj Brine | Form Brine |
|---|---|---|
| NACL | 0.486 | 2.570 |
| CACO3 | 0.008 | 0.042 |
| MGCL2 | 0.068 | 0.357 |
| CACL2 | 0.012 | 0.066 |
| NAHCO3 | 0.001 | 0.167 |
| NA2SO4 | 0.032 | 0.006 |

**Case 36**

| | IB | FB |
|---|---|---|
| NACL | 0.9719 | 2.570 |
| CACO3 | 0.016 | 0.042 |
| MGCL2 | 0.135 | 0.357 |
| CACL2 | 0.025 | 0.066 |
| NAHCO3 | 0.002 | 0.167 |
| NA2SO4 | 0.0016 | 0.006 |

**Case 127**

| | IB | FB |
|---|---|---|
| NACL | 0.664 | 2.570 |
| CACO3 | 0.012 | 0.042 |
| MGCL2 | 0.103 | 0.357 |
| CACL2 | 0.007 | 0.066 |
| NAHCO3 | 0.0004 | 0.167 |
| NA2SO4 | 0.0448 | 0.006 |

*Figure 45: Representative cases of the DoE including the brine speciation effect.*

Figure 46 shows a sensitivity analysis with different brine species, for the injections and formation brine. Brine species for the formation water are surrounded with a rectangle with continuous rounded corners, while brine species corresponding to the injection brine are surrounded with the same color rectangle, but with dashes. From this figure it can be observed the brine species for the formation water have more impact those same species for the injected water. Besides, the species with calcium and magnesium divalent cations are more impactful than the other salt species. Therefore, the higher the calcium and magnesium divalent cations in the formation brine compared with the injection brine, the higher the cumulative oil.

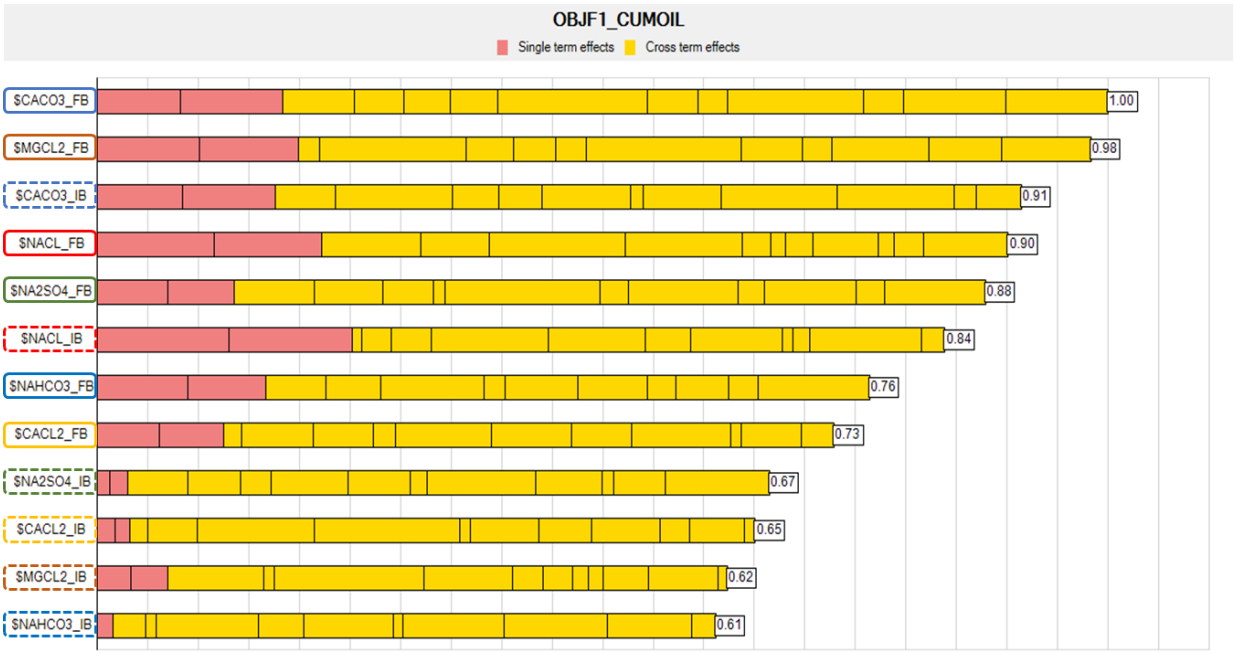


*Figure 46: Sensitivity analysis for the brine speciation for formation and injection brine.*

The maximum capillary pressure for high salinity is very impactful. The lower the maximum capillary pressure for high salinity, the higher the efficiency of the process. However, the maximum capillary pressure for low salinity has the least impact. Comparing the effect of the maximum capillary pressure, a slight change of the maximum capillary pressure for high salinity was more impactful than a huge change of the maximum capillary pressure for low salinity. In Figure 47 it is observed the effect of maximum capillary pressure on the recovery factor for all the cases of the design of experiments. The lower the maximum capillary pressure, the higher the recovery factor, indicating that the more oil-wet the reservoir, the better the effect of LSWI.

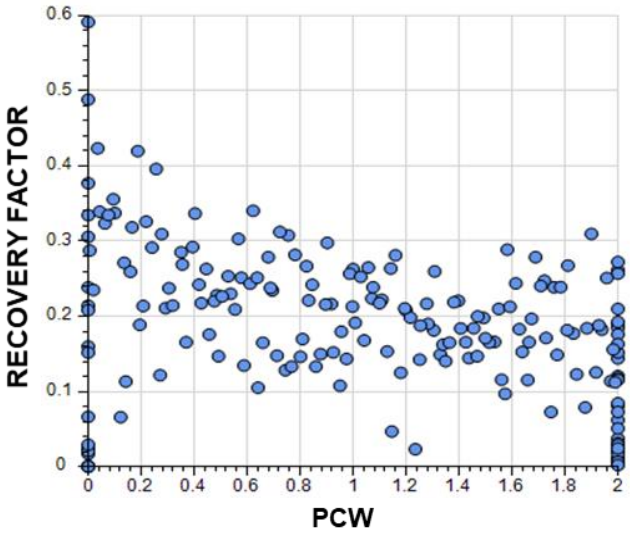


*Figure 47: Distribution of maximum capillary pressure of DoE cases Vs. Recovery factor.*

The API is another important parameter in the uncertainty. Figure 48 shows the impact of the API in the recovery factor, water cut and cumulative gas. The higher the API, the higher the cumulative gas in the system, the higher the recovery factor and the lower the water cut. This indicates LSWI has a better performance when the fluid in the reservoir has higher API, because increase the recovery factor and decrease the water cut.

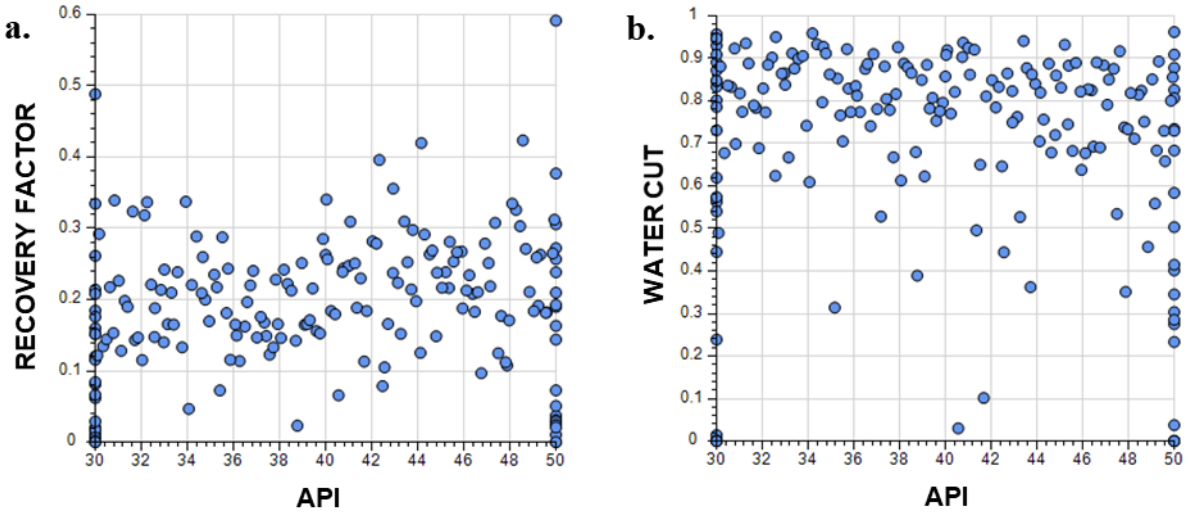

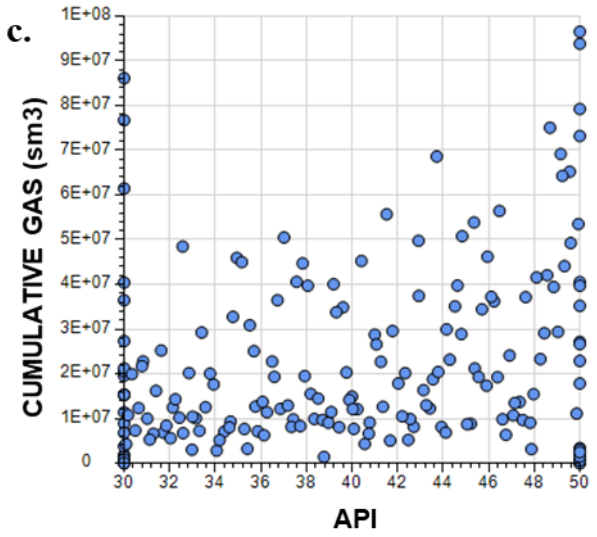


*Figure 48: Distribution of API for DoE cases Vs. Recovery factor (a), water cut (b) and cumulative gas (c)*

## 6. Effect of fluid model

So far, the evaluation of the low salinity water injection performance is done for high API fluid. This includes uncertainties and characterizations, results and analysis already presented in the last chapters. However, Low Salinity Water Injection (LSWI) evaluation was carried out for two different fluids: low API and high API. This was done with the aim to ascertain the effect of the two different fluids in the performance of LSWI.

In the next paragraphs will be summarized the contrasts between high and low API. In order to stated differences clear, it will be followed the same thesis organization so far, i.e. first, rock-physic saturation functions will be discussed, then brine speciation.

The low API crude has a base value of 25 API. The minimum and maximum values for the uncertainty are 20 and 30 API, respectively. The high API crude has base value of 40 API. The minimum and maximum values for the uncertainty are 30 and 50 API, respectively.

## 6.1 Rock-Physics Saturation Functions

The low salinity scaling function has a larger effect for high API than for low API. The water cut and the cumulative water are more affected by the low salinity scaling function. The effect of the scaling function on the water cut and recovery factor decreases from high to low API. Analyzing the recovery factor and the cumulative oil functions, the low salinity scaling function with capillary pressure is more relevant for low API than for high API. This can be observed in Figures 22 and 23.

The salt composition for the injection water and the salt compositions for the low salinity scaling function are less impactful for low API (Figures 24 and 25) than they are for high API (Figures 26 and 27). However, the most affecting variables in both low and high API are the saturation functions and the low salinity scaling function.

Figure 49 shows the effect of API in the recovery factor and water cut for the cases of the uncertainty and characterization, both for high and low API. An envelope is drawn to showcase the variation of the recovery factor with increasing API. Also, the water cut decreases with increasing the API, as shown in the envelope.

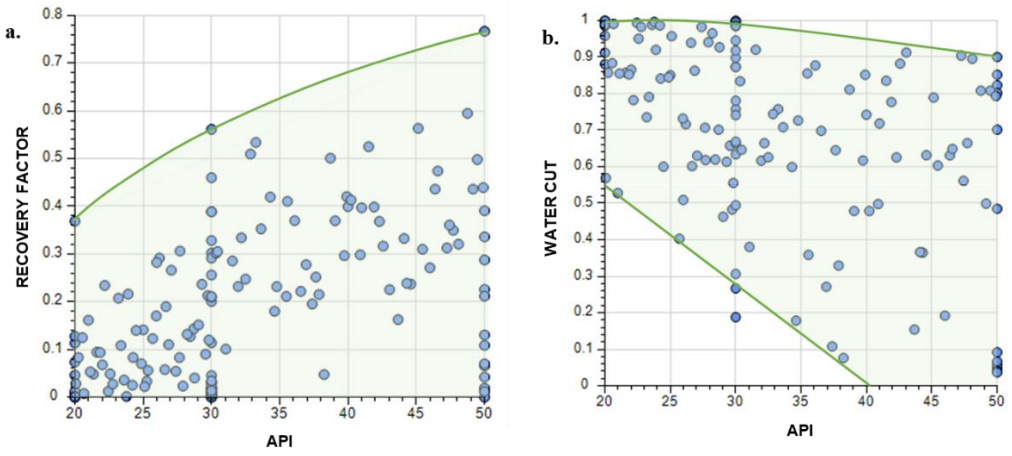


*Figure 49: Distribution of API for DoE cases Vs. Recovery factor (a) and water cut (b).*

From Figure 49 is possible to interpret that LSWI is more effective for high API fluids, because the recovery factor is increased, and the water cut is decreased. Higher recovery factor represents a higher profitability and lower water cut constitutes lower operating expenses. The values with recovery factor near to zero are acquired because the influence of other variables which are varying their values simultaneously with the change in API. Besides, the water cut values near zero are obtained by the changes of values for other variables.

## 6.2 Brine Speciation

Figure 50 shows the recovery efficiency for low and high API. Oil recovery efficiency for low API range from 0.01 to 0.09. For high API, oil recovery efficiency values go from 0.07 to 0.24. This huge difference in the oil recovery efficiency shows the effectiveness of LSWI for high API crudes. Nonetheless, this technique is applicable to low API crudes through an integrated reservoir evaluation.

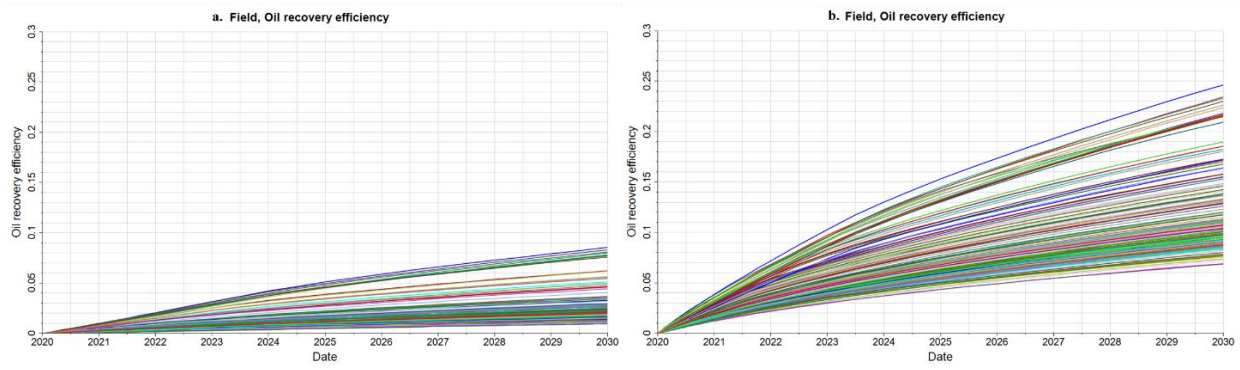


*Figure 50: Oil recovery efficiencies for low (a) and high (b) API DoE.*

# 7. Discussion/Limitations

Differences in the results of the rock saturation functions and the brine speciation evaluation rely on the ranges of the injected brine. The injected brine concentration values used for the rock saturation functions were up to 20 Kppm, while for brine speciation were up to 80 Kppm. Also, for the rock saturation functions evaluation the simulator used was ECLIPSE 100, while for the brine speciation evaluation the simulator used was INTERSECT.

Throughout the brine speciation assessment, the same percentage of brine species was maintained for the formation and injection brine. It is recommended to perform uncertainty and optimization for brine speciation with different ratios between the species. Also, the partition of each specie into its anions and cations could be assessed, in order to ascertain the impact of each ion in LSWI.

This study was limited to the API range from 20 to 50. However, the effect of low salinity water injection could be assessed in heavy oils, mainly where water flooding is being or is expected to be developed.

In this thesis, LSWI was evaluated as a single EOR mechanism. Nonetheless, the synergy of this process with other EOR techniques made it suitable to increase the application range. Other EOR techniques include polymer flooding, surfactant flooding and other chemical processes.

# 8. Conclusions

The saturation functions play a very important role in modeling LSWI EOR. Some of the salient observations and conclusions from the investigation are as follows:

- The most impactful factors affecting LSWI performance are relative-permeability scaling and to a lesser extent capillary-pressure scaling.
- Either the initial high salinity state or the change brought about due to the injection of low salinity water, both are relevant in the LSWI assessment. In other words, the initial wettability of the system and the wettability alteration effected by LSWI are important in the evaluation of this EOR technique. The allocation of saturation functions to each rock-type confirms the hypothesis from the literature regarding the initial wettability of the reservoir is an important parameter in the screening criteria.
- The performance LSWI may depend on the initial water saturation. The main reason can be attributed to the fact that the saturation functions are strongly dependent on the initial water saturation. Thus, with increasing initial water saturation, the impact of low salinity effect decreases.
- Rock-type dependency in saturation functions provides a more accurate approach to evaluation of LSWI project performance. This facies-dependency narrows the range of plausible results and provides better estimates of the recovery factor, water cut, cumulative oil, water and gas.

Brine speciation of water injection must be done in order to accurately model the effects of each brine on LSWI. In brine speciation, we introduce the presence of other salt ions in the aqueous phase than simply sodium chloride. In the study of LSWI without brine speciation, we overlook

the presence of other ions and the salinity of the water is based on equivalent sodium chloride concentration. The most salient conclusions from the brine speciation are as follows:

- Brine speciation reveals the capillary pressure can play prominent role in LSWI performance.
- Brine speciation reveals the native wettability of the system is more important than the change brought about by low salinity. This is a conflicting observation related to the relative permeability results. This is related to chemical interaction of different species with the rock and the in-situ brine. However, the influence of both native wettability and the change brought about by low salinity should be accurately modeled.

Low salinity water injection behaves differently with changing the fluid model. Therefore, differences between low and high API fluids were ascertained, with the following conclusion:

- LSWI has a better performance in high API crudes, because the recovery factor is increased, and the water cut is decreased. However, LSWI is still applicable to low API fluids.

## References

Al-Qattan A., Sanaseeri A., Al-Saleh Z., Singh B., Al-Kaaoud H., Delshad M., Hernandez R., Winoto W., Badham S., Bouma C., Brown J. and Kumer K. (2018). Low salinity waterflood and low salinity polymer injection in the Wara reservoir of the greater Burgan field. 26-28 March. EOR conference at oil and gas west Asia. Muscat, Oman. SPE. https://doi.org/10.2118/190481-MS

Brodie J. and Jerauld G. (2014) Impact of Salt Diffusion on Low-Salinity Enhanced Oil Recovery. Improved Oil Recovery Symposium. 12-16 April. Tulsa, Oklahoma, USA. BP. SPE. https://doi.org/10.2118/169097-MS

Callegaro C., Bartosek M., Nobili M., Masserano F., Pollero M., Mousa D. and Mahmoud M. (2015). Design and implementation of low salinity waterflood in a north African brown field. Abu Dhabi International Petroleum Exhibition and Conference. 9-12 November. UAE. SPE. https://doi.org/10.2118/177590-MS

Dang C., Nghiem L., Nguyen N. and Chen Z. (2015). Practical concerns and principle guidelines for screening, implementation, design and optimization of low salinity waterflooding. Western regional meeting. 27 -30 April. Garden Groove, California. SPE. https://doi.org/10.2118/174008-MS

Jerauld G., Lin C., Webb K. and Seccombe J. (2008). Modeling Low-Salinity Waterflooding. Annual Technical Conference and Exhibition. 24-27 September. San Antonio, Texas, USA. SPE. https://doi.org/10.2118/102239-MS

Lager A., Webb K., Black C., Singleton M. and Sorbie K. (2006). Low Salinity Oil Recovery – An experimental investigation. International symposium of the Society of Core Analysts. 12-16 September. Trondheim, Norway. SPWLA.

Nayar, Kishor G., Mostafa H. Sharqawy, Leonardo D. Banchik, and John H. Lienhard V. "Thermophysical Properties of Seawater: A Review and New Correlations That Include Pressure Dependence." Desalination 390 (July 2016): 1-24. http://dx.doi.org/10.1016/j.desal.2016.02.024

Romanuka J., Hofman J., Ligthelm D., Suijkerbuijk B., Marcelis A., Oedai S., Brussee N., van der Linde H., Aksulu H. and Austad T. (2012). Low Salinity EOR in Carbonates. Eighteenth Improved Oil Recovery Symposium. 14-18 April. Tulsa, Oklahoma, USA. SPE, Shell and University of Stavanger. https://doi.org/10.2118/153869-MS

Rostami P, Mehraban M, Sharifi M, Dejam M and Ayatollahi S (2019). "Effect of water salinity on oil/brine interfactial behavior during low salinity waterflooding: A mechanistic study". Science Direct. https://doi.org/10.1016/j.petlm.2019.03.005

Rotondi M., Callegaro C., Masserano F., and Bartosek M. (2014). Low Salinity Water Injection: ENI's Experience. Abu Dhabi International Petroleum Exhibition and Conference. 10-13 November. UAE. SPE. https://doi.org/10.2118/171794-MS

Sorop T., Suijkerbuijk B., Masalmeh S., Looijer M., Parker A., Dindoruk D., Goodyear S. and Al-Qarshubi I. (2013). Integrated approach in eploying Low Salinity Waterflooding. Enhanced Oil Recovery Conference. 2-4 July. Kuala Lumpur, Malaysia. SPE. https://doi.org/10.2118/165277-MS

Tang G. and Morrow N. (1999). Influence of brine composition and fines migration on crude oil/brine/rock interactions and oil recovery. University of Wyoming. USA. Journal of Petroleum Science and Engineering 24. https://doi.org/10.1016/S0920-4105(99)00034-0

Walid E. and Sepehrnoori K. (2017). Low salinity and engineered water injection for sandstone and carbonate reservoirs. USA. Elsevier.

Webb K., Black C. and Al-Ajeel H. (2004). Low Salinity Oil Recovery-Log-Inject-Log. Fourteenth Symposium on Improved Oil Recovery. 17-21 April. Tulsa, Oklahoma, USA. SPE. https://doi.org/10.2118/89379-MS

# Appendix. Sensitivity Analysis for all DoE

Sensitivity analysis for relative permeability scaling - Low API

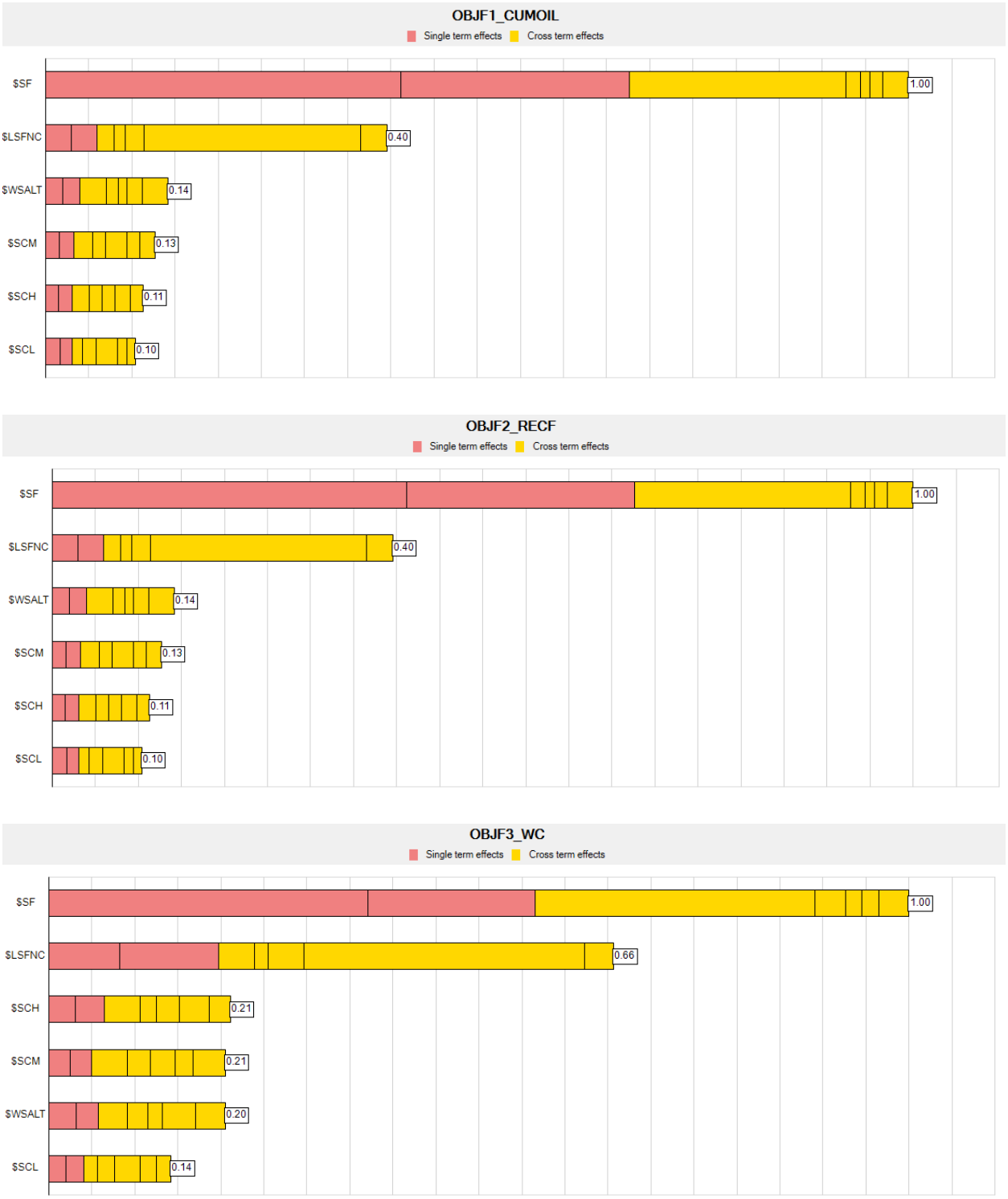

Sensitivity analysis for capillary pressure scaling - Low API

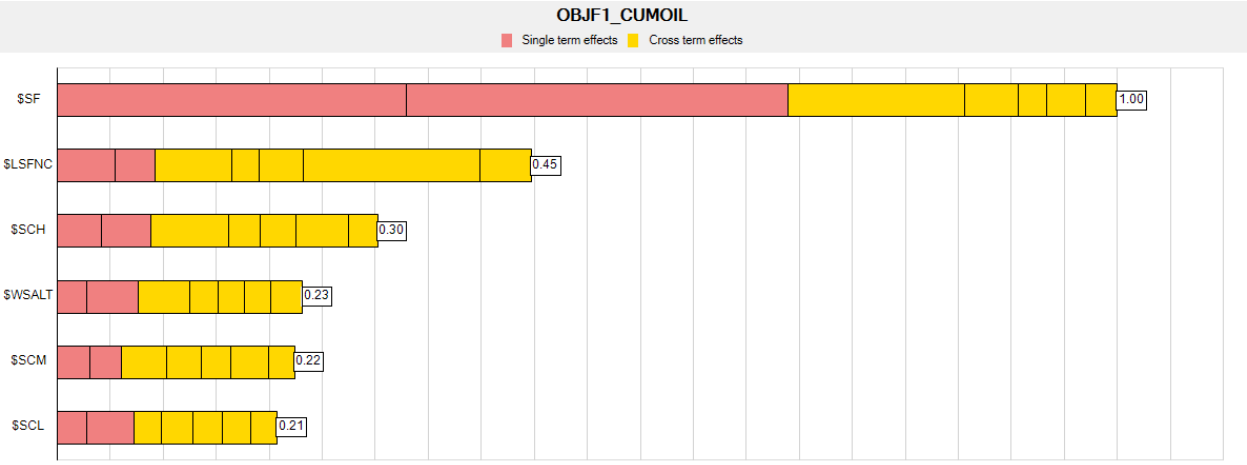


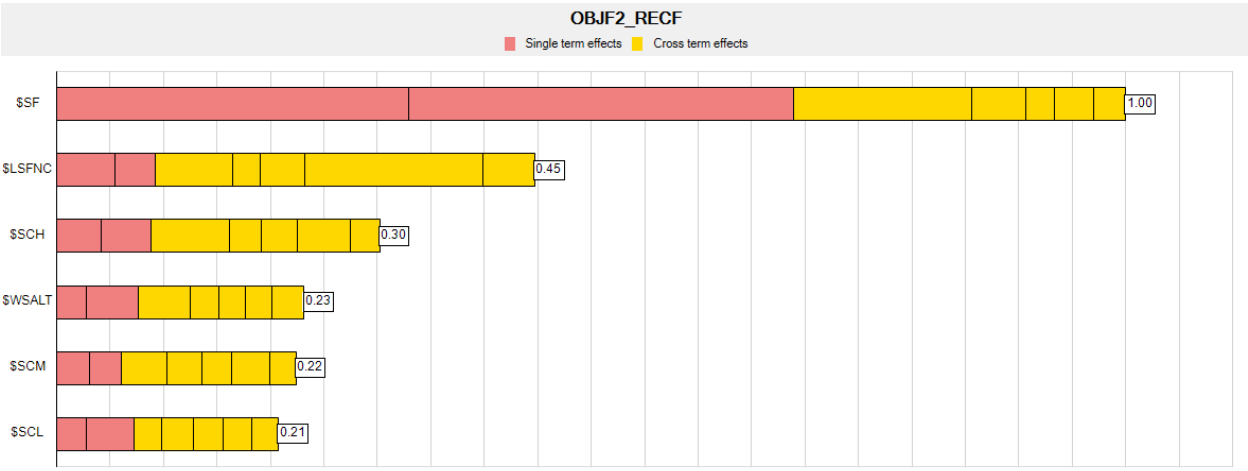


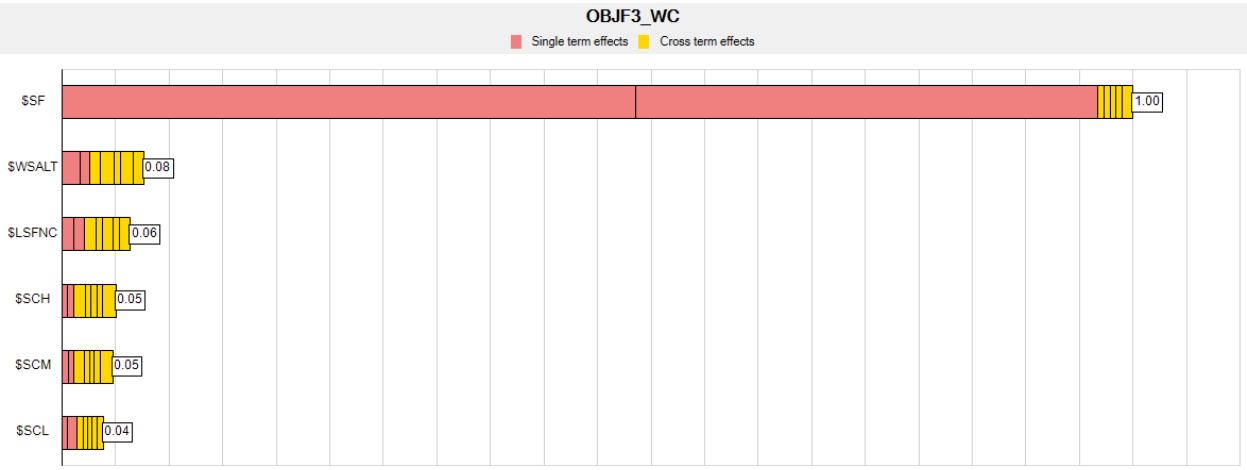

Sensitivity analysis for relative permeability and capillary pressure scaling - Low API

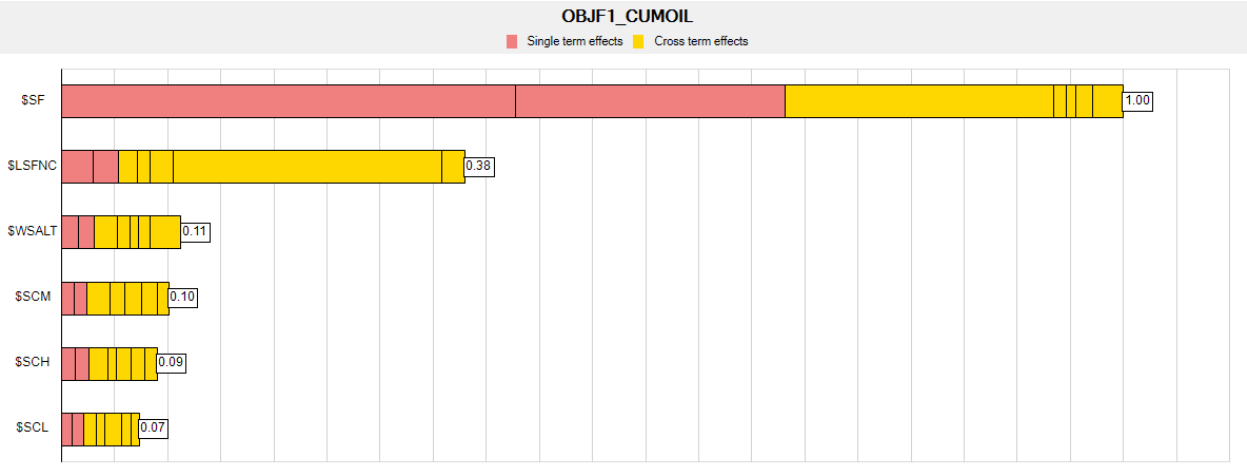


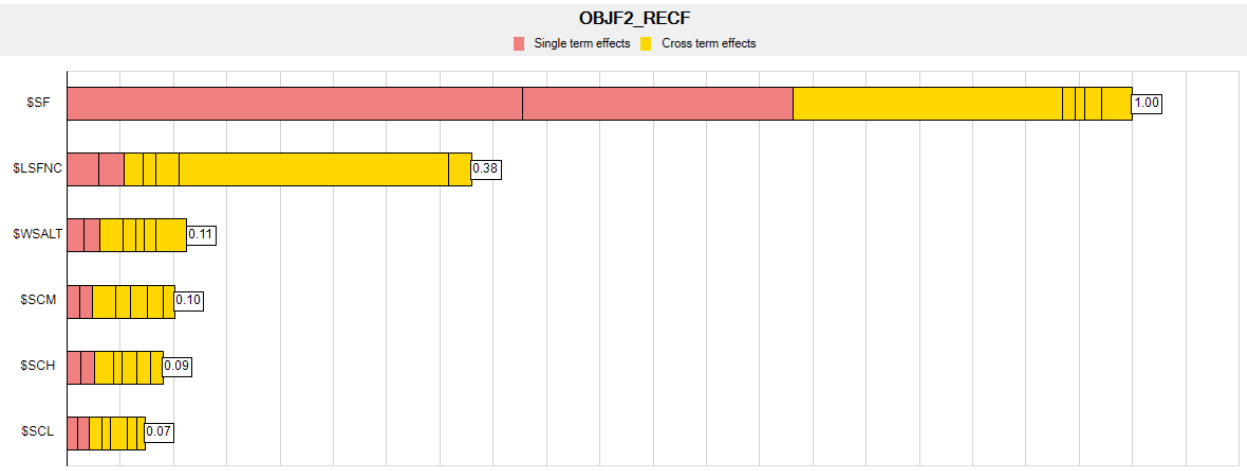


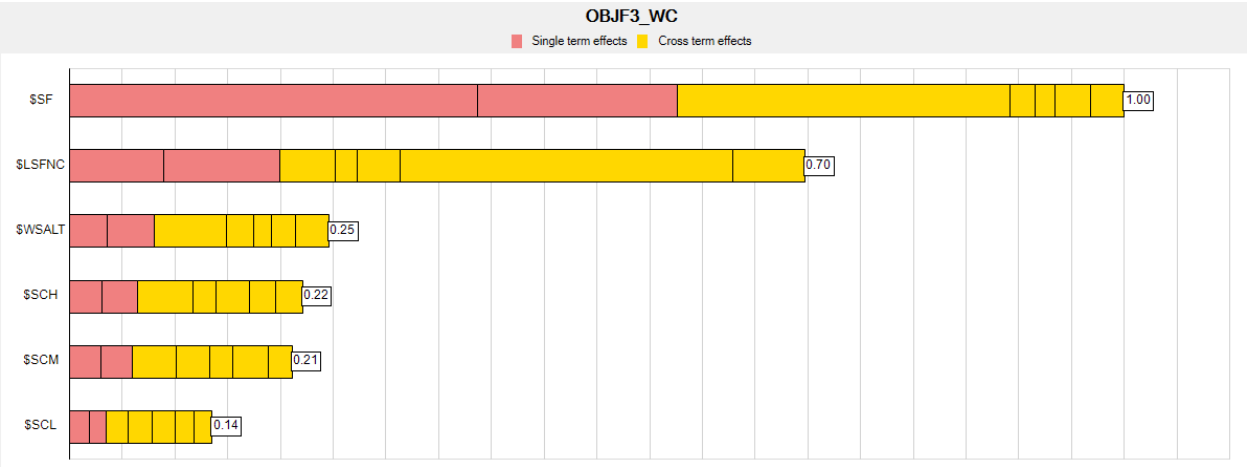

Sensitivity analysis for relative permeability scaling - High API

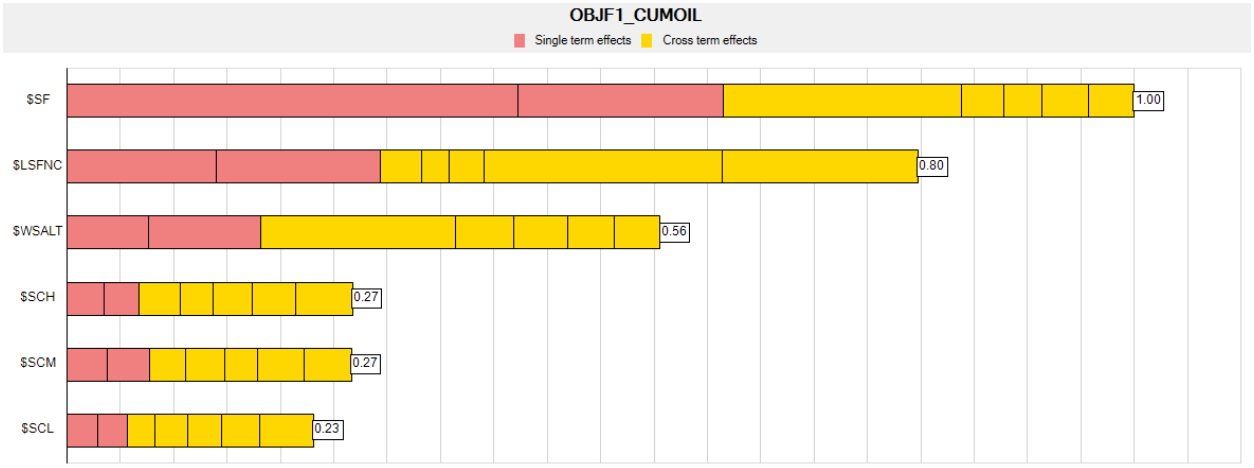


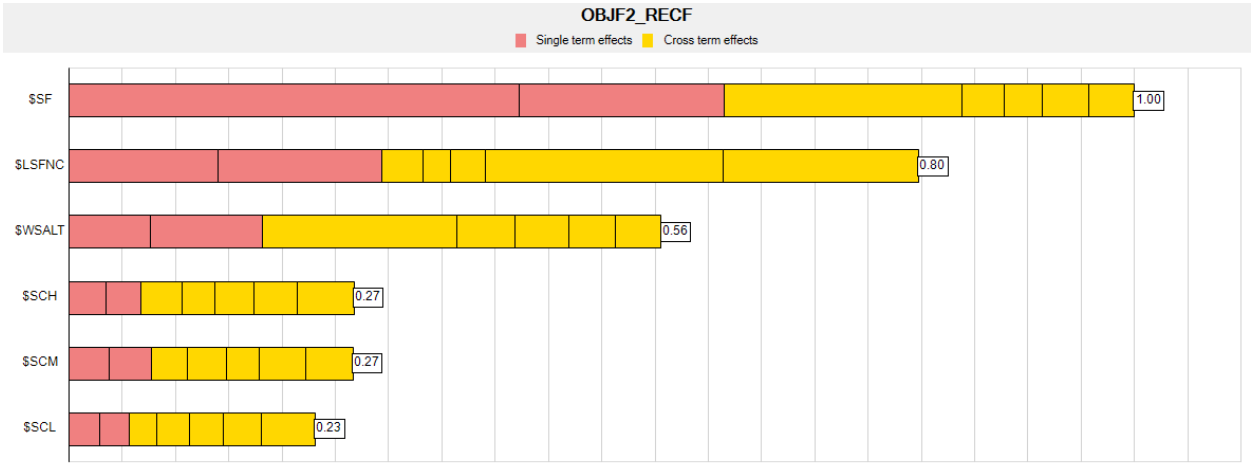


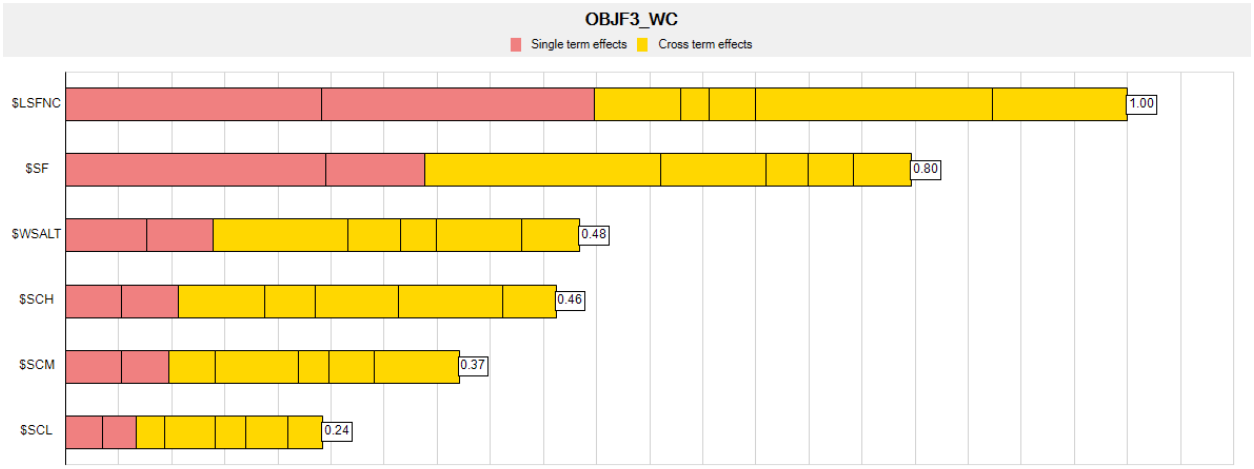

Sensitivity analysis for capillary pressure scaling - High API

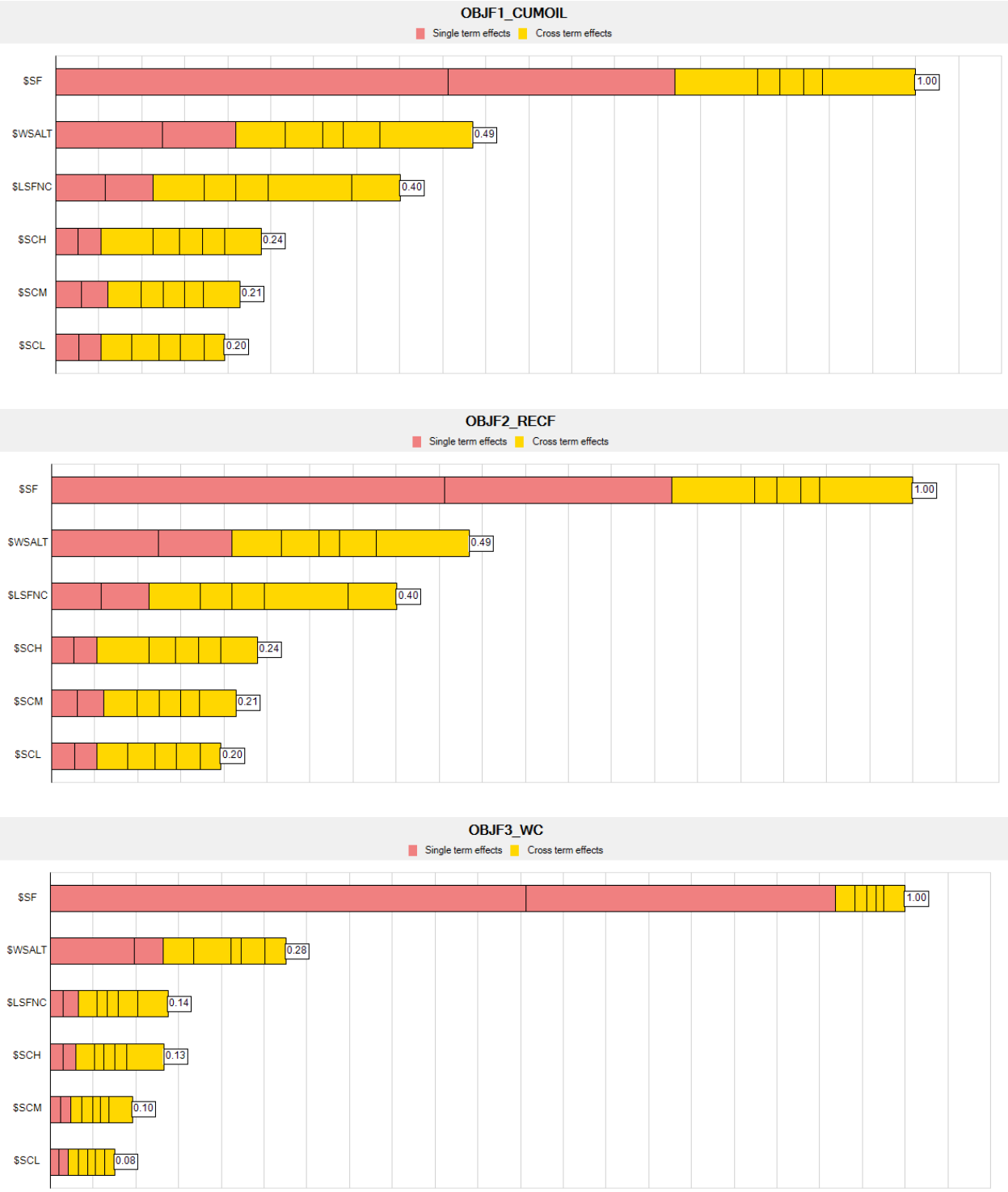

Sensitivity analysis for relative permeability and capillary pressure scaling - High API

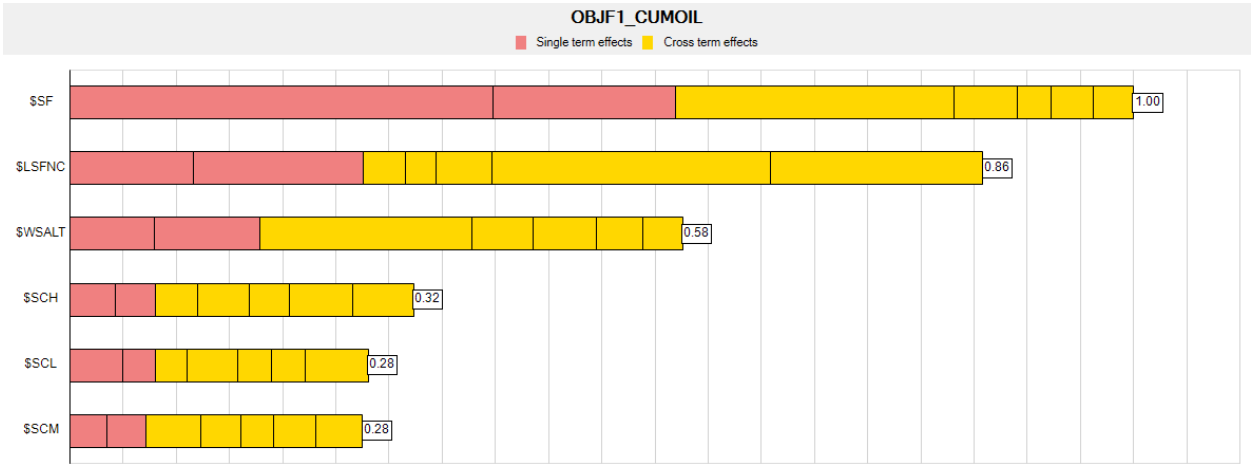


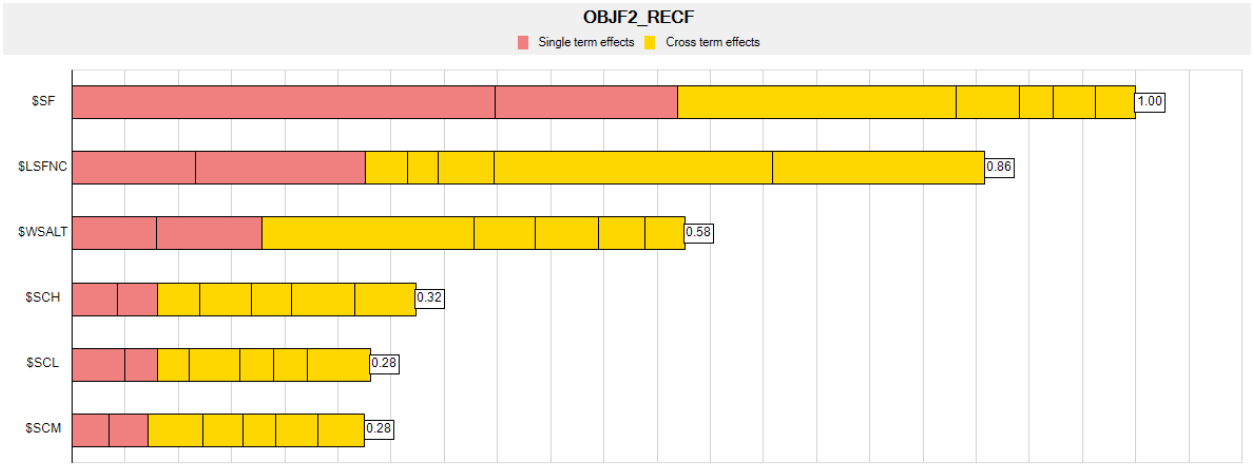


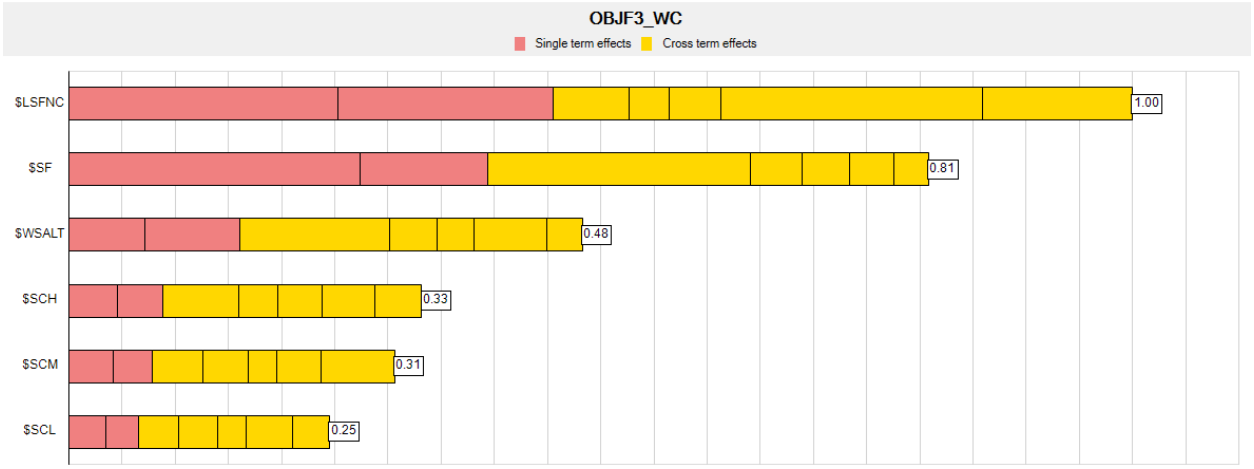

Sensitivity analysis for relative permeability and capillary pressure scaling with endpoints uncertainty - High API

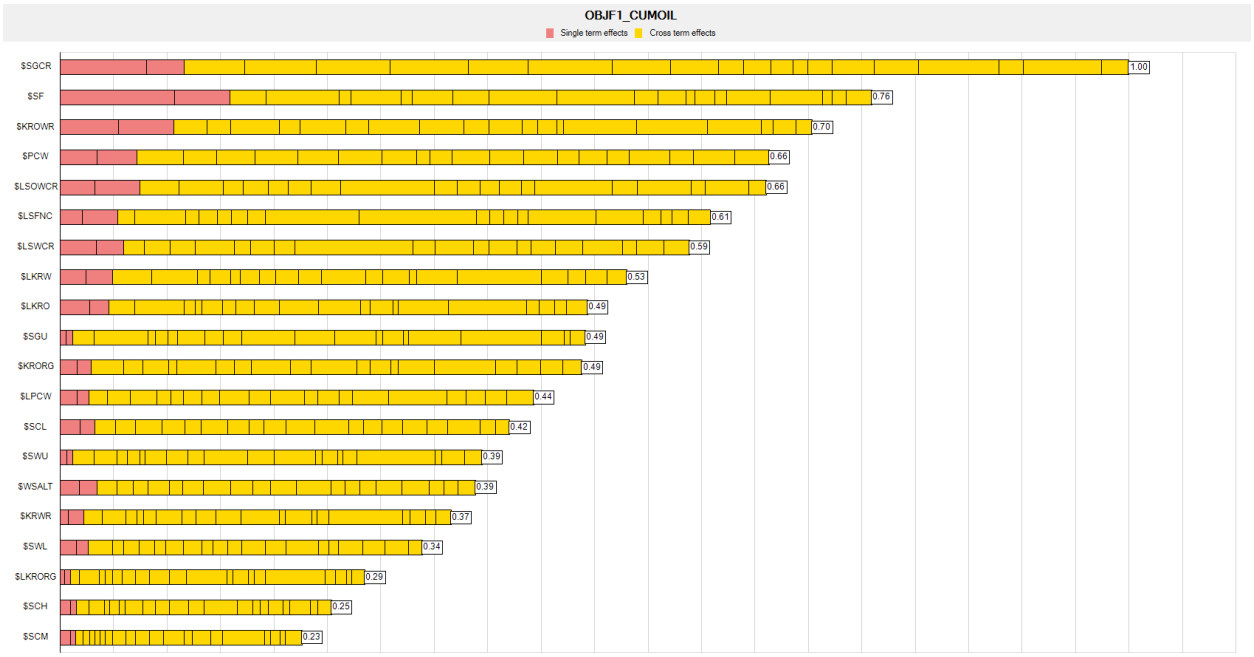


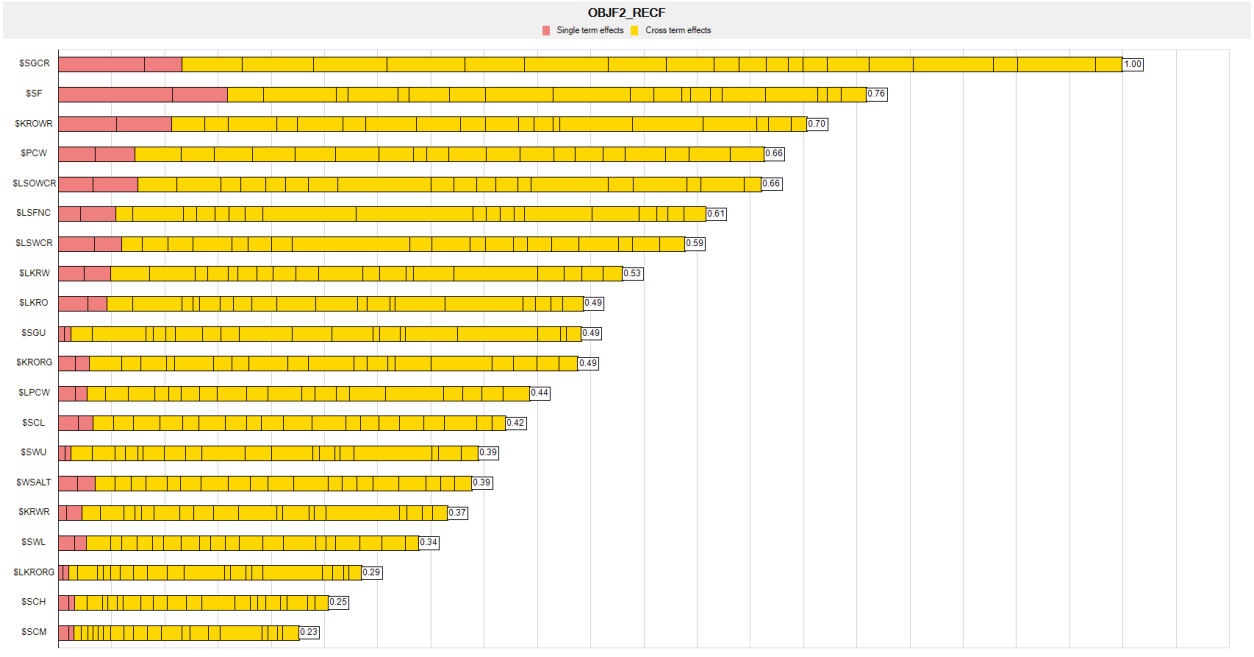

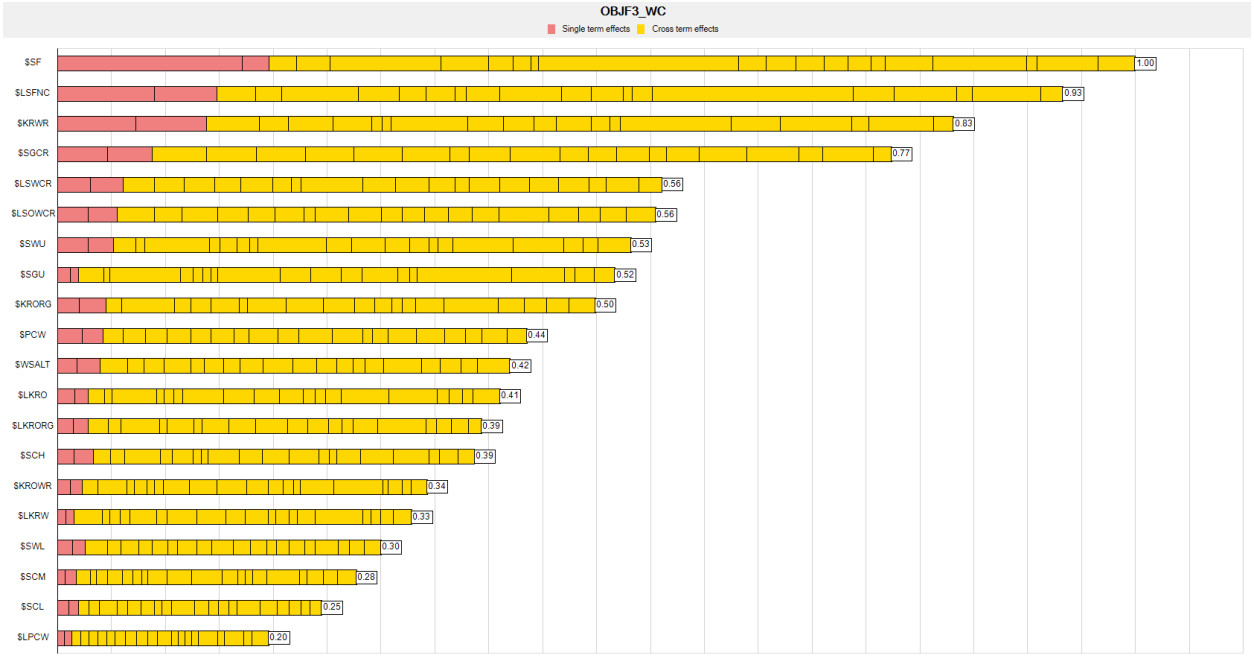
OBJF3_WC
Single term effects
Cross term effects
$SF 1.00
$LSFNC 0.93
$KRWR 0.83
$SGCR 0.77
$LSWCR 0.56
$LSOWCR 0.56
$SWU 0.53
$SGU 0.52
$KRORG 0.50
$PCW 0.44
$WSALT 0.42
$LKRO 0.41
$LKRORG 0.39
$SCH 0.39
$KROWR 0.34
$LKRW 0.33
$SWL 0.30
$SCM 0.28
$SCL 0.25
$LPCW 0.20

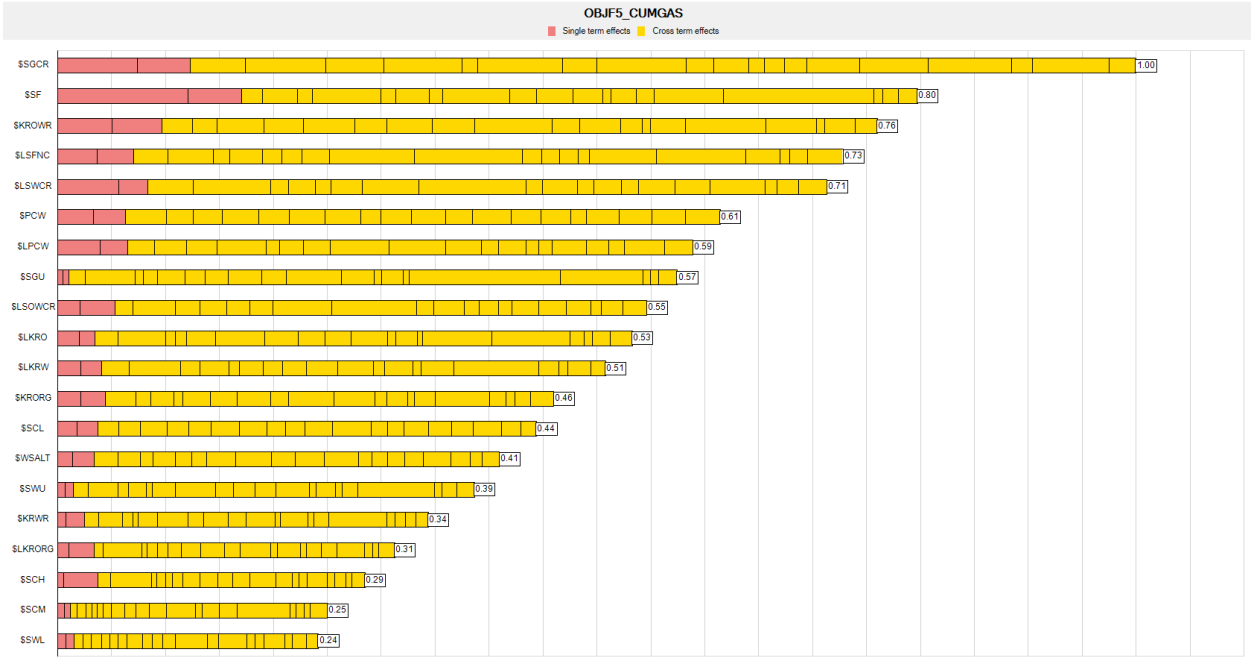
OBJF5_CUMGAS
Single term effects
Cross term effects
$SGCR 1.00
$SF 0.80
$KROWR 0.76
$LSFNC 0.73
$LSWCR 0.71
$PCW 0.61
$LPCW 0.59
$SGU 0.57
$LSOWCR 0.55
$LKRO 0.53
$LKRW 0.51
$KRORG 0.46
$SCL 0.44
$WSALT 0.41
$SWU 0.39
$KRWR 0.34
$LKRORG 0.31
$SCH 0.29
$SCM 0.25
$SWL 0.24

Sensitivity analysis for relative permeability and capillary pressure scaling with endpoints uncertainty - Low API

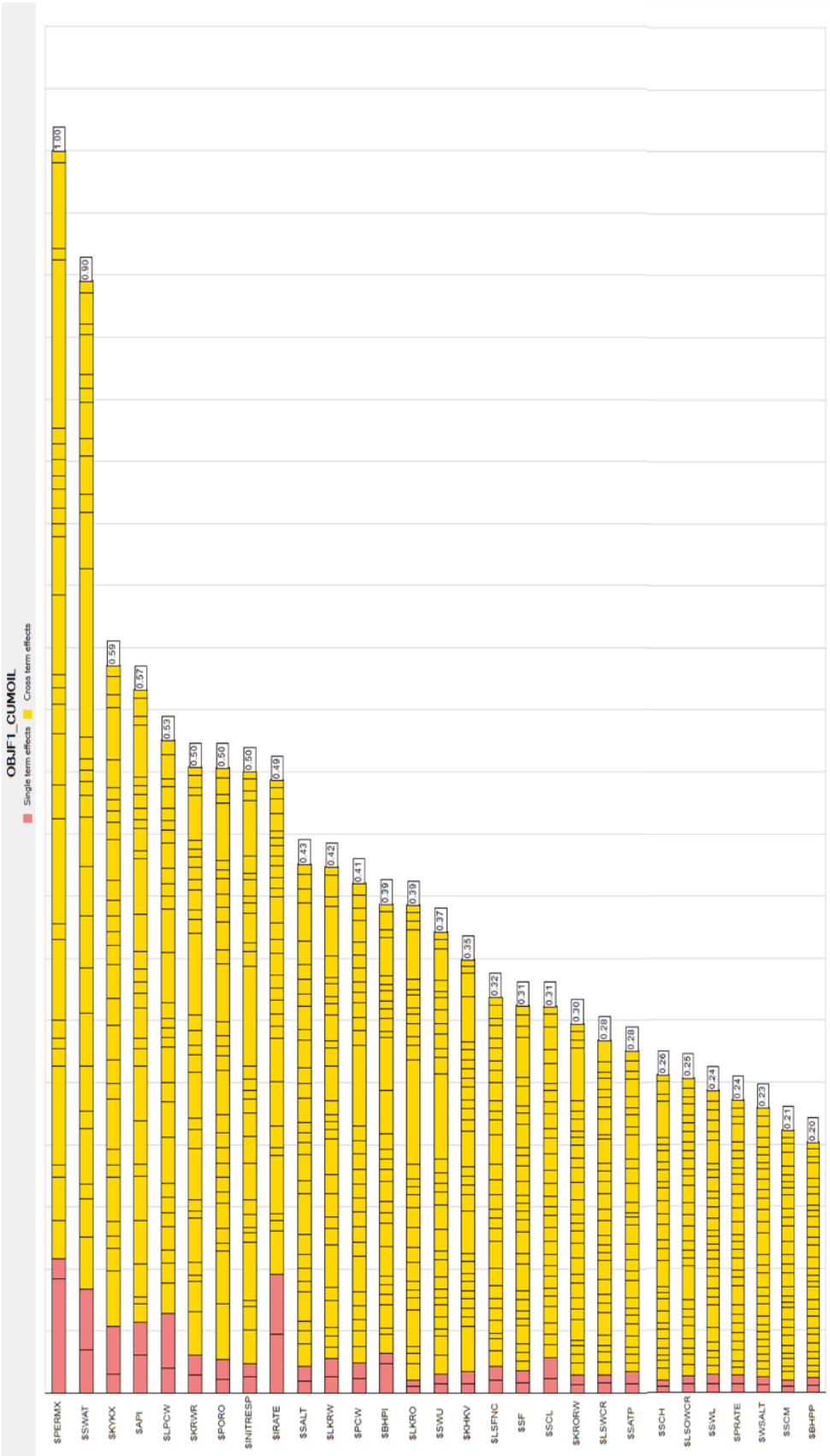
OBJF1_CUMOIL
Single term effects
Cross term effects
$PERMX
$SWAT
$KYKX
$API
$LPCW
$KRWR
$PORO
$INITRESP
$IRATE
$SALT
$LKRW
$PCW
$BHPI
$LKRO
$SWU
$KHKV
$LSFNC
$SF
$SCL
$KRORW
$LSWCR
$SATP
$SCH
$LSOWCR
$SWL
$PRATE
$WSALT
$SCM
$BHPP
1.00
0.90
0.59
0.57
0.53
0.50
0.50
0.50
0.49
0.43
0.42
0.41
0.39
0.39
0.37
0.35
0.32
0.31
0.31
0.30
0.28
0.28
0.26
0.25
0.24
0.24
0.23
0.21
0.20

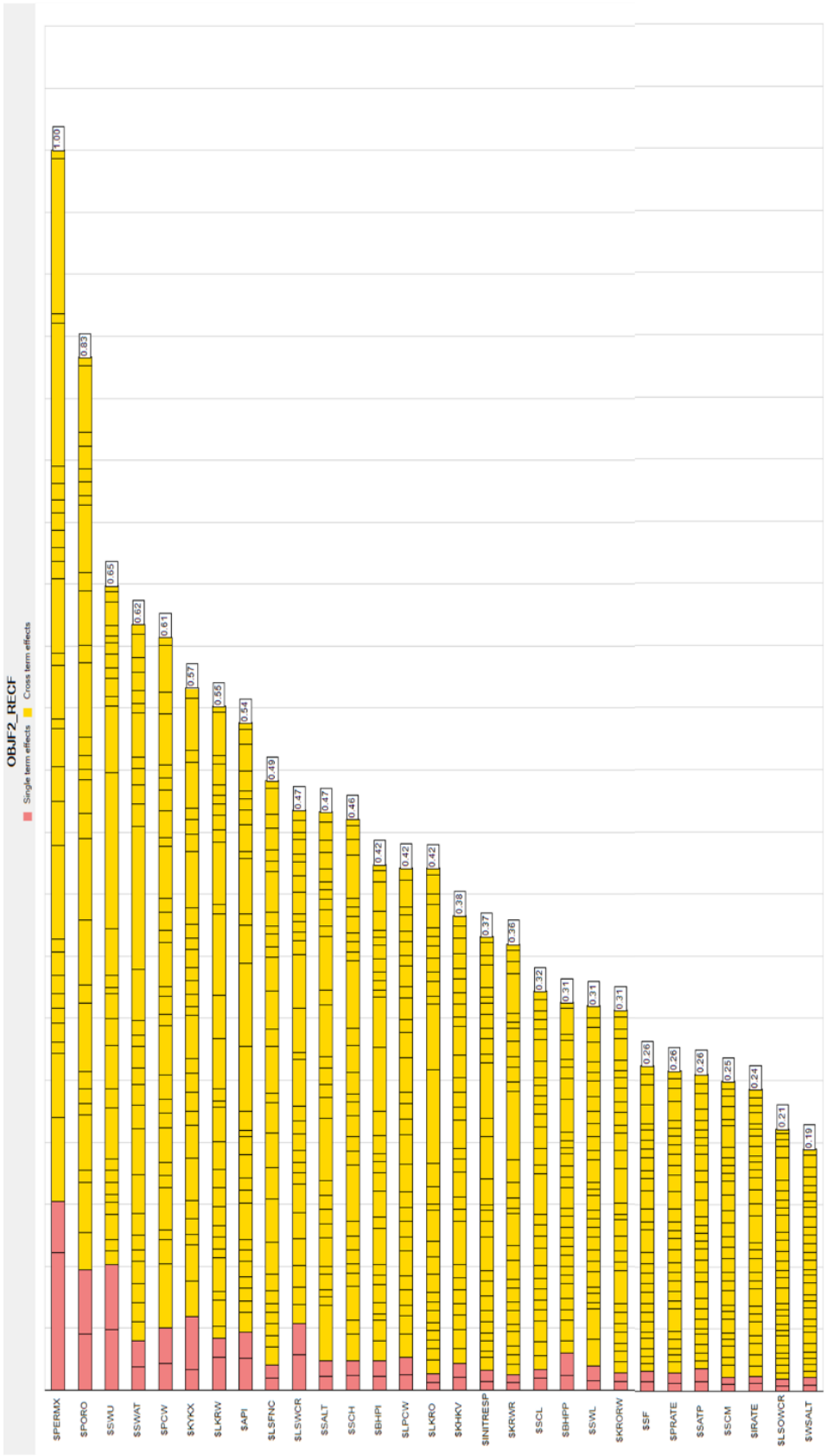
OBJF2_RECF
Single term effects
Cross term effects
1.00
0.83
0.65
0.62
0.61
0.57
0.55
0.54
0.49
0.47
0.47
0.46
0.42
0.42
0.42
0.38
0.37
0.36
0.32
0.31
0.31
0.31
0.26
0.26
0.26
0.25
0.24
0.21
0.19
$PERMX
$PORO
$SWU
$SWAT
$PCW
$KYKX
$LKRW
$API
$LSFNC
$LSWCR
$SALT
$SCH
$BHPI
$LPCW
$LKRO
$KHKV
$INITRESP
$KRWR
$SCL
$BHPP
$SWL
$KRORW
$SF
$PRATE
$SATP
$SCM
$IRATE
$LSOWCR
$WSALT

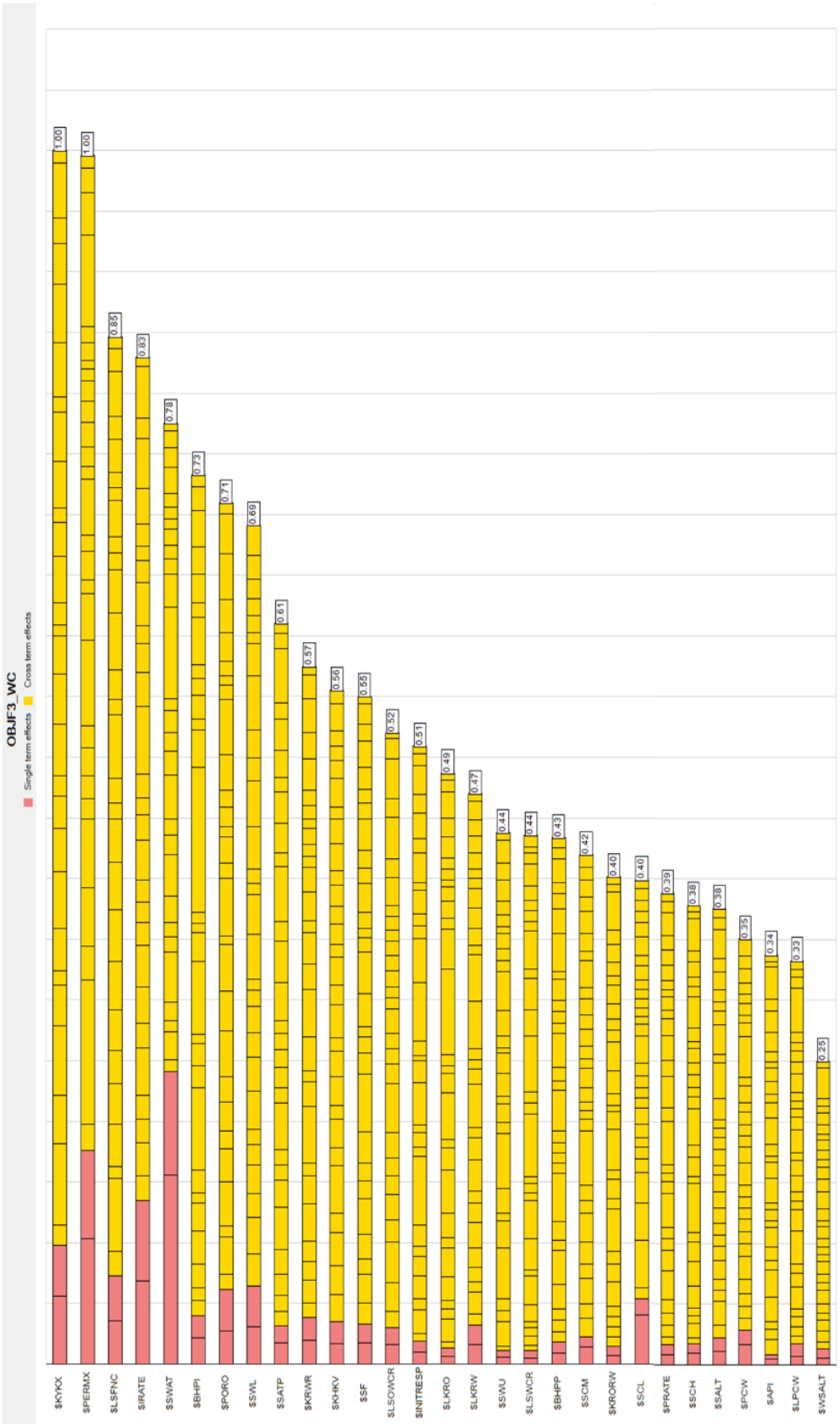
OBJF3_WC
Single term effects
Cross term effects
1.00
1.00
0.85
0.83
0.78
0.73
0.71
0.69
0.61
0.57
0.56
0.55
0.52
0.51
0.49
0.47
0.44
0.44
0.43
0.42
0.40
0.40
0.39
0.38
0.38
0.35
0.34
0.33
0.25
$KYKX
$PERMX
$LSFNC
$IRATE
$SWAT
$BHPI
$PORO
$SWL
$SATP
$KRWR
$KHKV
$SF
$LSOWCR
$INITRESP
$LKRO
$LKRW
$SWU
$LSWCR
$BHPP
$SCM
$KRORW
$SCL
$PRATE
$SCH
$SALT
$PCW
$API
$LPCW
$WSALT

Sensitivity analysis for relative permeability and capillary pressure scaling with endpoints uncertainty and other parameters - High API

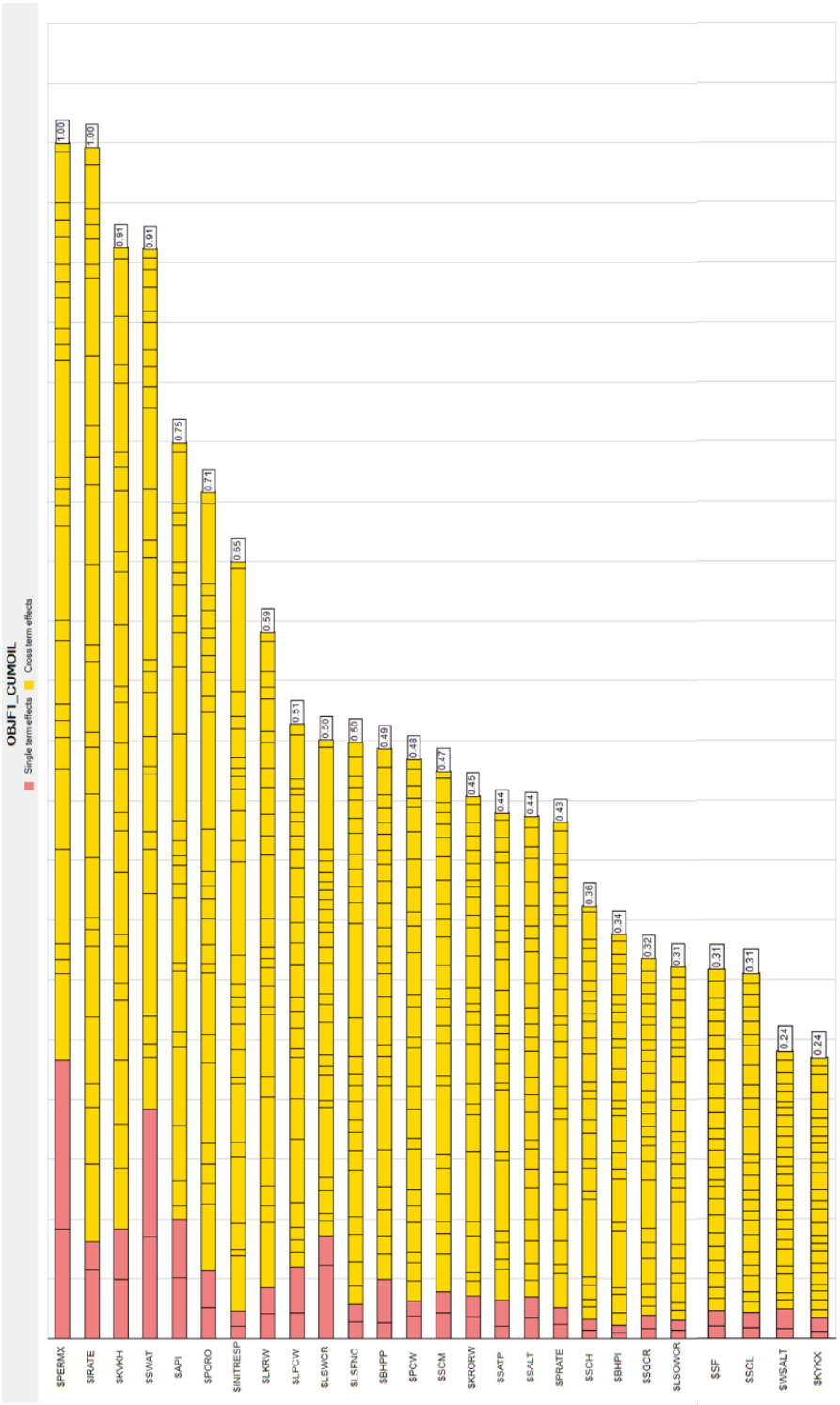

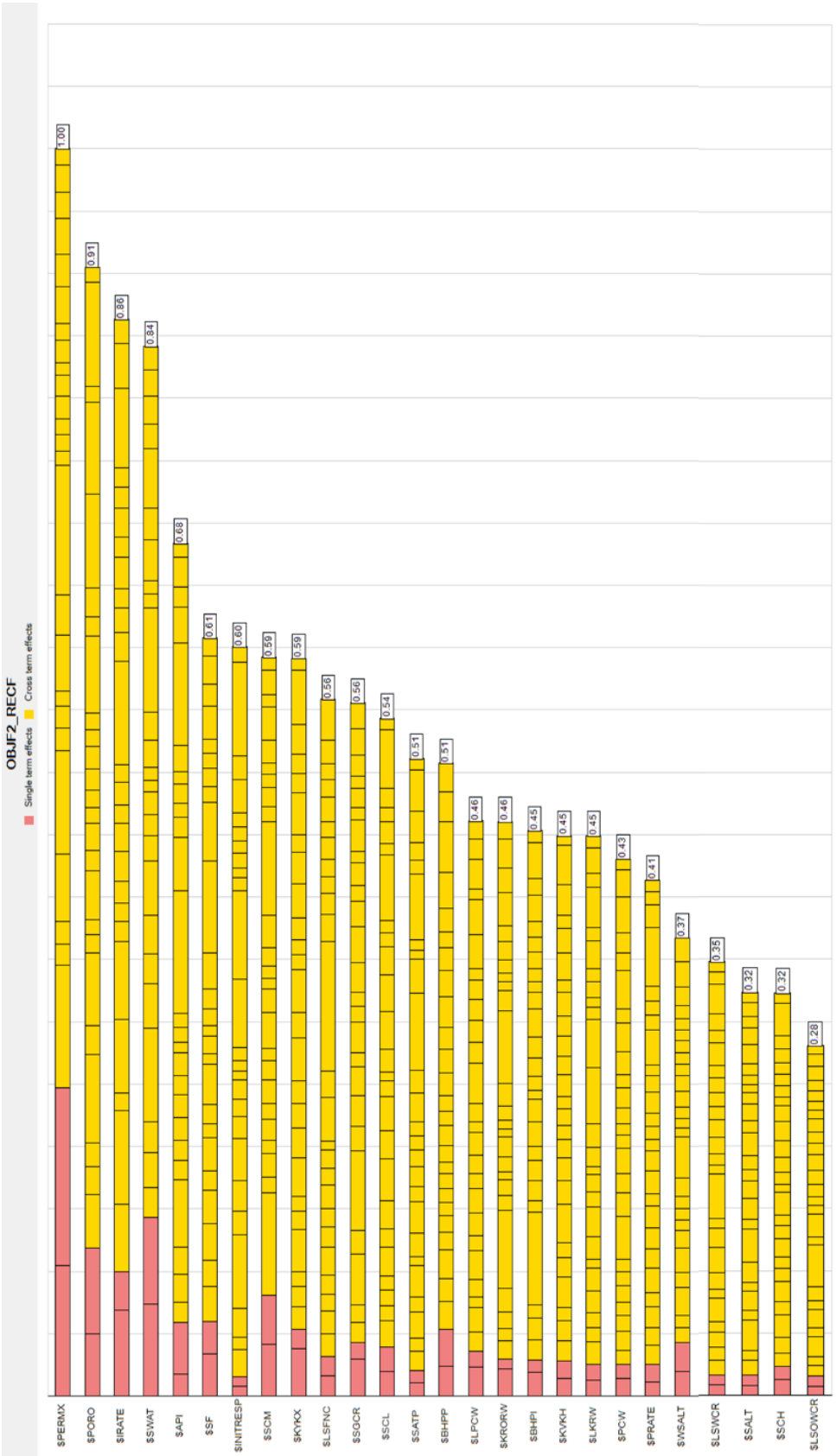
OBJF2_RECF
Single term effects
Cross term effects
1.00
0.91
0.86
0.84
0.68
0.61
0.60
0.59
0.59
0.56
0.56
0.54
0.51
0.51
0.46
0.46
0.45
0.45
0.45
0.43
0.41
0.37
0.35
0.32
0.32
0.28
$PERMX
$PORO
$IRATE
$SWAT
$API
$SF
$INITRESP
$SCM
$KYKX
$LSFNC
$SGCR
$SCL
$SATP
$BHPP
$LPCW
$KRORW
$BHPI
$KVKH
$LKRW
$PCW
$PRATE
$WSALT
$LSWCR
$SALT
$SOH
$LSOWCR

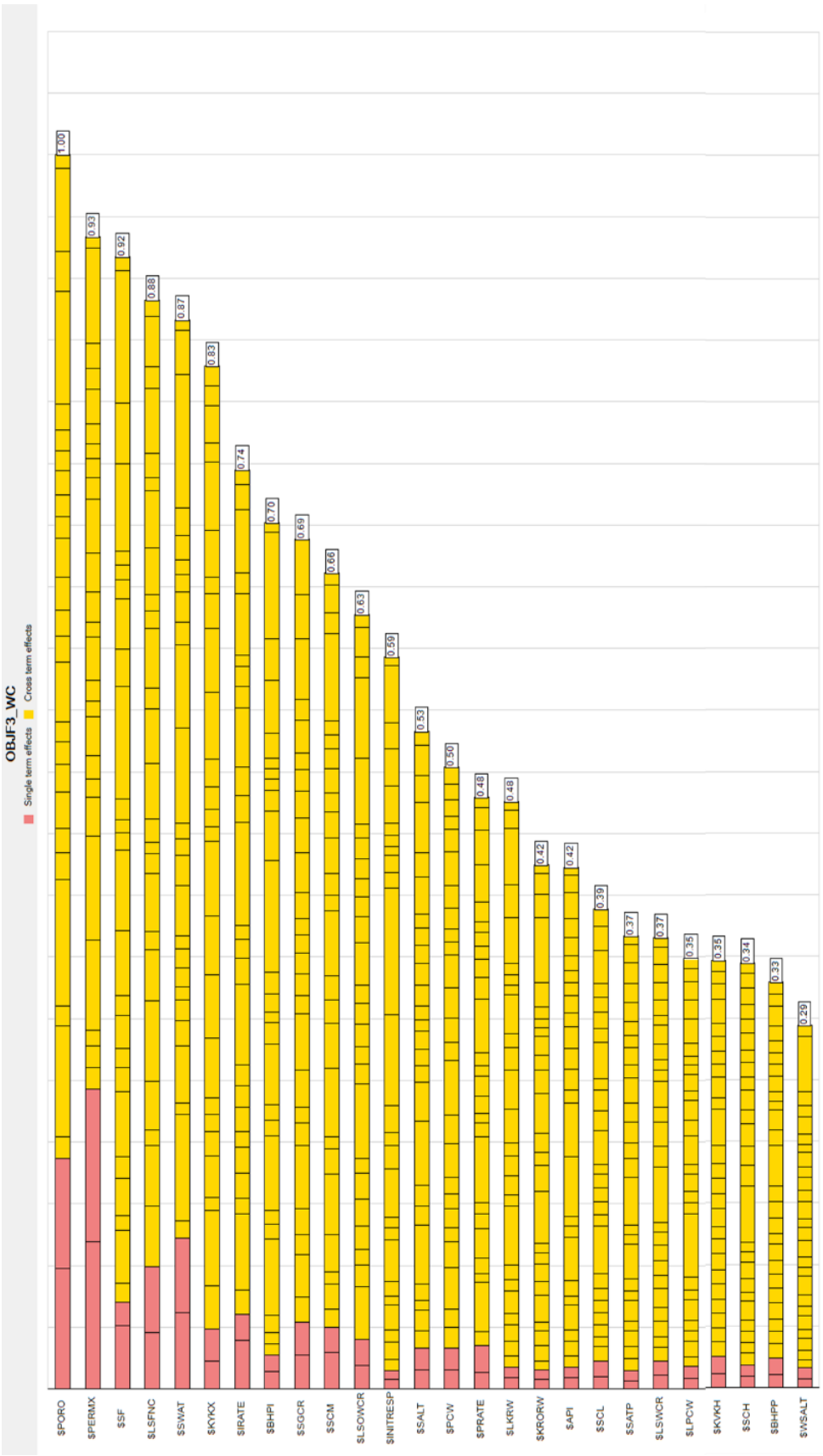
OBJF3_WC
Single term effects
Cross term effects
1.00
0.93
0.92
0.88
0.87
0.83
0.74
0.70
0.69
0.66
0.63
0.59
0.53
0.50
0.48
0.48
0.42
0.42
0.39
0.37
0.37
0.35
0.35
0.34
0.33
0.29
$PORO
$PERMX
$SF
$LSFNC
$SWAT
$KYKX
$IRATE
$BHPI
$SGCR
$SCM
$LSOWCR
$INITRESP
$SALT
$PCW
$PRATE
$LKRW
$KRORW
$API
$SCL
$SATP
$LSWCR
$LPCW
$KVKH
$SCH
$BHPP
$WSALT

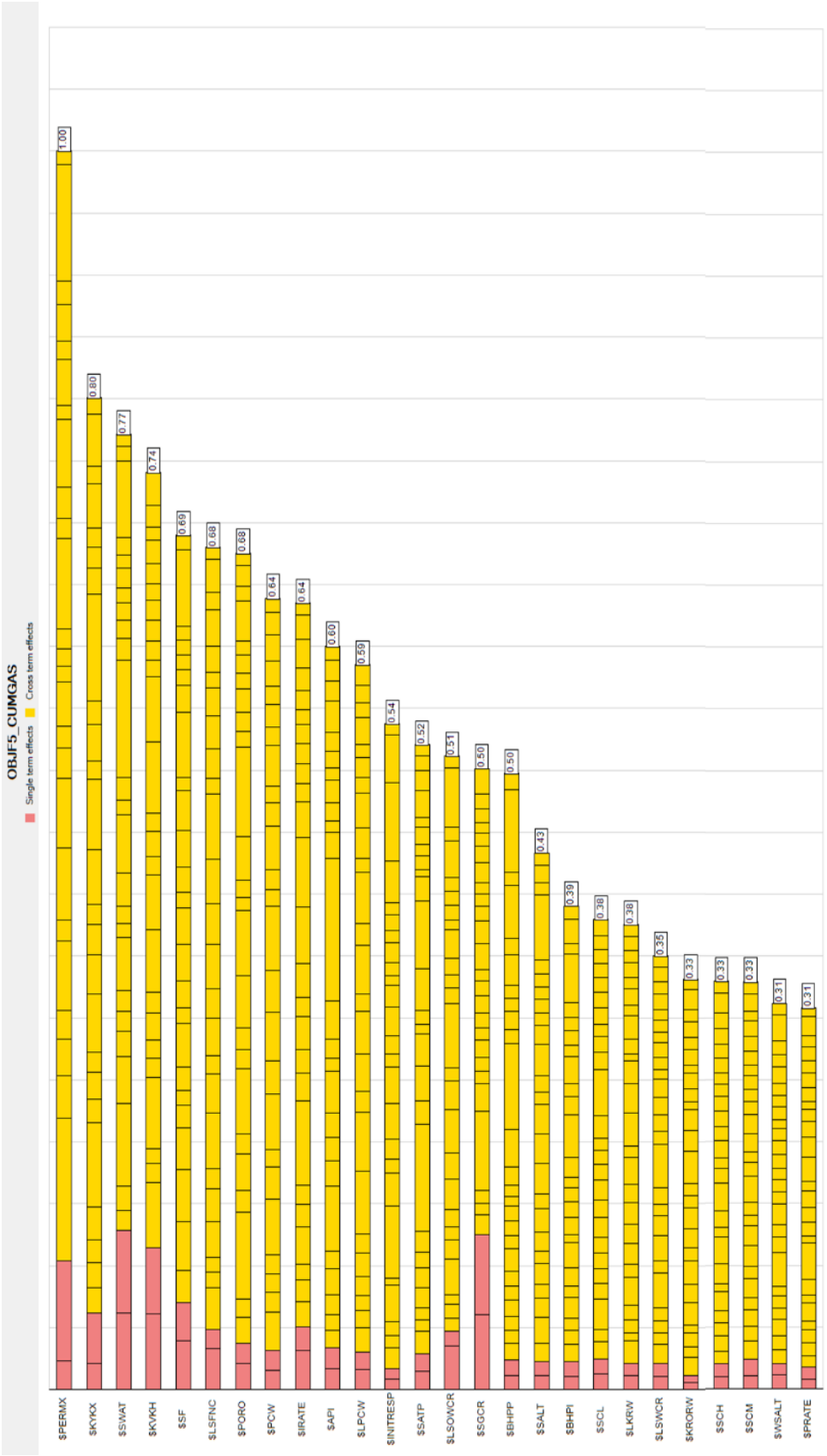
OBJF5_CUMGAS
Single term effects
Cross term effects
1.00
0.80
0.77
0.74
0.69
0.68
0.68
0.64
0.64
0.60
0.59
0.54
0.52
0.51
0.50
0.50
0.43
0.39
0.38
0.36
0.35
0.33
0.33
0.33
0.31
0.31
$PERMX
$KYKX
$SWAT
$KVKH
$SF
$LSFNC
$PORO
$PCW
$IRATE
$API
$LPCW
$INITRESP
$SATP
$LSOWCR
$SGCR
$BHPP
$SALT
$BHPI
$SCL
$LKRW
$LSWCR
$KRORW
$SCH
$SCM
$WSALT
$PRATE

Sensitivity analysis for relative permeability and capillary pressure scaling with endpoints uncertainty – Low API

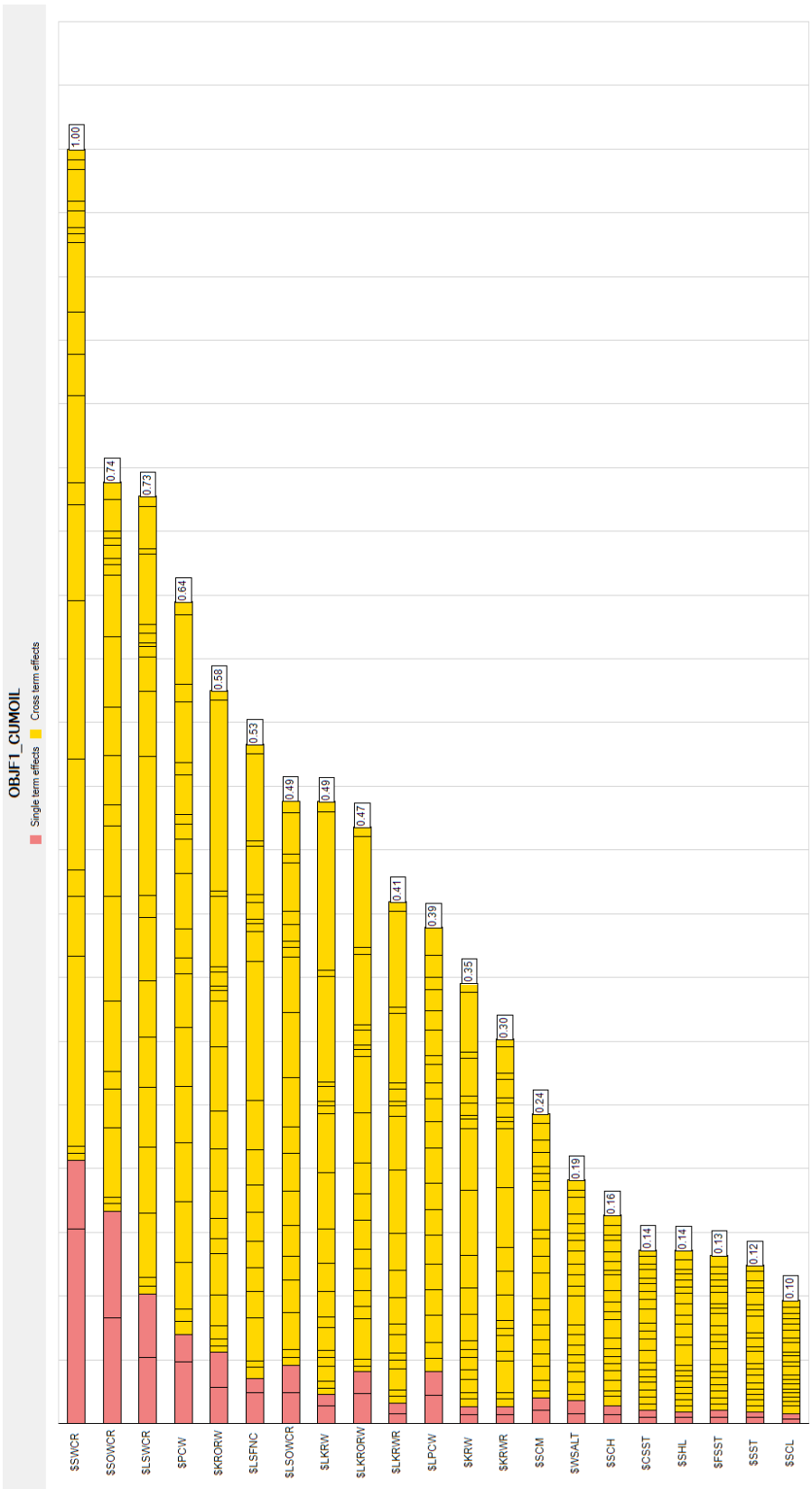
OBJF1_CUMOIL
Single term effects
Cross term effects
1.00
0.74
0.73
0.64
0.58
0.53
0.49
0.49
0.47
0.41
0.39
0.35
0.30
0.24
0.19
0.16
0.14
0.14
0.13
0.12
0.10
$SWCR
$SOWCR
$LSWCR
$PCW
$KRORW
$LSPNC
$LSOWCR
$LKRW
$LKRORW
$LKRWR
$LPCW
$KRW
$KRWR
$SCM
$WSALT
$SCH
$CSST
$SHL
$FSST
$SST
$SCL

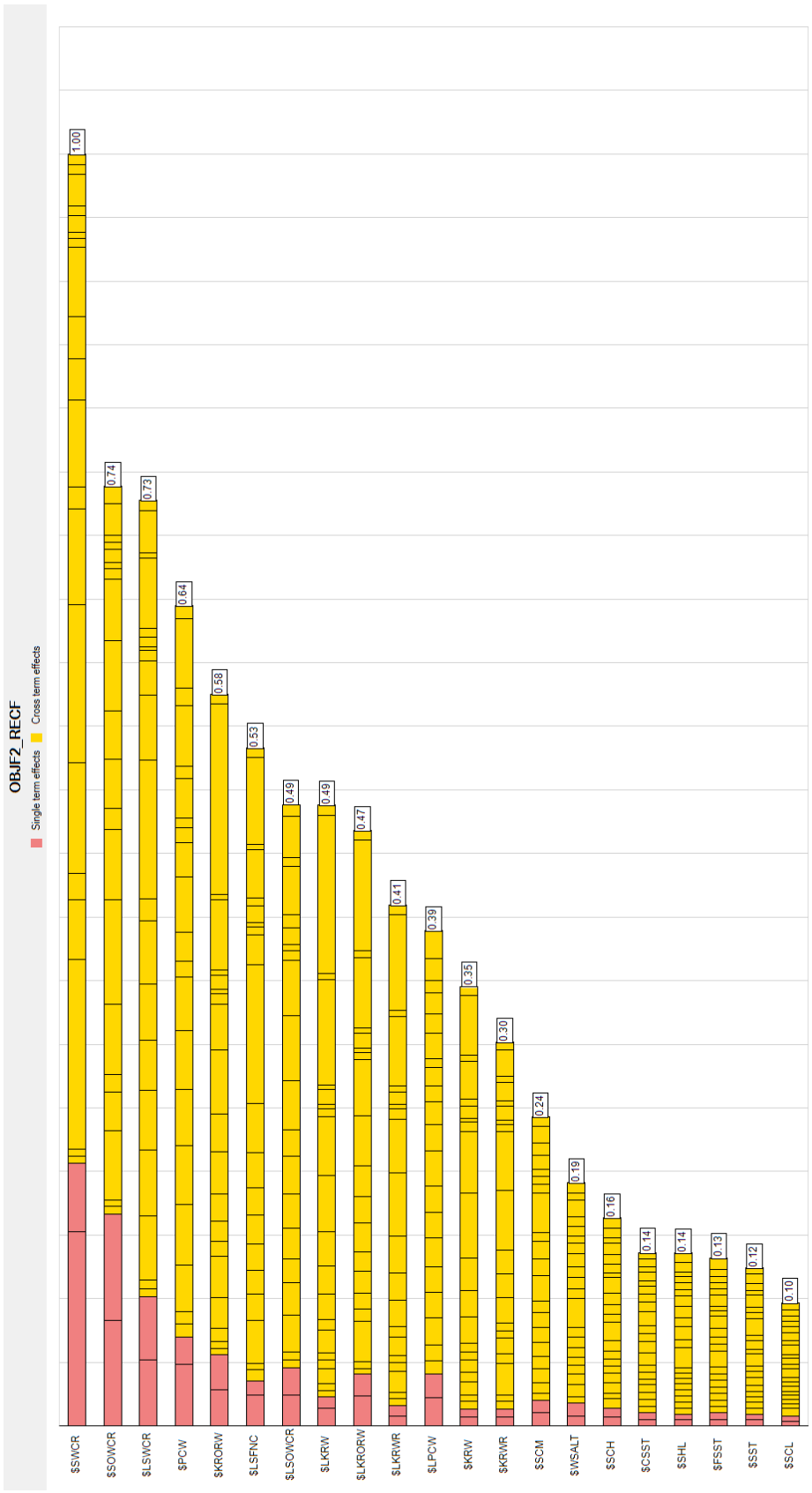
OBJF2_RECF
Single term effects
Cross term effects
1.00
0.74
0.73
0.64
0.58
0.53
0.49
0.49
0.47
0.41
0.39
0.35
0.30
0.24
0.19
0.16
0.14
0.14
0.13
0.12
0.10
$SWCR
$SOWCR
$LSWCR
$PCW
$KRORW
$LSFNC
$LSOWCR
$LKRW
$LKRORW
$LKRWR
$LPCW
$KRW
$KRWR
$SCM
$WSALT
$SCH
$CSST
$SHL
$FSST
$SST
$SCL

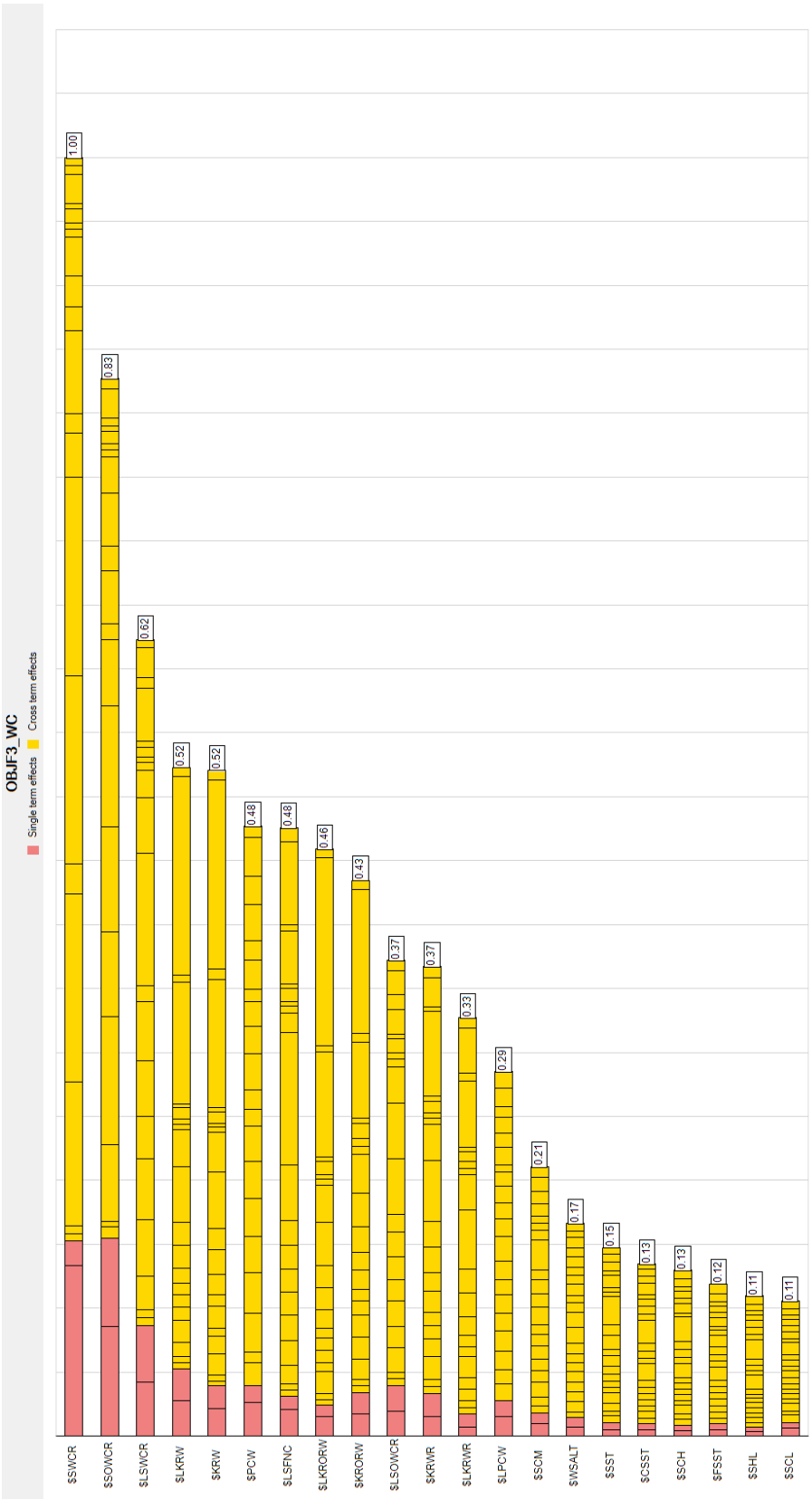
OBJF3_WC
Single term effects
Cross term effects
1.00
0.83
0.62
0.52
0.52
0.48
0.48
0.46
0.43
0.37
0.37
0.33
0.29
0.21
0.17
0.15
0.13
0.13
0.12
0.11
0.11
$SWCR
$SOWCR
$LSWCR
$LKRW
$KRW
$PCW
$LSFNC
$LKRORW
$KRORW
$LSOWCR
$KRWR
$LKRWR
$LPCW
$SCM
$WSALT
$SST
$CSST
$SCH
$FSST
$SHL
$SCL

Sensitivity analysis for relative permeability and capillary pressure scaling with endpoints uncertainty – High API

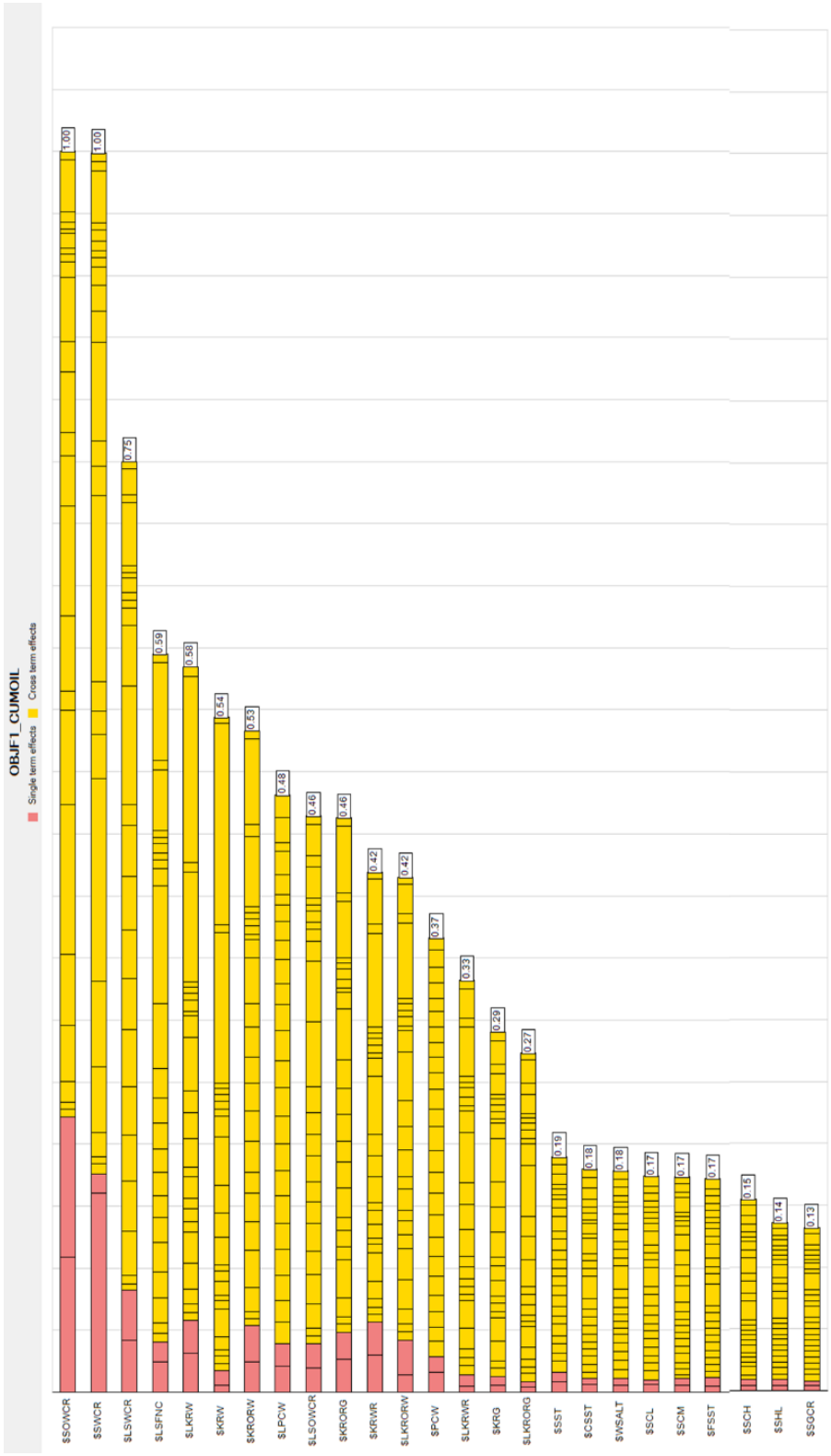

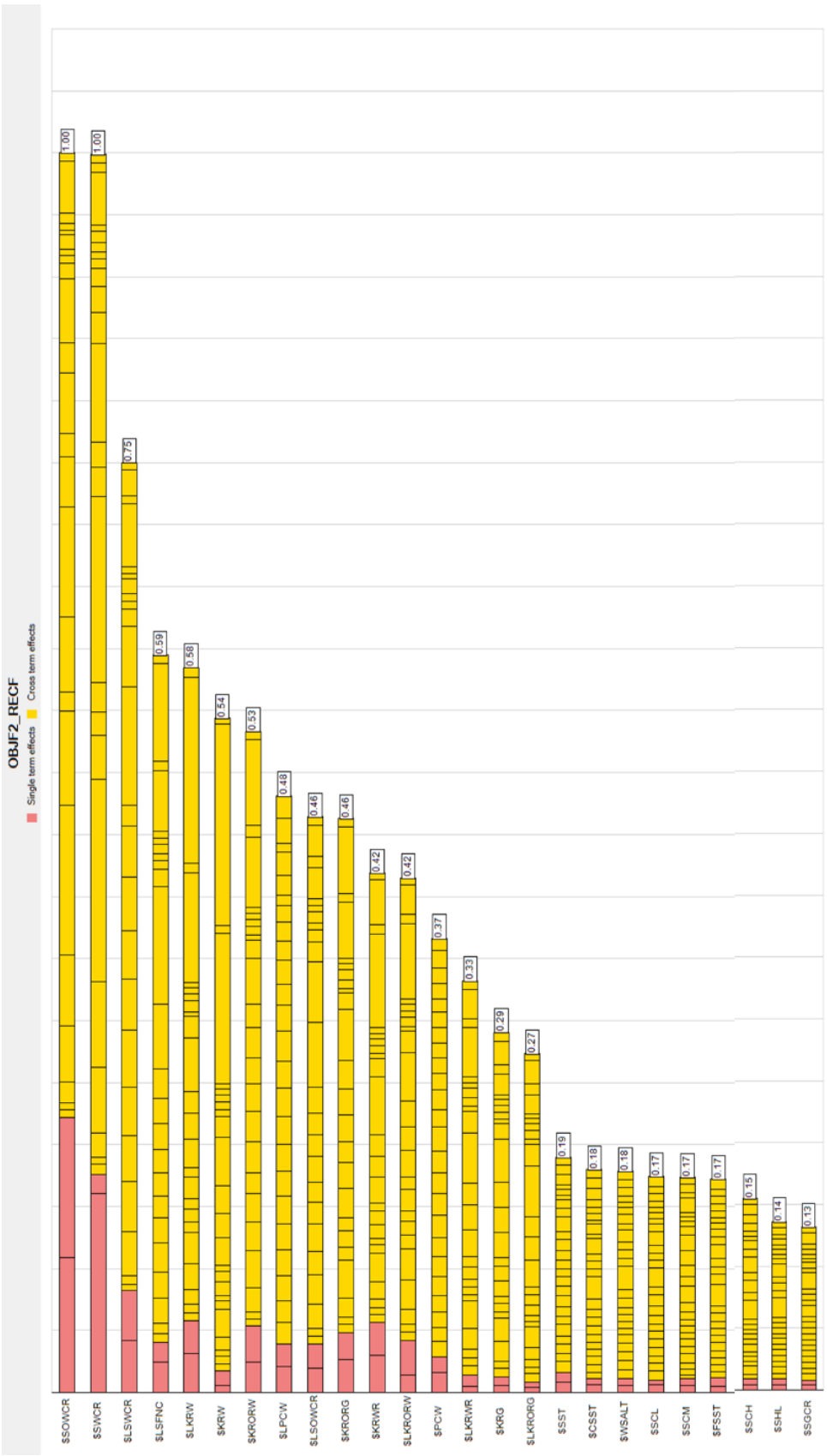
OBJF2_RECF
Single term effects
Cross term effects
1.00
1.00
0.75
0.59
0.58
0.54
0.53
0.48
0.46
0.46
0.42
0.42
0.37
0.33
0.29
0.27
0.19
0.18
0.18
0.17
0.17
0.17
0.15
0.14
0.13
$SOWCR
$SWCR
$LSWCR
$LSFNC
$LKRW
$KRW
$KRORW
$LPCW
$LSOWCR
$KRORG
$KRWR
$LKRORW
$PCW
$LKRWR
$KRG
$LKRORG
$SST
$CSST
$WSALT
$SCL
$SCM
$FSST
$SCH
$SHL
$SGCR

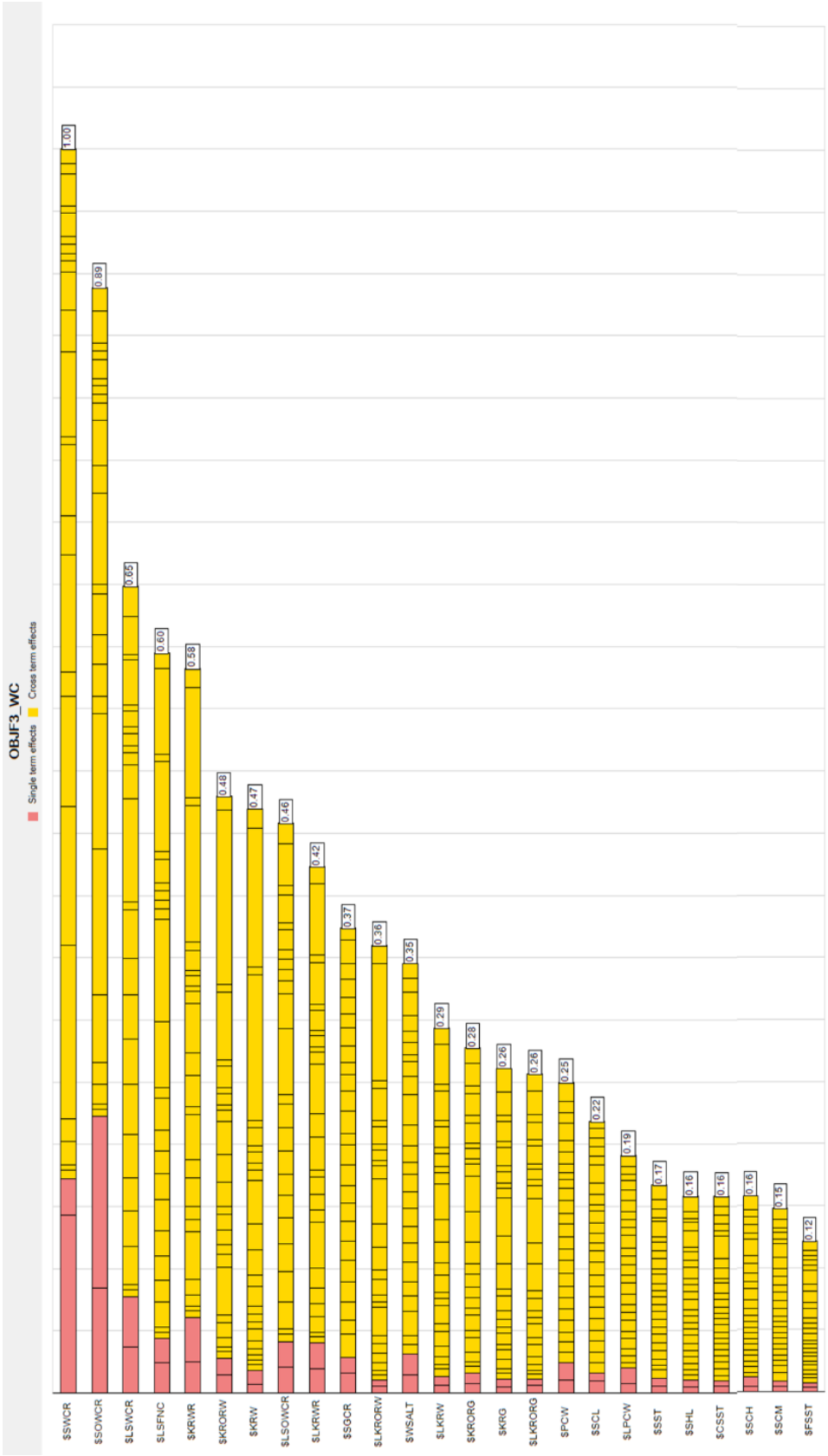
OBJF3_WC
Single term effects
Cross term effects
1.00
0.89
0.65
0.60
0.58
0.48
0.47
0.46
0.42
0.37
0.36
0.35
0.29
0.28
0.26
0.26
0.25
0.22
0.19
0.17
0.16
0.16
0.16
0.15
0.12
$SWCR
$SOWCR
$LSWCR
$LSFNC
$KRWR
$KRORW
$KRW
$LSOWCR
$LKRWR
$SGCR
$LKRORW
$WSALT
$LKRW
$KRORG
$KRG
$LKRORG
$PCW
$SCL
$LPCW
$SST
$SHL
$CSST
$SCH
$SCM
$FSST

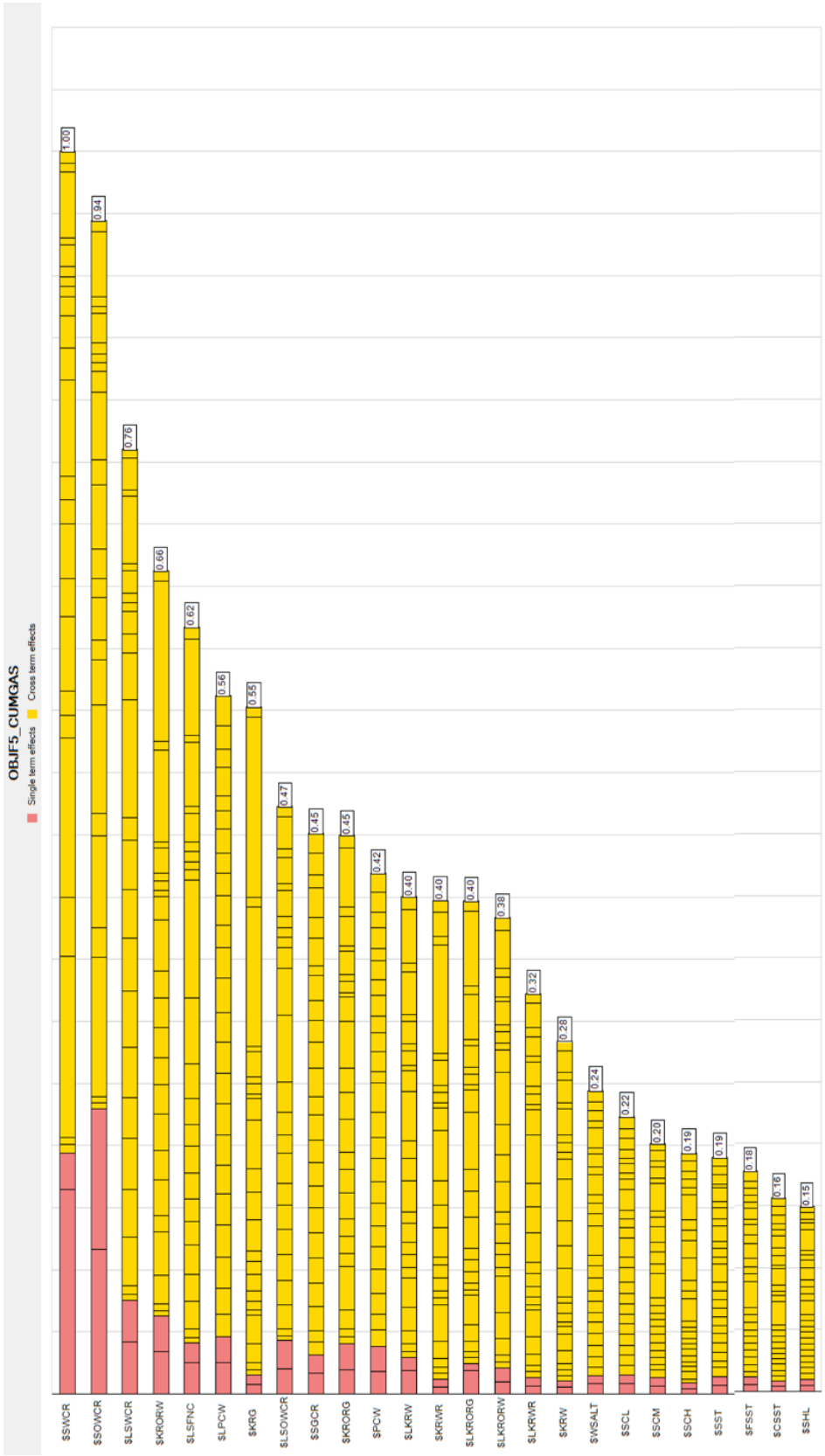
OBJF5_CUMGAS
Single term effects
Cross term effects
1.00
0.94
0.76
0.66
0.62
0.56
0.55
0.47
0.45
0.45
0.42
0.40
0.40
0.40
0.38
0.32
0.28
0.24
0.22
0.20
0.19
0.19
0.18
0.16
0.15
$SWCR
$SOWCR
$LSWCR
$KRORW
$LSFNC
$LPCW
$KRG
$LSOWCR
$SGCR
$KRORG
$PCW
$LKRW
$KRWR
$LKRORG
$LKRORW
$LKRWR
$KRW
$WSALT
$SCL
$SCM
$SCH
$SST
$FSST
$CSST
$SHL

Sensitivity analysis for rock-type saturation functions, relative permeability and capillary pressure scaling, endpoints and other parameters uncertainty – Low API

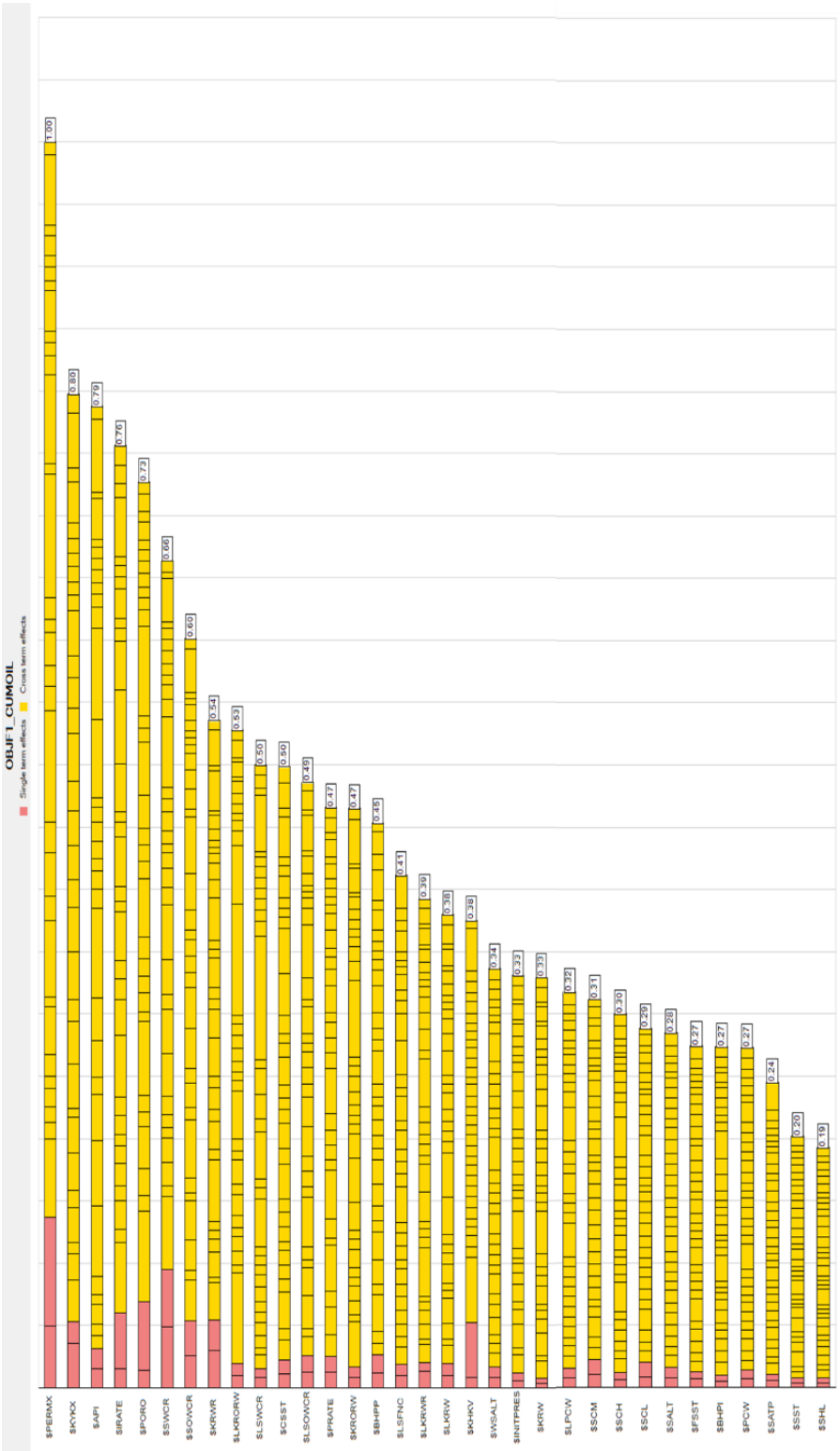

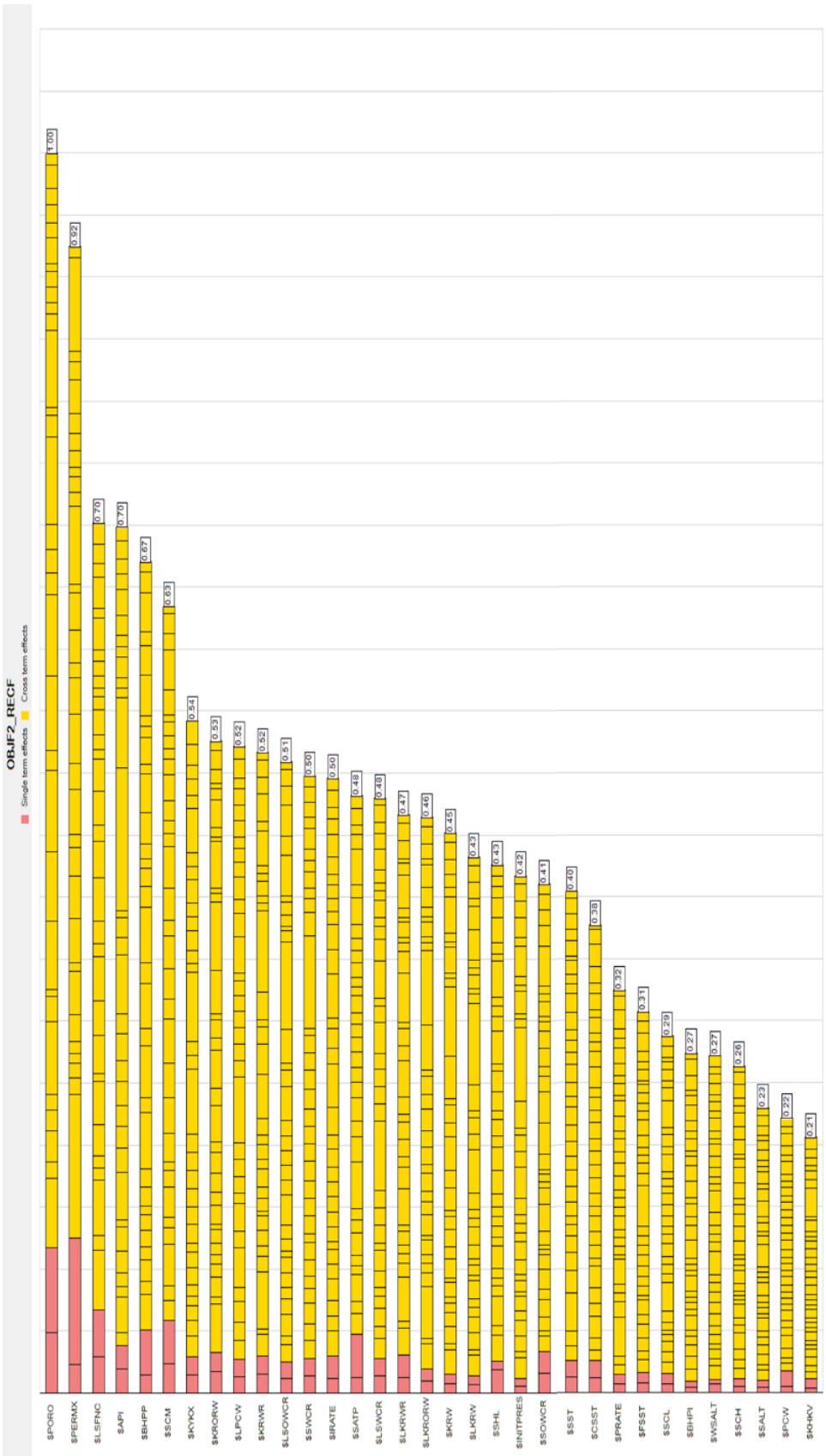
OBJF2_RECF
Single term effects
Cross term effects
1.00
0.92
0.76
0.70
0.67
0.63
0.54
0.53
0.52
0.52
0.51
0.50
0.50
0.48
0.48
0.47
0.46
0.45
0.43
0.43
0.42
0.41
0.40
0.38
0.32
0.31
0.29
0.27
0.27
0.26
0.23
0.22
0.21
$PORO
$PERMX
$LSFNC
$API
$BHPP
$SCM
$KYKX
$KRORW
$LPCW
$KRWR
$LSOWCR
$SWCR
$IRATE
$SATP
$LSWCR
$LKRWR
$LKRORW
$KRW
$LKRW
$SHL
$INITPRES
$SOWCR
$SST
$CSST
$PRATE
$FSST
$SCL
$BHPI
$WSALT
$SCH
$SALT
$PCW
$KHKV

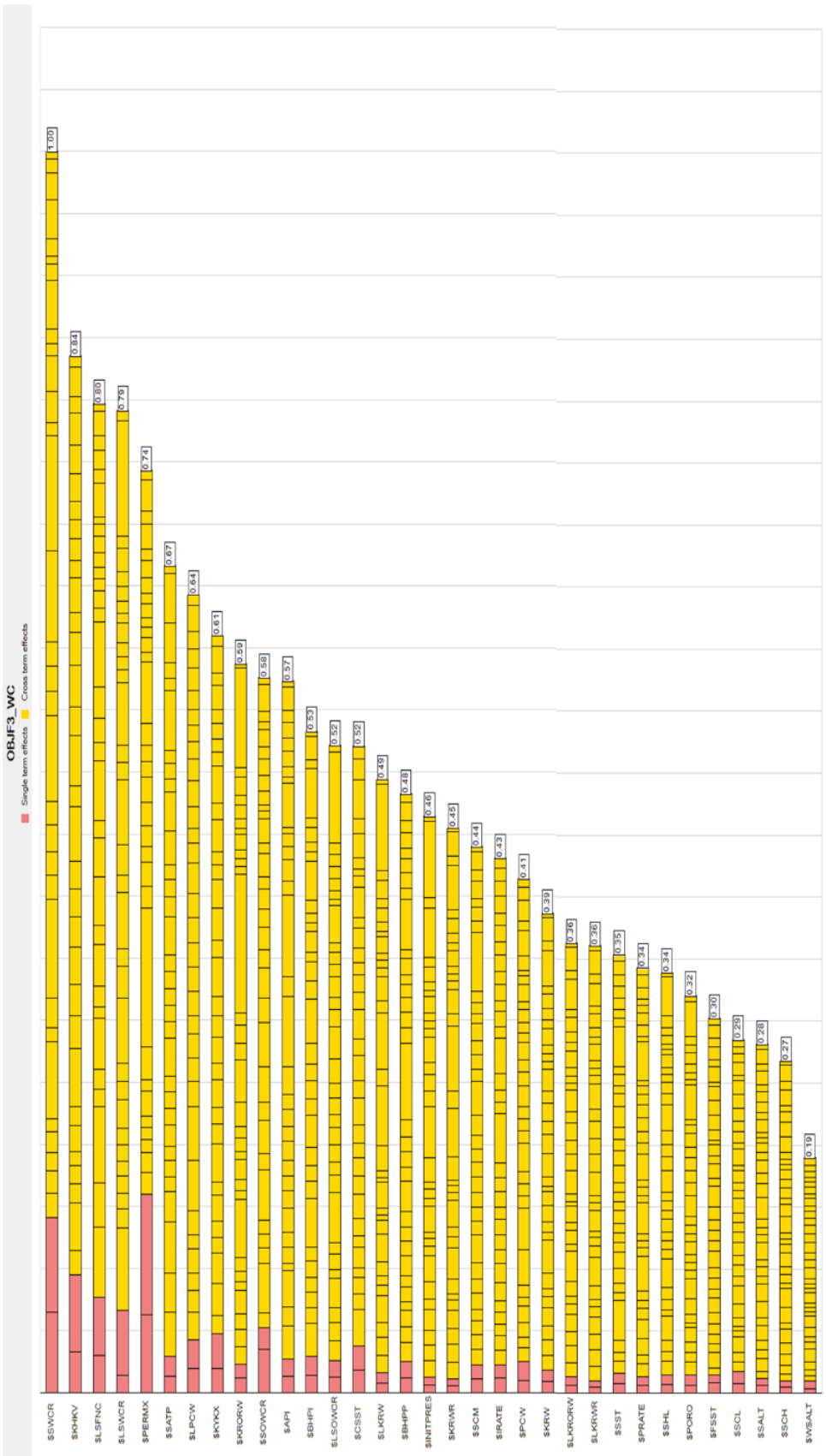
OBJF3_WC
Single term effects
Cross term effects
$SWCR
$KHKV
$LSFNC
$LSWCR
$PERMX
$SATP
$LPCW
$KYKX
$KRORW
$SOWCR
$API
$BHPI
$LSOWCR
$CSST
$LKRW
$BHPP
$INITPRES
$KRWR
$SCM
$IRATE
$PCW
$KRW
$LKRORW
$LKRWR
$SST
$PRATE
$SHL
$PORO
$FSST
$SCL
$SALT
$SCH
$WSALT
1.00
0.84
0.80
0.79
0.74
0.67
0.64
0.61
0.59
0.58
0.57
0.53
0.52
0.52
0.49
0.48
0.46
0.45
0.44
0.43
0.41
0.39
0.36
0.36
0.35
0.34
0.34
0.32
0.30
0.29
0.28
0.27
0.19

Sensitivity analysis for rock-type saturation functions, relative permeability and capillary pressure scaling, endpoints and other parameters uncertainty – High API

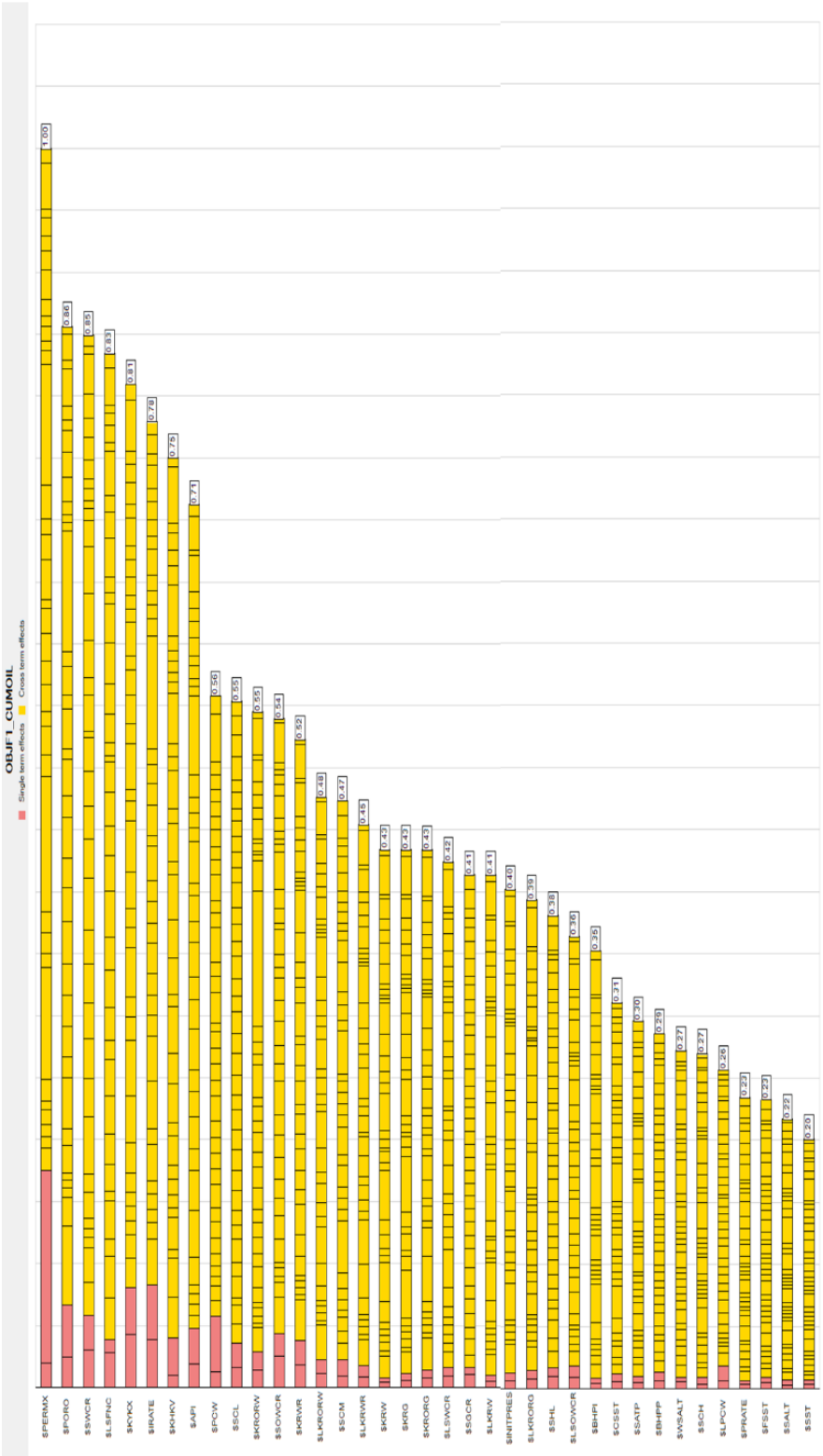

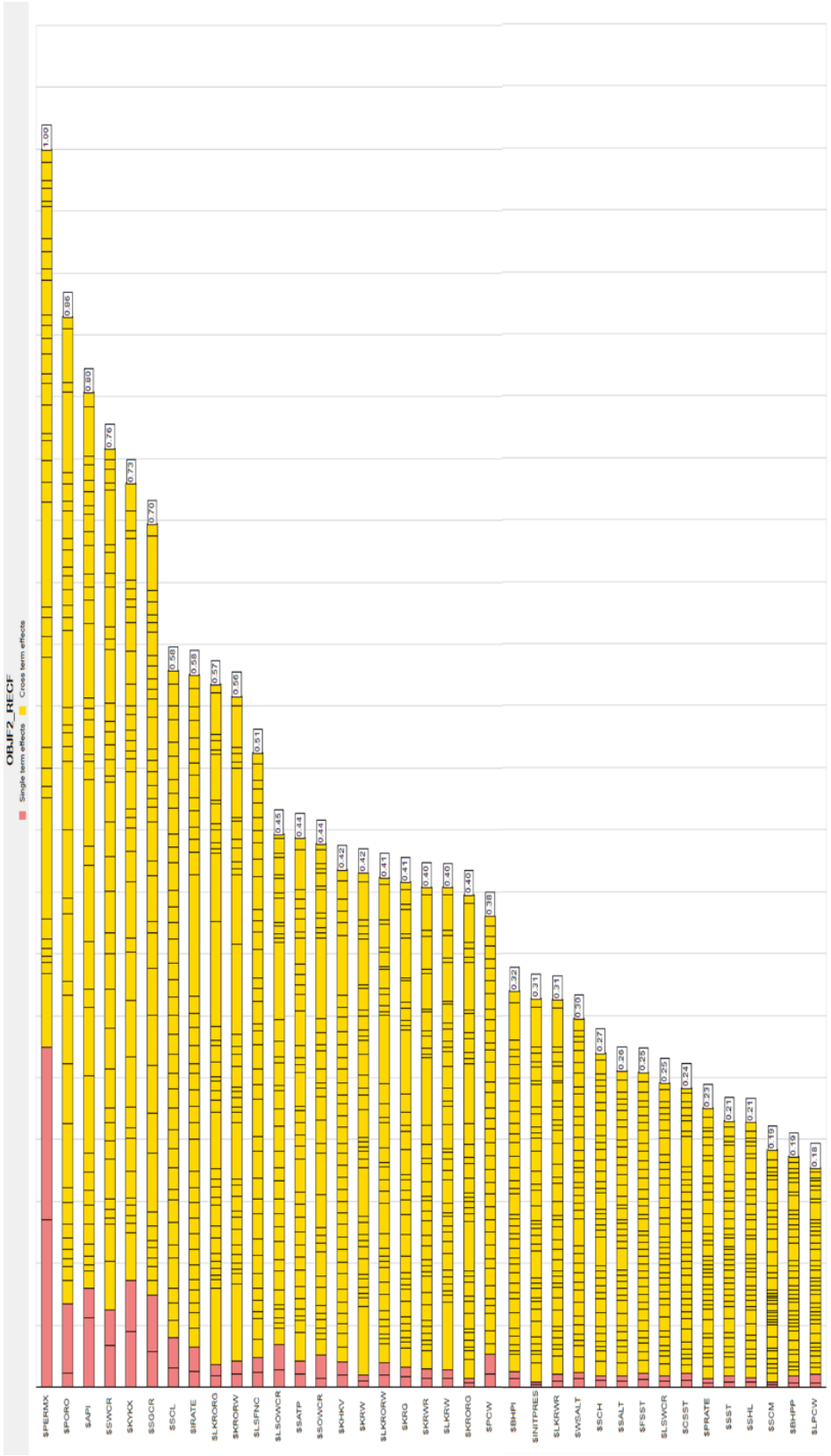
OBJF2_REGF
Single term effects
Cross term effects
$PERMX 1.00
$PORO 0.88
$API 0.80
$SWCR 0.76
$KYKX 0.73
$SGCR 0.70
$SCL 0.58
$IRATE 0.58
$LKRORG 0.57
$KRORW 0.56
$LSFNC 0.51
$LSOWCR 0.46
$SATP 0.44
$SOWCR 0.44
$KHKV 0.42
$KRW 0.42
$LKRORW 0.41
$KRG 0.41
$KRWR 0.40
$LKRW 0.40
$KRORG 0.40
$PCW 0.38
$BHPI 0.32
$INITPRES 0.31
$LKRWR 0.31
$WSALT 0.30
$SCH 0.27
$SALT 0.26
$FSST 0.25
$LSWCR 0.25
$CSST 0.24
$PRATE 0.23
$SST 0.21
$SHL 0.21
$SCM 0.19
$BHPP 0.19
$LPCW 0.18

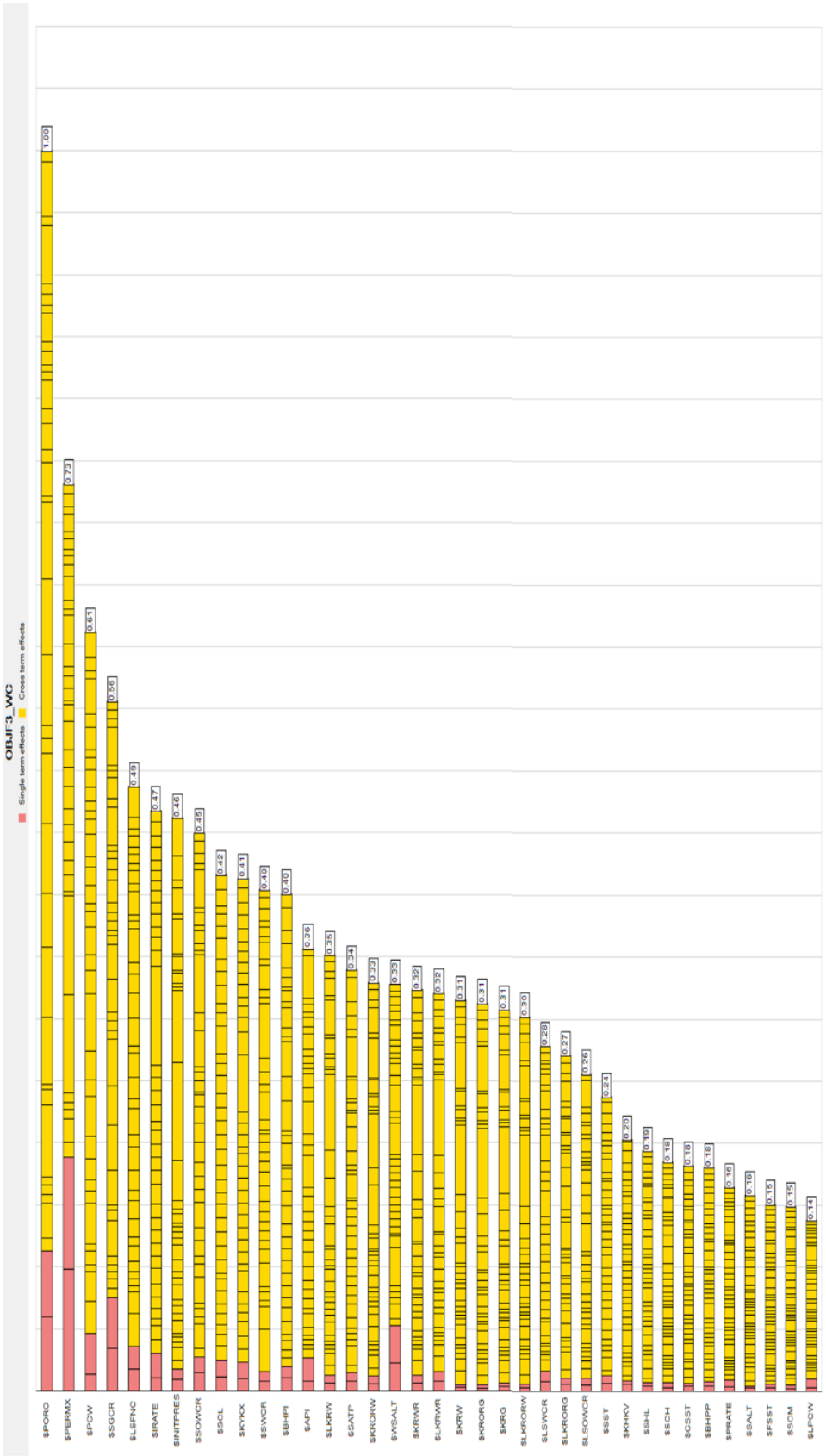
OBJF3_WC
Single term effects
Cross term effects
$PORO 1.00
$PERMX 0.79
$PCW 0.61
$SGCR 0.56
$LSFNC 0.49
$IRATE 0.47
$INITPRES 0.46
$SOWCR 0.45
$SCL 0.42
$KYKX 0.41
$SWCR 0.40
$BHPI 0.40
$API 0.36
$LKRW 0.35
$SATP 0.34
$KRORW 0.33
$WSALT 0.33
$KRWR 0.32
$LKRWR 0.32
$KRW 0.31
$KRORG 0.31
$KRG 0.31
$LKRORW 0.30
$LSWCR 0.28
$LKRORG 0.27
$LSOWCR 0.26
$SST 0.24
$KHKV 0.20
$SHL 0.19
$SCH 0.18
$CSST 0.18
$BHPP 0.18
$PRATE 0.16
$SALT 0.16
$FSST 0.15
$SCM 0.15
$LPCW 0.14

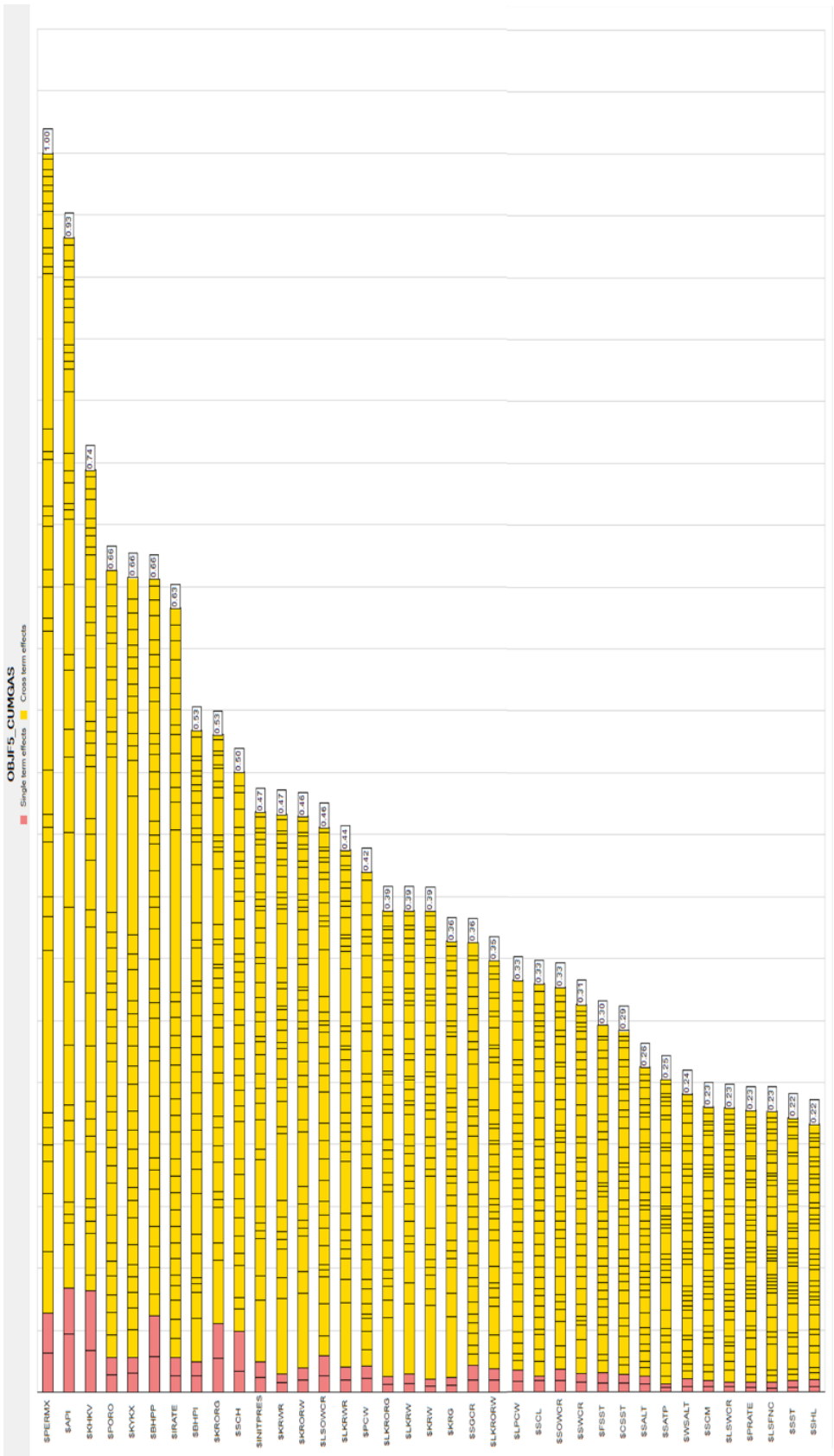
OBJF5_CUMGAS
Single term effects
Cross term effects
$PERMX
$API
$KHKV
$PORO
$KYKX
$BHPP
$IRATE
$BHPI
$KRORG
$SCH
$INITPRES
$KRWR
$KRORW
$LSOWCR
$LKRWR
$PCW
$LKRORG
$LKRW
$KRW
$KRG
$SGCR
$LKRORW
$LPCW
$SCL
$SOWCR
$SWCR
$FSST
$CSST
$SALT
$SATP
$WSALT
$SCM
$LSWCR
$PRATE
$LSFNC
$SST
$SHL
1.00
0.93
0.74
0.66
0.66
0.66
0.63
0.53
0.53
0.50
0.47
0.47
0.46
0.46
0.44
0.42
0.39
0.39
0.39
0.38
0.36
0.35
0.33
0.33
0.33
0.31
0.29
0.28
0.26
0.25
0.24
0.23
0.23
0.23
0.23
0.22
0.22

Sensitivity analysis for brine speciation, rock-type saturation functions, relative permeability and capillary pressure scaling, endpoints uncertainty – High API

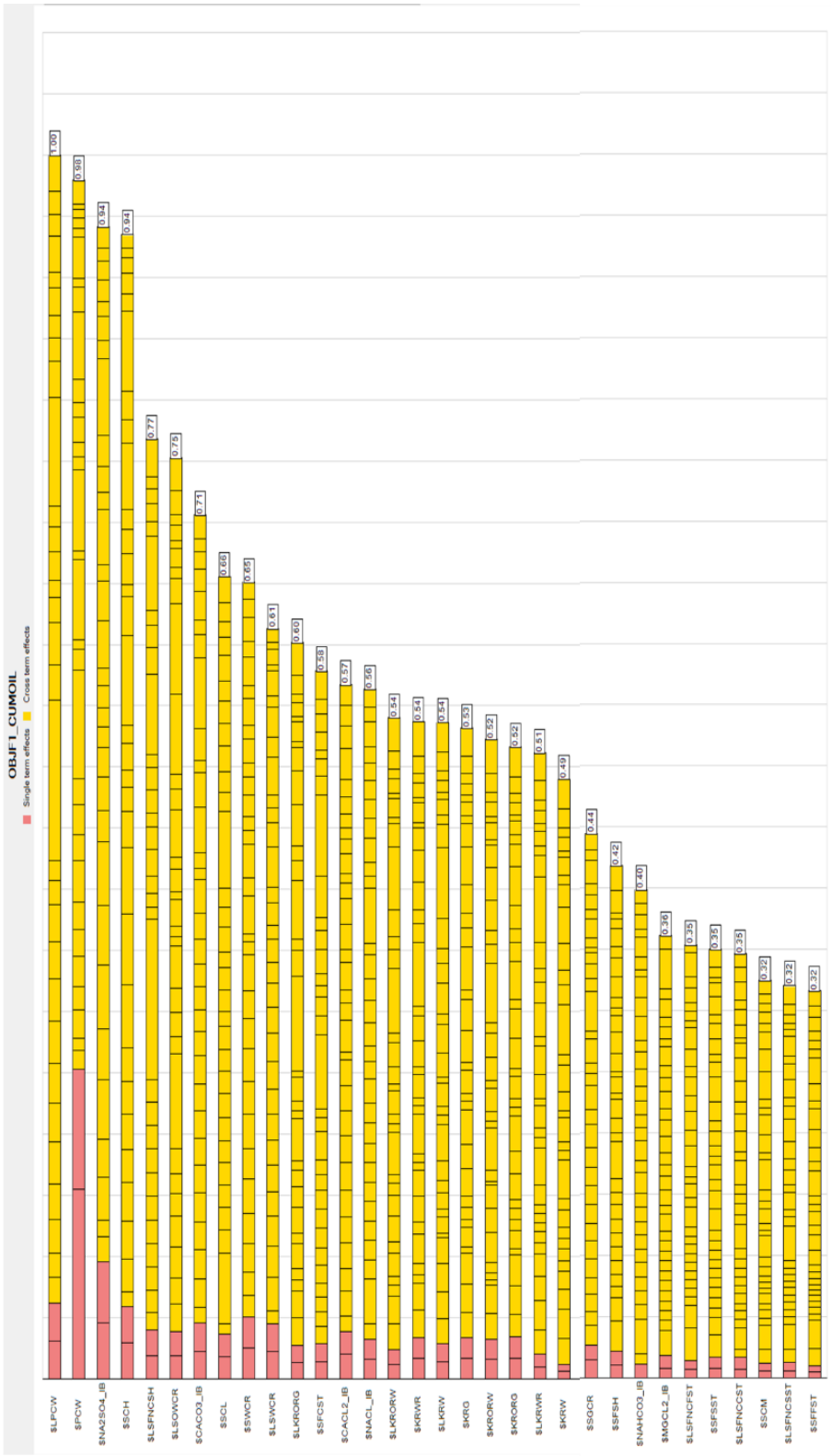

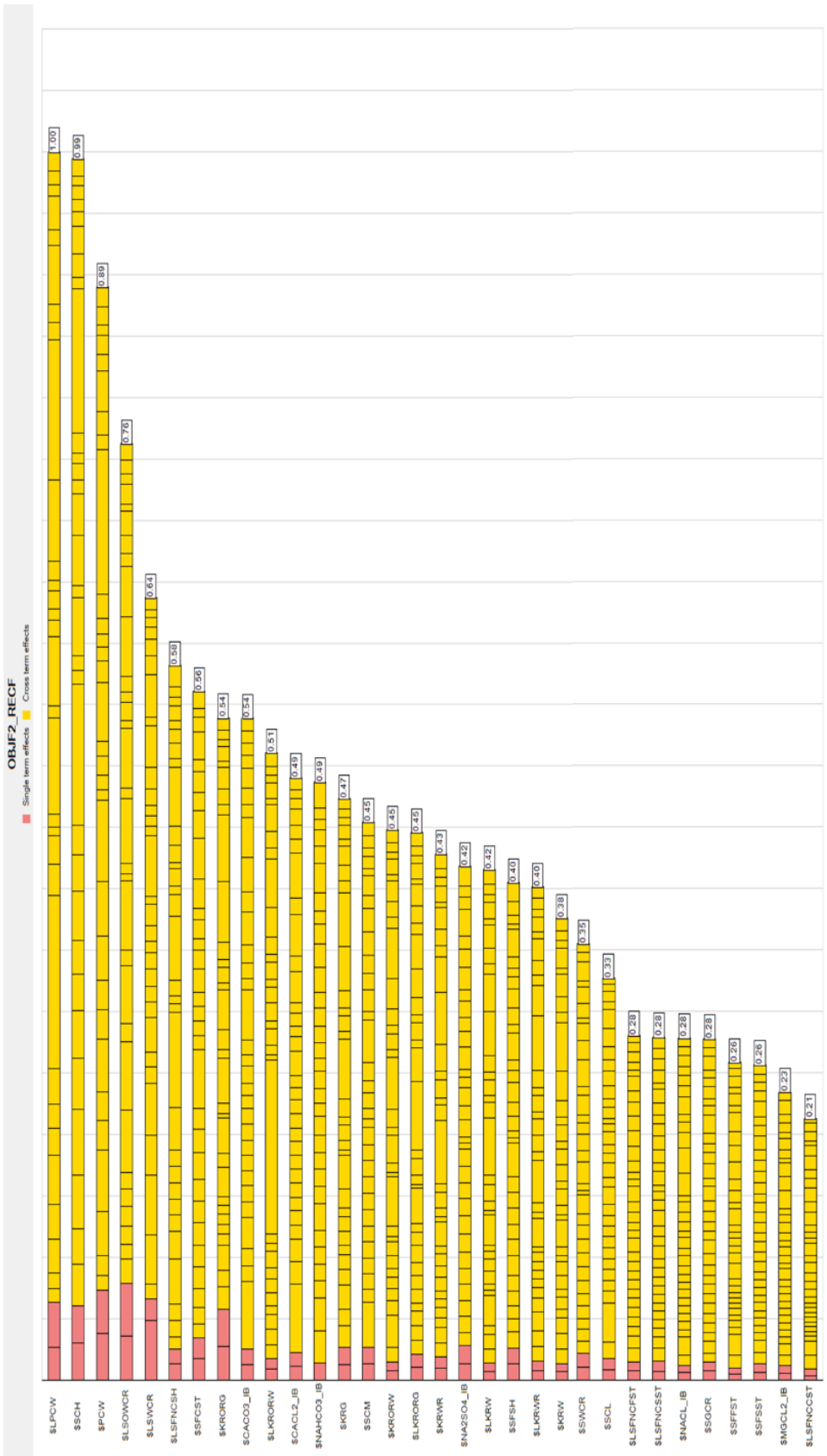
OBJF2_RECF
Single term effects
Cross term effects
1.00
0.99
0.89
0.76
0.64
0.58
0.56
0.54
0.54
0.51
0.49
0.49
0.47
0.45
0.45
0.45
0.43
0.42
0.42
0.40
0.40
0.38
0.35
0.33
0.28
0.28
0.28
0.28
0.26
0.26
0.23
0.21
$LPCW
$SCH
$PCW
$LSOWCR
$LSWCR
$LSFNCSH
$SFCST
$KRORG
$CACO3_IB
$LKRORW
$CACL2_IB
$NAHCO3_IB
$KRG
$SCM
$KRORW
$LKRORG
$KRWR
$NA2SO4_IB
$LKRW
$SFSH
$LKRWR
$KRW
$SWCR
$SCL
$LSFNCFST
$LSFNCSST
$NACL_IB
$SGCR
$SFFST
$SFSST
$MGCL2_IB
$LSFNCCST

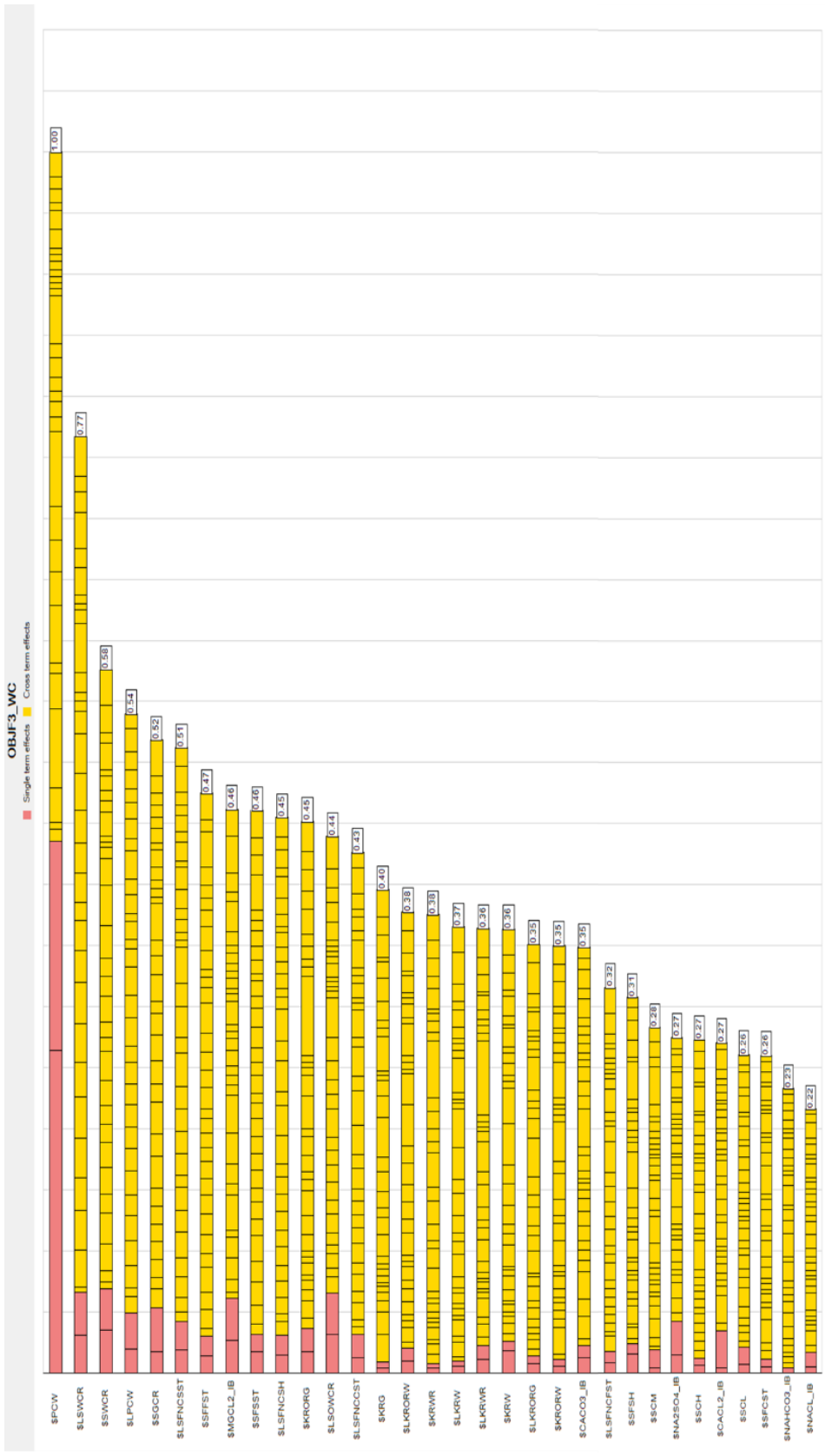
OBJF'3_WC
Single term effects
Cross term effects
1.00
0.77
0.58
0.54
0.52
0.51
0.47
0.46
0.46
0.45
0.45
0.44
0.43
0.40
0.38
0.38
0.37
0.36
0.36
0.35
0.35
0.35
0.32
0.31
0.28
0.27
0.27
0.27
0.26
0.26
0.23
0.22
$PCW
$LSWCR
$SWCR
$LPCW
$SGCR
$LSFNCSST
$SFFST
$MGCL2_IB
$SFSST
$LSFNCSH
$KRORG
$LSOWCR
$LSFNCCST
$KRG
$LKRORW
$KRWR
$LKRW
$LKRWR
$KRW
$LKRORG
$KRORW
$CACO3_IB
$LSFNCFST
$SFSH
$SCM
$NA2SO4_IB
$SCH
$CACL2_IB
$SGL
$SFCST
$NAHCO3_IB
$NACL_IB

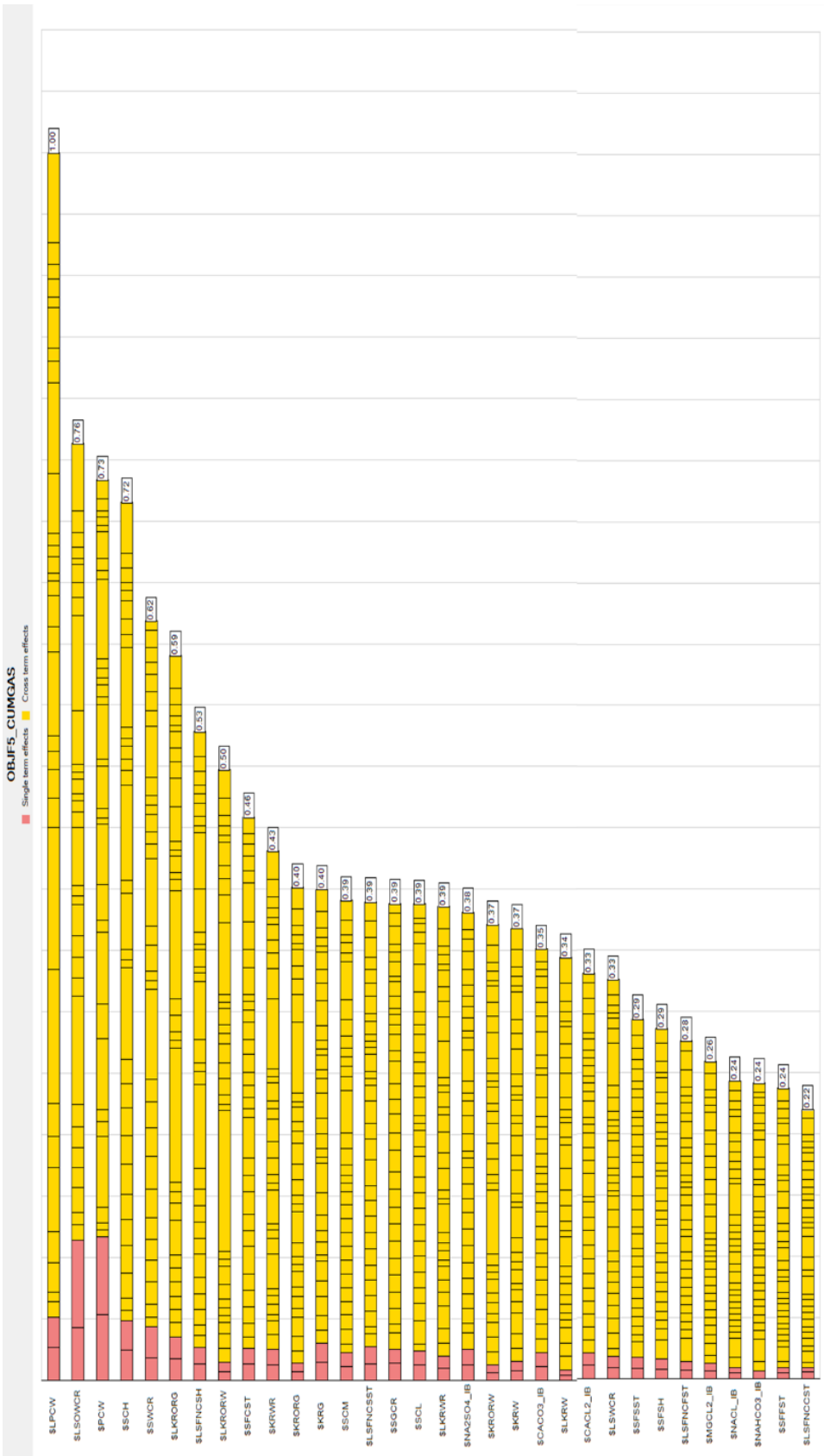
OBJF5_CUMGAS
Single term effects
Cross term effects
1.00
0.76
0.73
0.72
0.62
0.59
0.53
0.50
0.46
0.43
0.40
0.40
0.39
0.39
0.39
0.39
0.39
0.38
0.37
0.37
0.35
0.34
0.33
0.33
0.29
0.29
0.28
0.26
0.24
0.24
0.24
0.22
$LPCW
$LSOWCR
$PCW
$SCH
$SWCR
$LKRORG
$LSFNCSH
$LKRORW
$SFCST
$KRWR
$KRORG
$KRG
$SCM
$LSFNCSST
$SGCR
$SCL
$LKRWR
$NA2SO4_IB
$KRORW
$KRW
$CACO3_IB
$LKRW
$CACL2_IB
$LSWCR
$SFSST
$SFSH
$LSFNCFST
$MGCL2_IB
$NACL_IB
$NAHCO3_IB
$SFFST
$LSFNCCST

Sensitivity analysis for brine speciation, rock-type saturation functions, relative permeability and capillary pressure scaling, endpoints and other parameters uncertainty – High API

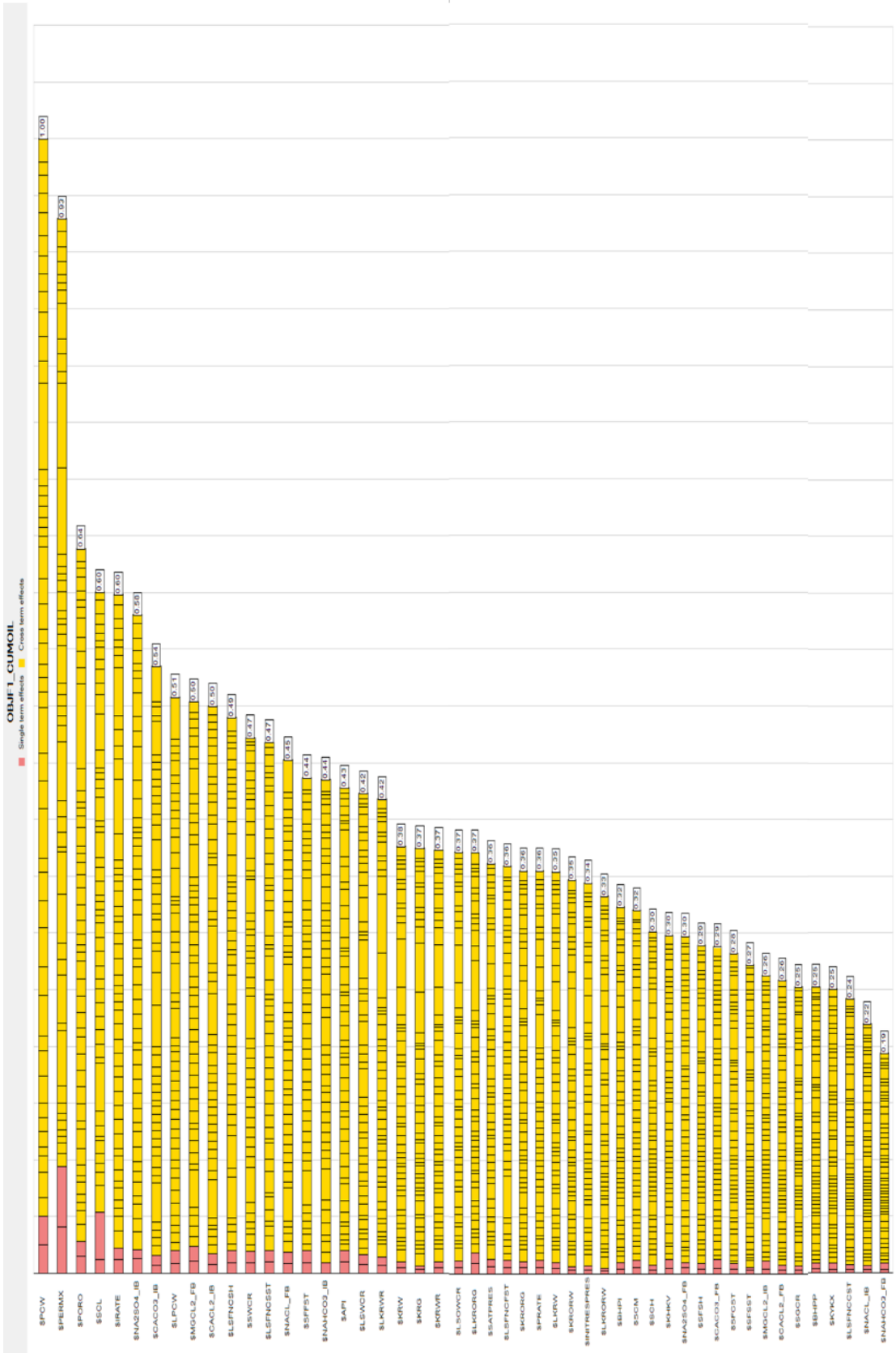
OBJF1_CUMOIL
Single term effects
Cross term effects
$PCW
$PERMX
$PORO
$SGL
$IRATE
$NA2SO4_IB
$CACO3_IB
$LPCW
$MGCL2_FB
$CACL2_IB
$LSFNCSH
$SWCR
$LSFNCSST
$NACL_FB
$SFFST
$NAHCO3_IB
$API
$LSWCR
$LKRWR
$KRW
$KRG
$KROWR
$LSOWCR
$LKRORG
$SATPRES
$LSFNCFST
$KRORG
$PRATE
$LKRW
$KRORW
$INITRESPRES
$LKRORW
$SHPI
$SCM
$SCH
$KHKV
$NA2SO4_FB
$SFSH
$CACO3_FB
$SFCST
$SFSST
$MGCL2_IB
$CACL2_FB
$SGCR
$SHPP
$KYK
$LSFNCCST
$NACL_IB
$NAHCO3_FB
1.00
0.93
0.64
0.60
0.60
0.56
0.54
0.51
0.50
0.50
0.49
0.47
0.47
0.45
0.44
0.44
0.43
0.42
0.42
0.38
0.37
0.37
0.37
0.37
0.36
0.36
0.36
0.36
0.35
0.35
0.34
0.33
0.32
0.32
0.30
0.30
0.30
0.30
0.29
0.29
0.28
0.27
0.26
0.26
0.25
0.25
0.25
0.24
0.22
0.19

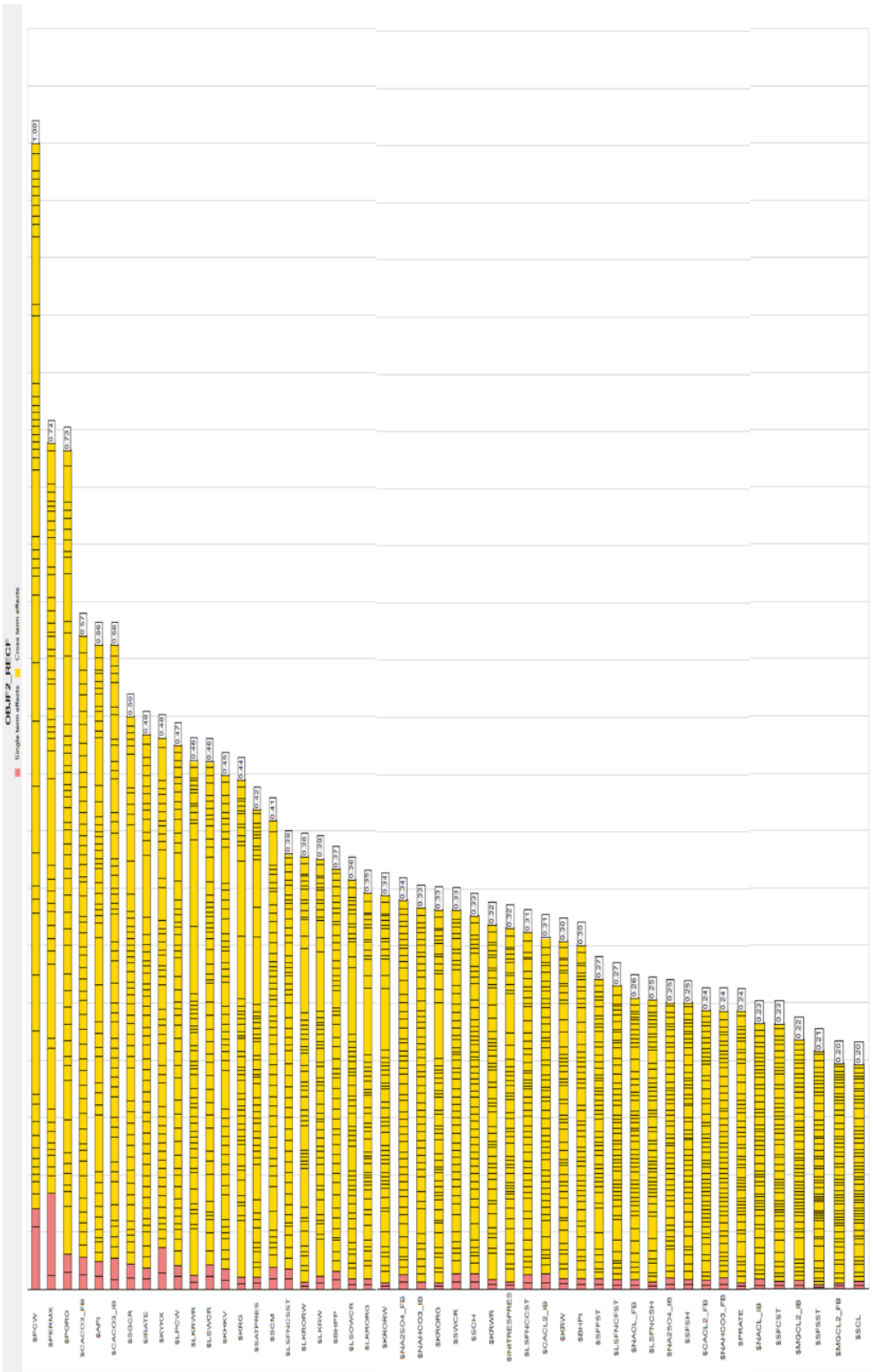
OBJF2_RFCF
Single term effects
Cross term effects
1.00
0.74
0.72
0.57
0.56
0.56
0.50
0.48
0.46
0.47
0.46
0.46
0.45
0.44
0.42
0.41
0.39
0.38
0.38
0.37
0.36
0.35
0.34
0.34
0.33
0.33
0.33
0.32
0.32
0.31
0.31
0.30
0.30
0.27
0.27
0.26
0.25
0.25
0.25
0.24
0.24
0.24
0.23
0.23
0.22
0.21
0.20
0.20
$PCW
$PERMX
$PORO
$CACO3_FB
$API
$CACO3_IB
$SGCR
$RATE
$KYKX
$LPCW
$LKRWR
$LSWCR
$KHKV
$KRG
$SATPRES
$SOM
$LSFNCSST
$LKRORW
$LKRW
$BHPP
$LSOWCR
$LKRORG
$KRORW
$NA2SO4_FB
$NAHCO3_IB
$KRORG
$SWCR
$SOH
$KRWR
$INITRESPRES
$LSFNCCST
$CACL2_IB
$KRW
$BHPI
$SFPST
$LSFNCPST
$NACL_FB
$LSFNCSH
$NA2SO4_IB
$SFSH
$CACL2_FB
$NAHCO3_FB
$PRATE
$NACL_IB
$SFCST
$MGCL2_IB
$SFSST
$MGCL2_FB
$SCL

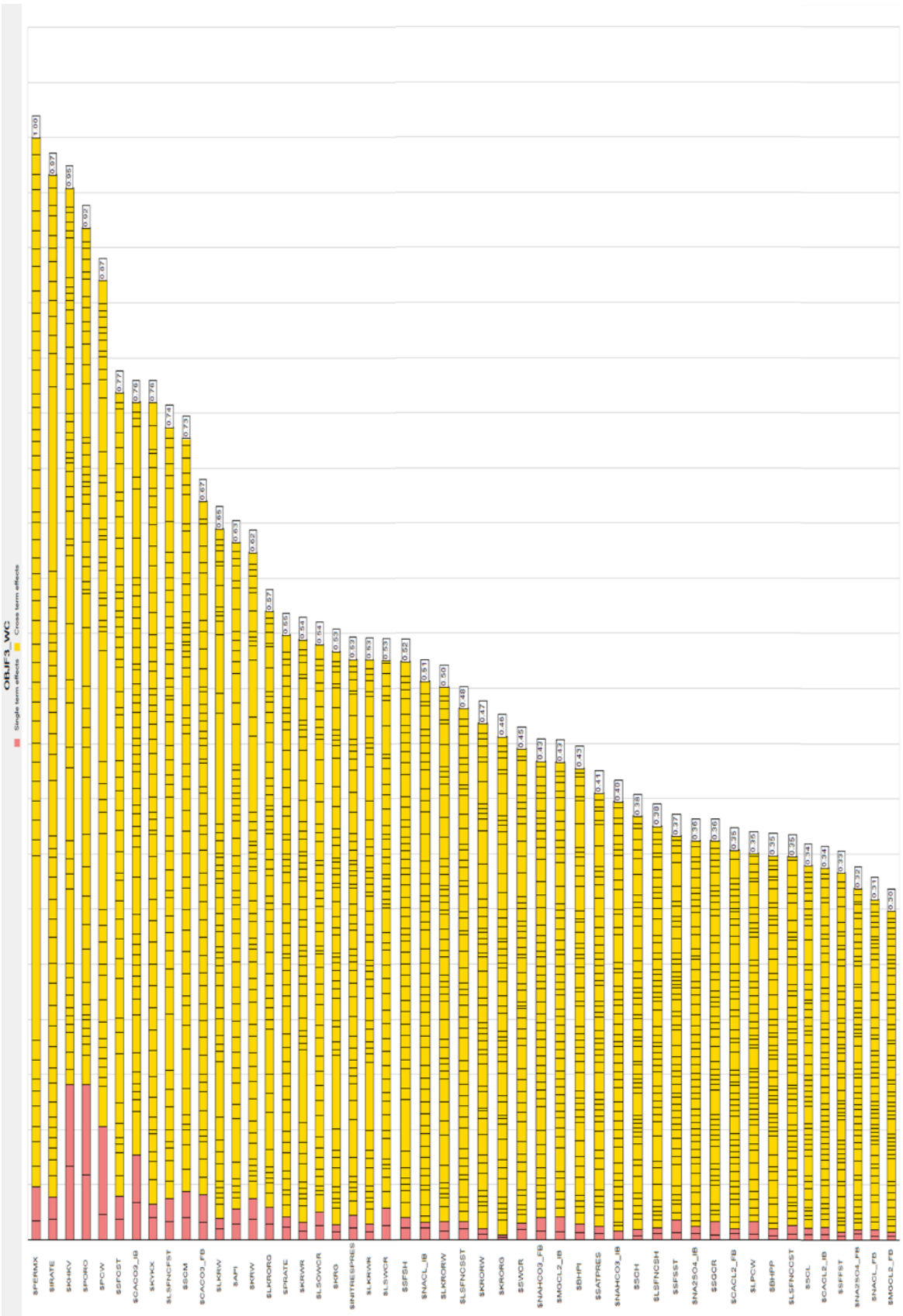
OBJF3_WC
Single term effects
Cross term effects
1.00
0.97
0.95
0.92
0.87
0.77
0.76
0.76
0.74
0.73
0.67
0.65
0.63
0.62
0.57
0.55
0.54
0.54
0.53
0.53
0.53
0.52
0.51
0.50
0.48
0.47
0.46
0.45
0.43
0.43
0.41
0.40
0.38
0.38
0.37
0.36
0.36
0.35
0.35
0.35
0.35
0.34
0.34
0.33
0.32
0.31
0.30
$PERMX
$IRATE
$KHKV
$PORO
$PCW
$SFCST
$CACO3_IB
$KYKX
$LSFNCFST
$SGM
$CACO3_FB
$LKRW
$API
$KRW
$LKRORG
$PRATE
$KRWR
$LSOWCR
$KRG
$PITRESPRES
$LKRWR
$LSWCR
$SFSH
$NACL_IB
$LKRORW
$LSFNCSST
$KRORW
$KRORG
$SWOR
$NAHCO3_FB
$MGCL2_IB
$BHPI
$SATPRES
$NAHCO3_IB
$SCH
$LSFNCSH
$SFSST
$NA2SO4_IB
$SGCR
$CACL2_FB
$LPCW
$BHPP
$LSFNCCST
$SCL
$CACL2_IB
$SFPST
$NA2SO4_FB
$NACL_FB
$MGCL2_FB

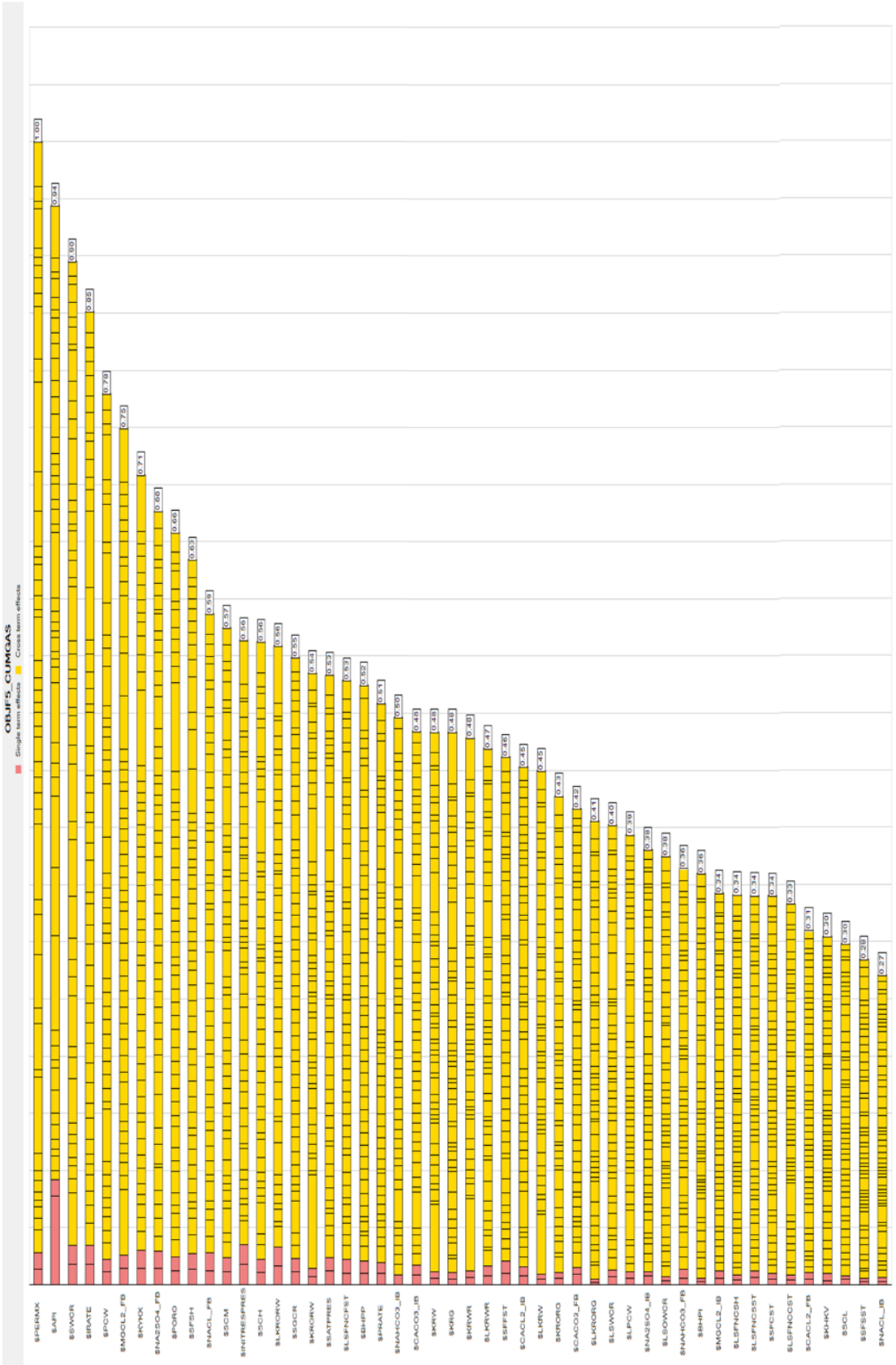
OBJF5_CUMGAS
Single term effects
Cross term effects
$PERMX
$API
$SWCR
$IRATE
$PCW
$MGCL2_FB
$KYKX
$NA2SO4_FB
$PORO
$SFSH
$NACL_FB
$SCM
$INITRESPRES
$SCH
$LKROKRW
$SOGCR
$KROKW
$SATPRES
$LSFNCPST
$BHPP
$PRATE
$NAHCO3_IB
$CACO3_IB
$KRW
$KRG
$KRWR
$LKRWR
$SFPST
$CACL2_IB
$LKRW
$KROKO
$CACO3_FB
$LKROKO
$LSWCR
$LPCW
$NA2SO4_IB
$LSGWCR
$NAHCO3_FB
$BHPI
$MGCL2_IB
$LSFNOSH
$LSFNOSST
$SFCST
$LSFNOCST
$CACL2_FB
$KHKV
$SOL
$SFSST
$NACL_IB
1.00
0.94
0.90
0.85
0.78
0.75
0.71
0.66
0.66
0.63
0.58
0.57
0.56
0.56
0.56
0.55
0.54
0.53
0.53
0.52
0.51
0.50
0.49
0.49
0.49
0.48
0.47
0.46
0.45
0.45
0.43
0.42
0.41
0.40
0.39
0.38
0.38
0.36
0.36
0.34
0.34
0.34
0.34
0.33
0.31
0.30
0.30
0.28
0.27